

# Estimating Solutions for the Ginzburg-Landau Superconductivity Model in Thin Disks

by Ty J. Thompson

A Thesis  
Submitted in Partial Fulfillment  
of the Requirements for the Degree of  
Master of Science  
in Mathematics

Northern Arizona University  
August, 2005

Approved:

---

James W. Swift, Ph.D., Co-Chair

---

John M. Neuberger, Ph.D., Co-Chair

---

Nándor Sieben, Ph.D.

## Abstract

# Estimating Solutions for the Ginzburg-Landau Superconductivity Model in Thin Disks

**Ty J. Thompson**

Numerical solutions to a nonlinear boundary value problem arising from the Ginzburg-Landau (GL) model for superconductivity are estimated using an augmented version of the Gradient-Newton-Galerkin-Algorithm (GNGA) provided by Neuberger, Swift and Sieben. After first characterizing the problem in terms of established PDE theory, a variational approach is used to recover a relationship between the critical points of the associated energy functional and the zeros of its derivative. The model is then applied to a nonmagnetic, homogeneous and isotropic thin cylindrical sample, estimated as a disk in  $\mathbb{R}^2$ , that is immersed in a normally incident and constant magnetic field near the critical superconducting temperature. The method produces branches of solution estimates of arbitrary stability, versus a bifurcation parameter that approximates the effect of decreasing temperature near superconductivity onset. Branch estimates that pass through three levels of bifurcation are studied, and several types of low-signature solutions observed are characterized in terms of the geometrical and mathematical symmetries inherent in the problem. Simulation results are provided at several stages to provide an intuitive perspective as the study develops, and to clarify the proposed theories.

# Acknowledgments

The author would like to thank Dr. James W. Swift for his expert guidance and many contributions to the body of this work. The most important results simply would not have been possible without the patient and consistent dedication that Professor Swift made. The numerical method used and its application to the Ginzburg-Landau model was first suggested to the author by Dr. John M. Neuberger, whose limitless encouragement and insight is truly an invaluable resource. The interested reader would be well-served to contact Dr. Swift or Dr. Neuberger to discuss the prospects of either extending this research, or of beginning a similar study in the field of applied mathematics.

# Contents

List of Figures . . . . .	vi
List of Tables . . . . .	vii
<b>Chapter 1 Introduction</b>	<b>1</b>
<b>Chapter 2 Ginzburg-Landau Theory</b>	<b>3</b>
2.1 Global Conditions and Unknowns . . . . .	3
2.2 Expressions for Energy Density . . . . .	4
2.3 Integrability Conditions for $u$ and $\mathbf{A}$ . . . . .	5
2.4 The General GL Model . . . . .	7
2.5 The Global Gauge Equivalence Relation . . . . .	9
2.6 The Disk $D \subseteq \mathbb{R}^2$ and the Magnetic Field . . . . .	11
<b>Chapter 3 Variational Formalism and the Linear Problem</b>	<b>14</b>
3.1 The <i>Regular Elliptic Problem</i> . . . . .	15
3.2 Trace on $\Gamma$ and a Green's Formula . . . . .	17
3.3 Equivalence of the Variational Problem . . . . .	19
3.4 The Eigenspace of $\mathcal{L}$ as a Basis for $L^2(D)$ . . . . .	22
3.5 The Eigenfunctions and Spectrum of $\mathcal{L}$ . . . . .	24
<b>Chapter 4 Newton's Method and GNGA</b>	<b>31</b>
4.1 The Newton Map and $J''(u)(v, w)$ . . . . .	32
4.2 Newton's Method in $\mathbb{R}^{2N}$ . . . . .	33
4.3 Numerical Integration on $D$ . . . . .	36
4.4 A Newton Map for Branch Following . . . . .	38
4.5 Computational Rules for Newton's Method . . . . .	40
4.6 A Generalized Algorithm and GNGA . . . . .	43

<b>Chapter 5</b>	<b>Equivalence, Equivariance and Invariance in <math>G^{2N}</math></b>	<b>46</b>
5.1	Notations for $G^{2N}$ Expansions . . . . .	46
5.2	The Energy Functional on Galerkin Space . . . . .	48
5.3	$J$ -Equivalence and the Group $\mathbb{T}^2$ . . . . .	48
5.4	$\mathbb{T}^2$ -Equivariance and Invariances of $\mathcal{N}$ . . . . .	52
5.5	The “Conjugate-Reflection” Action $C$ . . . . .	59
<b>Chapter 6</b>	<b>Solution Branch Estimation and Analysis</b>	<b>61</b>
6.1	Bifurcations from the Trivial Branch . . . . .	63
6.2	Bifurcations from the Primary Branches . . . . .	68
6.3	Bifurcations from the Secondary Branches . . . . .	79
<b>Chapter 7</b>	<b>Problem Extensions and Conclusions</b>	<b>91</b>
	<b>Bibliography</b>	<b>96</b>

# List of Figures

3.1	Estimated values for $n_{ L ,j}$ when $r_o = 4$ . . . . .	27
3.2	Eigenfunction squared modulus and phase plots. . . . .	29
6.1	Bifurcations from the trivial solution corresponding to the largest nine eigenvalues of $\mathcal{L}$ . . . . .	65
6.2	Squared modulus and phase plots for two primary solution examples. . . . .	67
6.3	Secondary branches bifurcating from the $(L, j) = (-9, 1)$ primary branch. . . . .	75
6.4	Squared modulus and phase plots for signature 0 secondary solution examples. . . . .	77
6.5	$J$ -Equivalent secondary solution estimates that are not related by a $\mathbb{T}^2$ action. . . . .	78
6.6	Secondary solution estimates similar to the two types of tertiary branch base solutions, near the minimum of the $(L, j) = (-12, 1)$ , $n = 12$ secondary branch. . . . .	85
6.7	Squared modulus plots for selected low signature tertiary solution estimates originating from the $(L, j) = (-12, 1)$ , $n = 12$ secondary branch. . . . .	87
6.8	Squared modulus plots for selected tertiary solution estimates originating from two different character 1 bifurcations of the $(L, j) = (-12, 1)$ , $n = 12$ secondary branch. . . . .	88
6.9	Squared modulus and phase plots for tertiary estimates originating from a secondary character 1 bifurcation estimate. Two approximately $J$ -Equivalent estimates are clearly not $\mathbb{T}^2$ -Equivalent. . . . .	89

# List of Tables

6.1	Signature 0 parameter and energy ranges for several secondary branch estimates. . . . .	76
6.2	Initial guess rules used to estimate two types of tertiary branches beginning from a character 2 secondary bifurcation estimate. .	84
6.3	Branch information for selected tertiary solution estimates originating from the $(L, j) = (-12, 1)$ , $n = 12$ secondary branch.	86

# Chapter 1

## Introduction

In this research, numerical solutions to the specific Ginzburg-Landau (GL) boundary value problem

$$\begin{aligned}(-i\nabla + \mathbf{A})^2 u + au + |u|^2 u &= 0 \text{ in } D \\ \frac{\partial u}{\partial r} &= 0 \text{ on } \partial D\end{aligned}\tag{1.1}$$

are estimated in a cylindrical coordinate system. The complex valued order parameter  $u$  is an unknown, the vector valued magnetic potential is  $\mathbf{A} = -r\hat{\theta}$ , and  $D \subset \mathbb{R}^2$  is an open disk centered at the origin. The problem (1.1) is a special case of the well-studied steady state GL boundary value problem, and arises when considering reasonable physical conditions and superconducting samples whose height-to-width ratio is sufficiently small [3]. The bounded, negative bifurcation parameter  $a$  models the effect of decreasing sample temperature.

To produce solution estimates, a version of the Gradient-Newton-Galerkin-Algorithm (GNGA) (see [17], [18]) is applied to finite-dimensional Galerkin expansions in the space  $L^2(D)$  for both the Euler-Lagrange equation in (1.1) and the unknown variable  $u$ . These Galerkin expansions are formed by linear combinations of appropriately selected sequences of eigenfunctions for the *realization* of Schrödinger differential operator  $(-i\nabla + \mathbf{A})^2$  on the expected solution space. Using a well selected initial guess, the iteration produces an expansion for a solution estimate  $\tilde{u}$  whose Euler-Lagrange derivative has an expansion that is arbitrarily small in  $L^2(D)$  norm.

A C++ program and several Perl and Mathematica scripts were written to execute the GNGA algorithm and produce solution branch estimates beginning at arbitrary points of bifurcation. The execution of these scripts is substantially automated, and rules used to decrease the number of computations performed based upon the characteristics of the current solution are built in. It is well established that nontrivial solutions to (1.1) are always degenerate; nevertheless a least squares linear system solver from the LAPACK routine library provides the needed computations for the numerical algorithm in all situations.

After applying the GL theory in the geometric context imposed by  $D$ , a variational approach is used to recover the PDE problem in Equation (1.1). The nontrivial solutions to the problem are never unique, therefore equivalence relations are used to distinguish between classes of estimates exhibiting different properties. The study of such relations is instrumental to the understanding of the different bifurcation phenomena that are observed.

There are many ways to extend this study, and there are specific questions that remain. Several variations to the solution-generating code are possible that might improve the level of automation or computational efficiency. Extensions to the problem itself might include applying the GL model in three dimensions, or modifying this model to account for more realistic material properties or high temperature effects. The use of a similar numerical method in these contexts introduces new mathematical challenges, although the additional insight provided over a more traditional approach may justify these efforts. Such possibilities are discussed separately in the concluding chapter.

# Chapter 2

## Ginzburg-Landau Theory

Mathematical approximations to (1.1) have context in the physics of superconductivity provided by the well known theory of Ginzburg and Landau, first presented in 1950 [15]. A complete theoretical development describing the relationship between the phenomenon of superconductivity, the GL model, and the system of equations (1.1) is beyond the scope of this study. However, a general connection is readily obtained, and illustrates the motivation of the work. Along the way, requisite conditions for the simplifying steps taken when obtaining the PDE problem from the general GL theory are specified. Most of these maneuvers are well-established in the current literature, but of course others deserve a more careful treatment. Examples of both situations are discussed briefly.

### 2.1 Global Conditions and Unknowns

The order parameter  $u$  is the unknown of interest throughout this work. In the GL model,  $|u|^2$  represents the density of superconducting electron pairs inside a given sample occupying some open domain  $\Omega \subseteq \mathbb{R}^3$ , with boundary  $\Gamma \subseteq \mathbb{R}^3$ . Always it is assumed that  $u$  is identically zero at all points outside of  $\bar{\Omega} = \Omega \cup \Gamma$ , and therefore  $u$  is often regarded as a function defined on subsets of  $\bar{\Omega}$ . Little generality is sacrificed when requiring the standard conditions that  $\Omega$  is a bounded set with the cone property; indeed the vast majority of sample geometries one might consider enjoy such properties.

The magnetic vector potential  $\mathbf{A} : \mathbb{R}^3 \rightarrow \mathbb{R}^3$  is generally an unknown quantity that satisfies the equation  $\nabla \times \mathbf{A} = \mu \mathbf{h}$ , where  $\mathbf{h} : \mathbb{R}^3 \rightarrow \mathbb{R}^3$  is

the magnetic field. In striving to preserve a general perspective, the applied magnetic field  $\mathbf{h}_o$  should only be required to be a measurable function in  $\mathbb{R}^3$  that is bounded pointwise on  $\Omega$ . The remaining parameters incorporated into the model are either taken to be physical constants, or material parameters with dependence on temperature. For the problem specific to this research, the corresponding adaptation of the GL model will provide insight into the response of a specific type of superconducting system to decreasing temperature.

## 2.2 Expressions for Energy Density

The form of the GL energy functional considered is obtained from the Gibbs free energy density  $g$  of a superconducting system in the presence of an applied magnetic field  $\mathbf{h}_o$ . This is expressed as

$$g = f_n + a|u|^2 + \frac{b}{2}|u|^4 + \frac{1}{2m}|(-i\hbar\nabla - 2e\mathbf{A})u|^2 + \frac{\mu}{2}\mathbf{h} \cdot (\mathbf{h} - 2\mathbf{h}_o), \quad (2.1)$$

where  $f_n$  is the constant free energy density in the normal (non-superconducting) state,  $a, b \in \mathbb{R}$  with  $b > 0$  are real valued material parameters with temperature dependence,  $m$  is taken to be twice the free electron mass,  $\hbar$  is Planck's constant,  $e$  is the (negative) electron charge and  $\mu$  is the material magnetic permeability. At this stage, the following global physical conditions are imposed on the system:

1. The applied magnetic field  $\mathbf{h}_o$  is spatially and dynamically constant.
2. The parameters  $a$  and  $b$  are spatially fixed for a given temperature.
3. The superconducting sample (occupying  $\Omega$ ) is surrounded by a non-magnetic, non-conducting material.
4. The sample is magnetically homogeneous and isotropic, so that  $\mu$  is a spatially constant scalar.
5. The sample is nonmagnetic (perhaps diamagnetic or paramagnetic).

These conditions numerically fix the quantity  $\frac{\mu}{2}\mathbf{h}_o \cdot \mathbf{h}_o$ , hence the energy density expression given by

$$f = \frac{\mu}{2}\mathbf{h}_o \cdot \mathbf{h}_o - f_n + g = a|u|^2 + \frac{b}{2}|u|^4 + \frac{1}{2m}|(-i\hbar\nabla - 2e\mathbf{A})u|^2 + \frac{\mu}{2}|\mathbf{h} - \mathbf{h}_o|^2 \quad (2.2)$$

may equivalently be considered. It is noted here that for a given sample temperature, all of the parameters (except  $u$ ,  $\mathbf{A}$  and  $\mathbf{h}$ ) in (2.2) are scalars.

## 2.3 Integrability Conditions for $u$ and $\mathbf{A}$

To recover the energy functional from the density expression (2.2), Lebesgue integrability for each of the four terms is required. In the standard way, let  $x = (x_1, x_2, \dots, x_N)$  denote a point in  $\mathbb{R}^N$ ; this notation is also used to denote vector valued maps in the same space. For any multi-index  $\alpha$ , let  $D^\alpha$  denote the product operator formed from the elementary partial derivative operators  $D_j = \partial/\partial x_j$  (see [4]). In defining  $u$  only on  $\Omega$ , the integrability of the first three terms of  $f$  is only required on  $\Omega$ . Thus, the familiar vector spaces of functions  $L^2(\Omega)$  and  $W^{1,2}(\Omega)$  given by

$$L^p(\Omega) \doteq \{f : \Omega \rightarrow \mathbb{C} \mid \int_{\Omega} |f(x)|^p dx < \infty\}$$

and

$$W^{m,p}(\Omega) \doteq \{f \in L^p(\Omega) \mid D^m f \in L^p(\Omega)\}$$

are used. When  $p = 2$ , for notational convenience the space  $W^{m,p}(\Omega)$  is written as  $H^m(\Omega)$ . Also, when  $m = 0$ , the simplification  $W^{0,2}(\Omega) = H^0(\Omega) = L^2(\Omega)$  is often useful. Results obtained from the well known Sobolev Imbedding and Hölder theorems, which are only stated here, are needed.

**Theorem 2.3.1** (*Sobolev Imbedding*) *Let  $m \geq 0$  be an integer and let  $p$  satisfy  $1 \leq p < \infty$ . Then, there exists the imbedding  $W^{m,p}(\Omega) \rightarrow L^q(\Omega)$  for  $p \leq q \leq Np/(N - mp)$ .*

**Theorem 2.3.2** (*Hölder*) *If  $f, g \in L^2(\Omega)$ , then  $fg \in L^1(\Omega)$ .*

The proofs for Theorems 2.3.1 and 2.3.2 are available in [1]. A straightforward extension of the Hölder theorem is next shown.

**Proposition 2.3.3** *If  $f, g \in L^4(\Omega)$ , then  $fg \in L^2(\Omega)$ .*

*Proof:* Let  $f, g \in L^4(\Omega)$ , so that  $\int_{\Omega} |f|^4 dx < \infty$  and  $\int_{\Omega} |g|^4 dx < \infty$ . Thus  $|f|^2, |g|^2 \in L^2(\Omega)$ , and by the Hölder theorem (Theorem 2.3.2)  $|f|^2|g|^2 \in L^1(\Omega)$ . But  $|f|^2|g|^2 = (|f||g|)^2 = |fg|^2$  and thus  $\int_{\Omega} |fg|^2 dx < \infty$ , whence  $fg \in L^2(\Omega)$ .  $\square$

Next, for  $N = 3$ , sufficient conditions for the integrability of the first three terms of (2.2) are provided.

**Proposition 2.3.4** *If  $u \in H^1(\Omega)$  and  $A_j|_{\Omega} \in H^1(\Omega)$  for  $j = 1, 2, 3$ , then*

$$\int_{\Omega} \left| a|u|^2 + \frac{b}{2}|u|^4 + \frac{1}{2m} |(-i\hbar\nabla - 2e\mathbf{A})u|^2 \right| dx < \infty,$$

hence  $(a|u|^2 + \frac{b}{2}|u|^4 + \frac{1}{2m}|(-i\hbar\nabla - 2e\mathbf{A})u|^2)$  is integrable on  $\Omega$  for  $a \in \mathbf{R}$  and  $b \in (0, \infty)$ .

*Proof:* General properties for integrable functions are used in the proof. For convenience, each restriction  $A_j|_{\Omega}$  is denoted simply by  $A_j$ . Let  $a \in \mathbf{R}$ , and  $b \in (0, \infty)$ . It is clear that  $\int_{\Omega} |a||u|^2 dx < \infty$ , since  $u \in H^1(\Omega) \subseteq L^2(\Omega)$  by definition. The imbedding result from Theorem 2.3.1 implies that  $u \in H^1(\Omega) \subseteq L^k(\Omega)$  for  $2 \leq k \leq 6$ , and thus  $u \in L^4(\Omega)$ , so that  $\int_{\Omega} \frac{b}{2}|u|^4 dx < \infty$  as well. Expanding the modulus of the last term gives

$$\begin{aligned} & \left| \frac{1}{2m} |(-i\hbar\nabla - 2e\mathbf{A})u|^2 \right| = \left| \frac{1}{2m} (-i\hbar\nabla u - 2e\mathbf{A}u) \cdot (i\hbar\nabla\bar{u} - 2e\mathbf{A}\bar{u}) \right| \\ &= \frac{1}{2m} |\hbar^2(\nabla u \cdot \nabla\bar{u}) + i2e\hbar(\nabla u \cdot \mathbf{A}\bar{u}) - i2e\hbar(\mathbf{A}u \cdot \nabla\bar{u}) + 4e^2(\mathbf{A}u \cdot \mathbf{A}\bar{u})| \\ &\leq \frac{\hbar^2}{2m} |\nabla u|^2 + \frac{|e|\hbar}{m} |\nabla u \cdot \mathbf{A}\bar{u}| + \frac{|e|\hbar}{m} |\mathbf{A}u \cdot \nabla\bar{u}| + \frac{2e^2}{m} |\mathbf{A}u|^2 \end{aligned}$$

where

$$\begin{aligned} |\nabla u|^2 &= |(D_1u, D_2u, D_3u)|^2 = \sum_{i=1}^3 |D_iu|^2 \\ |\nabla u \cdot \mathbf{A}\bar{u}| &\leq \sum_{i=1}^3 |(D_iu)A_i\bar{u}| \\ |\mathbf{A}u \cdot \nabla\bar{u}| &\leq \sum_{i=1}^3 |A_iu(D_i\bar{u})| \end{aligned}$$

and

$$|\mathbf{A}u|^2 = |(A_1u, A_2u, A_3u)|^2 = \sum_{i=1}^3 |A_iu|^2.$$

For each  $i$ ,  $|D_i u| \in L^2(\Omega)$  and it follows that  $|\nabla u| \in L^2(\Omega)$  and  $\int_{\Omega} (\frac{\hbar^2}{2m} |\nabla u|^2) dx$  is finite. Also, by Theorem 2.3.1,  $A_i, u, \bar{u} \in L^4(\Omega)$  so that  $A_i u, A_i \bar{u} \in L^2(\Omega)$  and also  $(D_i u) A_i \bar{u}, A_i u (D_i \bar{u}) \in L(\Omega)$ . The last three expressions above then imply that  $\int_{\Omega} (\frac{|e|\hbar}{m} |\nabla u \cdot \mathbf{A} \bar{u}|) dx$ ,  $\int_{\Omega} (\frac{|e|\hbar}{m} |\mathbf{A} u \cdot \nabla \bar{u}|) dx$ , and  $\int_{\Omega} (\frac{2e^2}{m} |\mathbf{A} u|^2) dx$  are all finite. The result follows by the triangle inequality; the modulus expression in the original integral is less than or equal to the positive, integrable function  $|a||u|^2 + \frac{b}{2}|u|^4 + |\frac{1}{2m}|(-i\hbar\nabla - 2e\mathbf{A})u|^2|$  on  $\Omega$ .  $\square$

Since  $\mathbf{A}$  is defined on  $\mathbb{R}^3$ , conditions for the integrability of the fourth term are somewhat less specific. A sufficiently strong condition is that

$$|\nabla \times \mathbf{A} - \mu \mathbf{h}_{\mathbf{o}}| \rightarrow 0 \quad \text{as} \quad |x| \rightarrow \infty \quad \text{“sufficiently fast”,} \quad (2.3)$$

so as to guarantee that  $(\nabla \times \mathbf{A} - \mu \mathbf{h}_{\mathbf{o}})_j \in L^2(\mathbb{R}^3)$  for  $j = 1, 2, 3$ . Certainly it is natural to expect that any induction effects should deteriorate reasonably quickly as distance from the superconducting sample increases [6]. Thus,  $\mathbf{A}$  should be an element of

$$\tilde{\mathbf{H}}^1(\Omega) \doteq \{\mathbf{A} : \mathbb{R}^3 \rightarrow \mathbb{R}^3 \mid A_j \in H^1(\Omega) \text{ and } (\nabla \times \mathbf{A} - \mu \mathbf{h}_{\mathbf{o}})_j \in L^2(\mathbb{R}^3)\}.$$

Therefore, for various allowable applied fields  $\mathbf{h}_{\mathbf{o}}$ , there are vector functions whose components are elements of  $H^1(\Omega)$  that are excluded from the domain of the energy density  $f$  in (2.2). In the literature, the condition that  $\nabla \times \mathbf{A} = \mu \mathbf{h}_{\mathbf{o}}$  ( $\mathbf{h} = \mathbf{h}_{\mathbf{o}}$ ) outside  $\bar{\Omega}$  is often supposed, in which case the simplification

$$\tilde{\mathbf{H}}^1(\Omega) = \{\mathbf{A} : \mathbb{R}^3 \rightarrow \mathbb{R}^3 \mid A_j \in H^1(\Omega)\} \doteq \mathbf{H}^1(\Omega)$$

is apparent [8]. Authors often let  $\mathbf{h}_{\mathbf{o}} \in L^2(\Omega)$ , but when considering samples for which the applied field is apparently constant, this may not be desirable. Of course many other perspectives are available; here an attempt to preserve maximum generality while establishing the integrability of  $f$  has been made. For this numerical study, standard approximations used to obtain the problem (1.1) will allow the above mentioned result that  $\tilde{\mathbf{H}}^1(\Omega) = \mathbf{H}^1(\Omega)$ .

## 2.4 The General GL Model

Having suitably defined integrability conditions for the energy density  $f$ , the real valued energy functional  $\mathcal{E} : H^1(\Omega) \times \tilde{\mathbf{H}}^1(\Omega) \rightarrow \mathbb{R}$  is defined as

$$\mathcal{E}(u, \mathbf{A}) = \int_{\Omega} a|u|^2 + \frac{b}{2}|u|^4 + \frac{1}{2m}|(-i\hbar\nabla - 2e\mathbf{A})u|^2 d\Omega + \int_{\mathbb{R}^3} \frac{\mu}{2} |\mathbf{h} - \mathbf{h}_{\mathbf{o}}|^2 d\mathbb{R}^3, \quad (2.4)$$

where additionally  $\nabla \times \mathbf{A} = \mu \mathbf{h}$  is assumed. In order to obtain a nondimensionalized form of  $\mathcal{E}$ , the mappings

$$\begin{aligned} \mathbf{A} &\rightarrow -\frac{\hbar\sqrt{\gamma}}{2e} \tilde{\mathbf{A}}, & u &\rightarrow \frac{1}{2e}\sqrt{\frac{m\gamma}{\mu}} \tilde{u}, \\ a &\rightarrow \frac{\hbar^2\gamma}{2m} \tilde{a}, & b &\rightarrow \frac{2\hbar^2\mu e^2}{m^2} \tilde{b}, \\ r &\rightarrow \tilde{r}/\sqrt{\gamma}, & \mathbf{h} &\rightarrow -\frac{\hbar\gamma}{2e\mu} \tilde{\mathbf{h}} \quad \text{and} \quad \mathbf{h}_o \rightarrow -\frac{\hbar\gamma}{2e\mu} \tilde{\mathbf{h}}_o \end{aligned} \quad (2.5)$$

are defined, where  $\gamma = \frac{e\mu\mathbf{h}_o}{\hbar}$ . Thus, the nondimensionalized functional

$$\mathcal{E}(u, \mathbf{A}) = \int_{\Omega} a|u|^2 + \frac{b}{2}|u|^4 + |(-i\nabla + \mathbf{A})u|^2 d\Omega + \int_{\mathbb{R}^3} |\nabla \times \mathbf{A} - \mathbf{h}_o|^2 d\mathbb{R}^3 \quad (2.6)$$

is obtained, after suppressing the “ $\sim$ ” notation. By using the mappings (2.5), the scaling factors have no temperature dependence. Therefore, a good indication of how the unknowns vary with temperature is provided when variations in the material parameters  $a$  and  $b$  in (2.6) are considered.

To apply the calculus of variations, the variables  $u$  and  $\mathbf{A}$  are assumed in the literature to be “sufficiently smooth,” so as to allow the integration of the functional derivative by parts. A derivative is taken separately with respect to each variable. The result is the Euler-Langrange system

$$\begin{aligned} (-i\nabla + \mathbf{A})^2 u + au + b|u|^2 u &= 0 \quad \text{on } \Omega \\ \nabla \times \nabla \times \mathbf{A} &= \frac{i}{2}(u^* \nabla u - u \nabla u^*) - |u|^2 \mathbf{A} \quad \text{on } \Omega \\ (-i\nabla + \mathbf{A})u \cdot \hat{n} &= 0 \quad \text{on } \Gamma, \end{aligned} \quad (2.7)$$

where  $\hat{n}$  denotes the outward unit vector normal to the boundary  $\Gamma$ . Reference [8] includes a proof asserting the existence of a “global minimizer” for  $\mathcal{E}$ . In the next chapter, the existence of critical points for the specific adaptation of the GL model used in this research will be discussed.

It is necessary here to require at least two additional conditions for the domain  $\Omega$ . First,  $\Omega$  should everywhere lie on only one side of its boundary; this is true whenever any one of several regularity conditions (additional to the cone condition) is imposed [1]. Secondly, the unit vector  $\hat{n}$  must be well-defined at each boundary point. To recover this property, one generally specifies that there exists some  $\mathbb{R}^2 \rightarrow \mathbb{R}^3$  parameterization of  $\Gamma$  whose components are differentiable. The boundary condition in Equation (2.7) is required whenever  $\Omega$  is surrounded by a non-conducting material (see [3], [15]). The details regarding these calculations as they pertain to the PDE problem in (1.1) are provided in the next chapter.

## 2.5 The Global Gauge Equivalence Relation

The fact that solution space is partitioned by gauge equivalence classes is built in to the GL model. Gauge equivalence has far-reaching implications for the adaptation of the global model to that used in this research. Several known results are discussed as they will apply to the simplified model on  $D$  in two dimensions.

**Definition 2.5.1** *The elements  $(u, \mathbf{A}), (v, \mathbf{B}) \in H^1(\Omega) \times \tilde{\mathbf{H}}^1(\Omega)$  are **gauge equivalent** if there is a real function  $\phi \in H^2(\Omega)$  such that  $v = ue^{i\phi}$  and  $\mathbf{B} = \mathbf{A} - \nabla\phi$ .*

It is clear that gauge equivalence induces a linear transformation in  $H^1(\Omega) \times \tilde{\mathbf{H}}^1(\Omega)$ , and defines an equivalence relation on the same space. The next result is well known; the proof follows from that provided in [8], and the containment  $\tilde{\mathbf{H}}^1(\Omega) \subseteq \mathbf{H}^1(\Omega)$ .

**Lemma 2.5.2** *Every  $(u, \mathbf{A}) \in H^1(\Omega) \times \tilde{\mathbf{H}}^1(\Omega)$  is gauge equivalent to some  $(v, \mathbf{B}) \in H^1(\Omega) \times \tilde{\mathbf{H}}^1(\Omega)$  such that  $\nabla \cdot \mathbf{B} = 0$  and  $\mathbf{B} \cdot \hat{n} = 0$  on  $\Gamma$ .*

Next, a particularly important property (only stated in [8]) regarding gauge equivalence is established.

**Lemma 2.5.3** *Let  $C$  be a gauge equivalence class in  $H^1(\Omega) \times \tilde{\mathbf{H}}^1(\Omega)$ . Then, there is a unique function  $\mathbf{B} \in \tilde{\mathbf{H}}^1(\Omega)$  satisfying  $\nabla \cdot \mathbf{B} = 0$  and  $\mathbf{B} \cdot \hat{n} = 0$  on  $\Gamma$  such that  $(v, \mathbf{B}) \in C$  for some  $v \in H^1(\Omega)$ . Moreover, for any  $(u, \mathbf{B}) \in C$  it follows that  $u = ve^{ic}$  for some  $c \in [0, 2\pi)$ .*

*Proof:* Let  $(u, \mathbf{A}) \in C$ . The existence of  $(v, \mathbf{B}) \in C$  such that  $\mathbf{B}$  is solenoidal and has no normal component on  $\Gamma$  is provided by Lemma 2.5.2. The property of uniqueness must be shown. Suppose  $\mathbf{A} \neq \mathbf{B}$ , and choose a real function  $\phi \in H^2(\Omega)$  such that  $\nabla\phi \neq 0$ . If  $\nabla\phi$  is constant, then because of the regularity of  $\Omega$  there is  $\gamma \in \Gamma$  for which  $\nabla\phi(\gamma) \cdot \hat{n} \neq 0$ . Since  $\mathbf{A}(\gamma) \cdot \hat{n} = \mathbf{B}(\gamma) \cdot \hat{n} + \nabla\phi(\gamma) \cdot \hat{n} = \nabla\phi(\gamma) \cdot \hat{n}$ , it follows that  $\mathbf{A} \cdot \hat{n} \neq 0$ . Otherwise  $\nabla\phi$  is not constant, and  $\Delta\phi$  is not the zero function. But then since  $\nabla \cdot \mathbf{A} = \nabla \cdot \mathbf{B} + \Delta\phi = \Delta\phi$ , it follows that  $\nabla \cdot \mathbf{A} \neq 0$ . This shows that any vector potential  $\mathbf{A}$  other than  $\mathbf{B}$  that is the second coordinate for some point in  $C$  is either not solenoidal, or has some nonzero component on  $\Gamma$ . Thus, the chosen  $\mathbf{B}$  is unique.

Next, considering  $(v, \mathbf{B}) \in C$  as above, pick any  $(u, \mathbf{B}) \in C$ . By gauge equivalence, let  $\phi \in H^2(\Omega)$  according to Definition 2.5.1. Then it must be that  $\nabla\phi = 0$  on  $\Omega$ , that is  $\phi$  is constant on  $\Omega$ . Thus  $u = ve^{i\phi}$  or  $v = ue^{i\phi}$ , and for some  $c \in [0, 2\pi)$  it follows that  $u = ve^{ic}$ .  $\square$

The gauge invariance of  $\mathcal{E}$  is of primary importance; it allows for both a simplified mathematical treatment as well as substantial insight into the nature of the model. To paraphrase Lemma 2.5.3, if  $(u, \mathbf{A})$  is a point in the product function space such that  $\nabla \cdot \mathbf{A} = 0$  and  $\mathbf{A} \cdot \hat{n} = 0$  on  $\Gamma$ , then the collection of all points formed by pairing with  $\mathbf{A}$  all complex functions whose phase is within a constant of  $u$  is contained in a single gauge equivalence class; this collection represents all points in the same equivalence class that have  $\mathbf{A}$  as a second coordinate. After the geometry of the problem is specified in the next section, this rule will be used to concisely describe the gauge equivalence class of a given point. Next, a well-known theorem is available that describes one of the most important properties of the functional  $\mathcal{E}$ . The proof is implied by a direct computation.

**Theorem 2.5.4** (*Gauge Invariance*) For all  $\phi \in H^2(\Omega)$  and  $(u, \mathbf{A}) \in H^1(\Omega) \times \tilde{\mathbf{H}}^1(\Omega)$ ,  $\mathcal{E}(u, \mathbf{A}) = \mathcal{E}(ue^{i\phi}, \mathbf{A} - \nabla\phi)$ .

*Proof:* Let  $\phi \in H^2(\Omega)$ ,  $(u, \mathbf{A}) \in H^1(\Omega) \times \tilde{\mathbf{H}}^1(\Omega)$ , and fix the parameters  $a \in \mathbb{R}$ ,  $b \in (0, \infty)$ . Clearly it follows that  $a|ue^{i\phi}|^2 = a|u|^2|e^{i\phi}|^2 = a|u|^2$ , and similarly that  $\frac{b}{2}|ue^{i\phi}|^4 = \frac{b}{2}|u|^4$ . Since  $\nabla \times (\mathbf{A} - \nabla\phi) = \nabla \times \mathbf{A} - \nabla \times (\nabla\phi) = \nabla \times \mathbf{A}$ , actually  $|\nabla \times (\mathbf{A} - \nabla\phi) - \mathbf{h}_o|^2 = |\nabla \times \mathbf{A} - \mathbf{h}_o|^2$ , and it remains to examine the third term. But, since

$$|(-i\nabla + \mathbf{A} - \nabla\phi)ue^{i\phi}| = |-i\nabla(ue^{i\phi}) + \mathbf{A}ue^{i\phi} - (\nabla\phi)ue^{i\phi}|$$

$$\begin{aligned}
&= |(-i\nabla u)e^{i\phi} - iu(ie^{i\phi}\nabla\phi) + \mathbf{A}ue^{i\phi} - (\nabla\phi)ue^{i\phi}| \\
&= |(-i\nabla u)e^{i\phi} + \mathbf{A}ue^{i\phi}| = |(-i\nabla + \mathbf{A})u|,
\end{aligned}$$

the result follows.  $\square$

After specifying the particular choice of  $\Omega$  and  $\mathbf{h}_0$  for the current problem in the next section, the implications of gauge invariance will be more apparent.

## 2.6 The Disk $D \subseteq \mathbb{R}^2$ and the Magnetic Field

With the goal of producing and studying mathematical solution estimates, the applied magnetic field  $\mathbf{h}_0$  and sample geometry is next specified. The application of the numerical method can then proceed after several assumptions and well-documented simplifications are made.

To realize a system of only a single parameter, the dependence of  $b$  on temperature is ignored, and the assignment  $b = 1$  is made in the dimensionless equations. As stated, this dependence is generally regarded as “weak;” with this assumption a good investigation of the nonlinearity in the first PDE from (2.7) is possible. The structure and evolution of solution estimates will be studied with respect to the remaining parameter  $a$ ; however, it should be noted that the scaling formalism provided in (2.5) allows for the specification of both  $a$  and  $b$  versus temperature, allowing one to regard the impact of temperature variation in more detail if needed.

Perhaps the most significant simplification imposed is the requirement that the sample be sufficiently “thin” in one dimension. In the Cartesian coordinate system, the boundary of  $\Omega$  is to be contained in the planes  $z = -t/2$  and  $z = t/2$ , where  $t$  denotes the sample thickness, and the sample itself is then contained in the intermediate region. As discussed in [3] and in other sources, if  $t$  is very small compared to the (London) penetration depth  $\lambda$ , variations in the vector potential  $\mathbf{A}$  are negligible. The parameter  $\lambda$  quantifies the penetration of  $\mathbf{h}_0$  into good conductors. For a thin sample immersed in an applied field, the estimate  $\mathbf{h} = \mathbf{h}_0$  on  $\mathbb{R}^3$  is reasonable. In nondimensional variables, the effect is to impose the equation  $\nabla \times \mathbf{A} = \mathbf{h}_0$  everywhere, and thus the last term in the energy functional equation (2.6) vanishes. Furthermore, dependence of the remaining quantity  $u$  in the  $z$ -direction is disregarded. The model is equivalently considered in only the

$xy$ -plane, since in this case it is clear that variations in energy density  $e$  must be identical in any plane intersecting  $\bar{\Omega}$  and normal to the  $z$ -axis.

A cylindrical system of coordinates with the standard unit vectors  $\hat{r}$ ,  $\hat{\theta}$ , and  $\hat{z}$  is adopted. Hence, the sample domain is formally specified as follows:

$$\Omega = \{(r, \theta, z) \in \mathbb{R}^3 \mid r < r_o \text{ and } -t/2 < z < t/2\}. \quad (2.8)$$

As discussed, solutions to the problem will actually be estimated on the plane disk  $D$  in  $\mathbb{R}^2$  and its boundary. The former is given by

$$D = \{(r, \theta) \in \mathbb{R}^2 \mid r < r_o\}, \quad (2.9)$$

where the constant  $r_o$  may vary from one estimation to the next. Next, the assignment  $\mathbf{h}_o = h_o \hat{z}$  is imposed, so that the applied magnetic field is normally applied to  $D$ .

In dimensionless quantities, a vector potential function satisfying  $\nabla \times \mathbf{A} = \mathbf{h}_o$  everywhere must next be chosen. As previously noted, a function that is both solenoidal and without a normal component on  $\Gamma$  allows for the convenient identification of gauge equivalence classes. According to the analysis of the linearized problem resulting from the above simplifications, the dimensionless magnetic field is  $\mathbf{h}_o = -2\hat{z}$ , whence  $\mathbf{A} = -r\hat{\theta}$  is the unique choice. Neglecting variations in the vector potential  $\mathbf{A}$  in the system (2.7), the reduced system (1.1) in  $D$  with the single unknown  $u$  is obtained. This motivates the definition of the spaces

$$L^p(D) \doteq \left\{ f : D \rightarrow \mathbb{C} \mid \int_D |f|^2 dx < \infty \right\},$$

$$H_B^{m,p}(D) \doteq \left\{ f \in L^p(D) \mid D^m f \in L^p(D) \text{ and } \frac{\partial f}{\partial r}(r_o) = 0 \right\},$$

and the functional  $J : H_B^1(D) \rightarrow \mathbb{R}$  as

$$J(u) = \int_D a|u|^2 + \frac{1}{2}|u|^4 + |(i\nabla + r\hat{\theta})u|^2 dx, \quad (2.10)$$

where  $B$  indicates the Neumann boundary condition. In chapter 3, the variational calculus necessary to obtain the system (1.1) from  $J$  is demonstrated. Unless otherwise stated, all subsequent discussions and results should be understood in the context of the selections of geometry, magnetic field and vector potential made in this section.

The analysis is more specific in the next chapter. The differential operator in the PDE problem (1.1) is a special case of the linear Schrödinger operator with magnetic vector potential. Although its properties are well understood, the estimation method chosen requires further theoretical considerations. Next, the variational approach is discussed in more detail, and the solutions of the linearized problem are introduced. It is this collection that spans the Galerkin spaces that contain the estimates needed for the numerical algorithms.

## Chapter 3

# Variational Formalism and the Linear Problem

The strength of a variational approach is that one expects a correspondence between the critical points of a given energy functional, and the zeros (or solutions) of its associated PDE. When approaching this desirable result, at least two obvious questions arise. Firstly, do solutions always exist for given parameter values, and if so do they enjoy any other properties such as continuity or differentiability? Secondly, there are natural concerns regarding how the elements of solution space may be related to one another, with respect to their energy. For the problem considered here, the last statement corresponds to the question of uniqueness.

Thus, the correspondence between the physical model applied on  $D$  and the numerical method requires an equivalence of the *critical points* for  $J$  in Equation (2.10), and the *solutions* for the specific boundary value problem given in Equation (1.1). To establish this, a theoretical framework is developed. Only those proofs for the most important results are detailed.

In the following sections, it is convenient to denote the Schrödinger operator  $(i\nabla + r\hat{\theta})^2$  by  $\mathcal{L}$ , and the boundary operator  $\partial/\partial r$  by  $B$ . Of primary interest are the properties of  $\mathcal{L}$  as an elliptic differential operator on the spaces  $H^2(D)$ ,  $H_B^2(D)$  and the well-known spaces

$$C^m(D) \doteq \{f : D \rightarrow \mathbb{C} \mid D^\alpha f \text{ is continuous on } D \text{ for each } |\alpha| \leq m\},$$

$$C_0^m(D) \doteq \{f \in C^m(D) \mid f \text{ has compact support in } D\},$$

and

$$\mathcal{D}(D) \doteq \{f : D \rightarrow \mathbb{C} \mid f \in C_0^\infty(D)\},$$

where the latter has the standard locally convex topology rendering it complete. The space  $C_0^\infty(D)$  denotes the set of continuous functions  $f : D \rightarrow \mathbb{C}$  with compact support in  $D$ , and having continuous derivatives of arbitrary order. Also, the theory requires the use of the spaces

$$C(\overline{D}) \doteq \{f \in C(D) \mid f \text{ is bounded and uniformly continuous on } D\},$$

and

$$C^m(\overline{D}) \doteq \{f \in C^m(D) \mid D^\alpha f \in C(\overline{D}) \text{ for each } |\alpha| \leq m\}.$$

Perhaps most importantly, each  $f \in \mathcal{D}(D)$  has compact support in  $D$ . Thus, each such  $f$  is bounded and uniformly continuous on  $D$ , and vanishes on some neighborhood of each boundary point. The space  $\mathcal{D}(\overline{D})$  is defined by identifying each such  $f$  with its unique continuous extension to  $\overline{D}$  as

$$\mathcal{D}(\overline{D}) \doteq \{f : \overline{D} \rightarrow \mathbb{C} \mid f \in \mathcal{D}(D) \text{ and } f|_\Gamma = 0\}.$$

Much of the following formalism is a specific application of the work available in [1] and [16], among others, and is readily applied because  $D$  possesses many useful regularity properties. Clearly, the boundary  $\Gamma$  may be parameterized on  $\mathbb{R}$  by component functions that have derivatives of arbitrary order; that is,  $\Gamma$  is of class  $C^\infty$ . Also, it is clear that  $\overline{D}$  is a compact subset of  $\mathbb{R}^2$ . First, a basic classification of the PDE system is needed.

### 3.1 The *Regular Elliptic Problem*

The operators  $\mathcal{L}$  and  $B$  enjoy properties that will allow for an extremely useful classification of the PDE problem, thus making several important theoretical developments subsequently possible. The elliptic properties of  $\mathcal{L}$  are first needed, and for these it suffices to regard  $\mathcal{L}$  on  $\mathbb{R}^2$  and to examine its characteristic form. The operator may be written in rectangular coordinates as

$$\mathcal{L} = -\frac{\partial^2}{\partial x_1^2} - \frac{\partial^2}{\partial x_2^2} - i2x_2 \frac{\partial}{\partial x_1} + i2x_1 \frac{\partial}{\partial x_2} + x_1^2 + x_2^2, \quad (3.1)$$

and equivalently in the general form

$$\mathcal{L}u = \sum_{|p|, |q| \leq 1} (-1)^{|p|} D^p (a_{pq} D^q u), \quad (3.2)$$

in terms of the multi-indices  $p, q$ . The coordinate functions are given by

$$a_{(0,0),(0,0)} = x_1^2 + y_1^2, \quad a_{(0,0),(0,1)} = i2x_1, \quad a_{(0,0),(1,0)} = -i2x_2,$$

$$a_{(0,1),(0,1)} = 1 \quad \text{and} \quad a_{(1,0),(1,0)} = 1.$$

The *characteristic form* of  $\mathcal{L}$ , denoted by  $\mathcal{L}_0$ , is then

$$\mathcal{L}_0 = \sum_{|p|,|q|=1} -a_{pq}\zeta^{p+q} = (-1)(\zeta_1^2 + \zeta_2^2), \quad (3.3)$$

for  $\zeta = (\zeta_1, \zeta_2) \in \mathbb{R}^2$ . Since  $|\zeta|^2 = -\mathcal{L}_0$  for all  $\zeta \in \mathbb{R}^2$  and  $x \in \overline{\mathbb{D}}$ , it may be concluded that  $\mathcal{L}$  is *uniformly strongly elliptic* in  $\overline{\mathbb{D}}$ . Furthermore, note that the coefficients  $a_{pq}$  have derivatives of arbitrary order in  $\overline{\mathbb{D}}$ . Also, since

$$-\Delta u = \sum_{|p|,|q|=1} (-1)^{|p|} D^p(a_{pq}D^q u), \quad (3.4)$$

exactly the same computations apply when considering the operator  $-\Delta$ .

In a similar fashion, the boundary operator  $B$  is considered on  $\mathbb{R}^2$ . The following conclusions rely upon the fact that  $B$  maps to a function defined on the boundary  $\Gamma$ ; a more complete treatment of the operator is postponed until the next section. First,  $B$  is *normal* on  $\Gamma$ . The order of  $B$  is 1, and the characteristic form is constructed from the general definition

$$Bu = \sum_{|h|\leq 1} b_h D^h u. \quad (3.5)$$

In rectangular coordinates, the operator is written

$$B = \left( x_1 \frac{\partial}{\partial x_1} + x_2 \frac{\partial}{\partial x_2} \right) / r_o,$$

so that

$$b_{(0,0)} = 0, \quad b_{(0,1)} = x_2/r_o \quad \text{and} \quad b_{(1,0)} = x_1/r_o.$$

The characteristic form of  $B$  is therefore  $x_1\zeta_1/r_o + x_2\zeta_2/r_o$ . When  $\zeta \in \mathbb{R}^2 - \{\mathbf{0}\}$  is normal to  $\Gamma$  at  $x = (x_1, x_2)$ , it follows that  $\zeta = k(x_1, x_2)$  for some nonzero real number  $k$ , in which case the form is clearly nonzero. Thus  $B$  is *normal* on  $\Gamma$ , and furthermore each coefficient function  $b_h$  may be differentiated through

arbitrary order. Secondly,  $B$  should *cover* the operator  $\mathcal{L}$  with respect to  $\Gamma$ . The polynomial in the complex variable  $\tau$  given by

$$\sum_{|h|=1} b_h(\zeta + \tau\zeta')^h, \quad (3.6)$$

where  $\zeta \in \mathbb{R} - \{0\}$  is tangent to  $\Gamma$  at  $x$  and  $\zeta' \in \mathbb{R} - \{0\}$  is normal to  $\Gamma$  at  $x$ , is first formed. Now  $\zeta = k_1(-x_2, x_1)$  for nonzero  $k_1 \in \mathbb{R}$ , and  $\zeta' = k_2(x_1, x_2)$  for nonzero  $k_2 \in \mathbb{R}$ . The polynomial in equation (3.6) is therefore  $k_2\tau(x_1^2 + x_2^2)/r_o = k_2\tau$ , which is not the zero polynomial. Since the boundary system consists only of a single operator, this result is sufficient to conclude that  $B$  *covers* both  $\mathcal{L}$  and  $-\Delta$  on  $\Gamma$ .

The collection of the properties demonstrated regarding  $\mathcal{L}$  and  $B$  mean that the PDE system in (1.1) is a *regular elliptic problem*. These conditions are to be called upon when developing the theory presented in the following sections.

## 3.2 Trace on $\Gamma$ and a Green's Formula

Several intermediate theoretical and computational necessities are next demonstrated. First, the space in which numerical estimates are to be produced is considered more carefully. Since every function in  $H^2(D)$  has well-defined derivatives (perhaps in the sense of distributions) through order 2 in  $L^2(D)$ , it is natural to define the domain of the operator  $\mathcal{L}$  (and  $-\Delta$ ) within this space. Although it has been suggested that the results below hold equally well for all  $u \in H^1(D)$ , presently the functions  $u \in H^2(D)$  will be of primary interest; it is solutions in this space which are sought by estimation.

Now, the boundary operator  $B$  is defined explicitly by applying the trace theorem in the above mentioned Sobolev space. The proof of this theorem, available in [16], utilizes the result that  $\mathcal{D}(\overline{D})$  is dense in  $H^2(D)$ .

**Theorem 3.2.1** *The mapping  $u \mapsto (u, Bu)$  of  $\mathcal{D}(\overline{D}) \rightarrow (\mathcal{D}(\Gamma))^2$  extends by continuity to a continuous linear mapping of  $H^2(D) \rightarrow H^{3/2}(\Gamma) \times H^{1/2}(\Gamma)$ . This mapping is surjective, and there exists a continuous linear right inverse  $\mathcal{R} : H^{3/2}(\Gamma) \times H^{1/2}(\Gamma) \rightarrow H^2(D)$ ,  $(g_1, g_2) \mapsto \mathcal{R}(g_1, g_2)$  such that  $\mathcal{R}(g_1, g_2) = g_1$  and  $B\mathcal{R}(g_1, g_2) = g_2$ .*

This theorem clearly has far-reaching implications. For each  $u \in H^2(D)$ , the well-defined map  $u \mapsto (u, Bu)$  allows for the specification of both a value for

$u$  and a normal first partial derivative for  $u$  on  $\Gamma$ , a set on which  $u$  itself is not even formally defined. The existence of the right inverse function  $\mathcal{R}$  puts the space  $H^2(D)/H_0^2(D) = \{u + H_0^2(D) \mid u \in H^2(D)\}$  into a one-to-one correspondence with  $H^{3/2}(\Gamma) \times H^{1/2}(\Gamma)$ , where  $H_0^2(D)$  is exactly the kernel of the same mapping above. Therefore, the operator  $B$  is a well-defined mapping given by

$$B : H^2(D) \rightarrow H^{1/2}(\Gamma) , \quad u \mapsto Bu = \frac{\partial u}{\partial r}(r_o) \quad (3.7)$$

in the sense of Theorem 3.2.1. Next, an intermediate result available by the use of a Green's formula is computed.

Let  $\langle \cdot, \cdot \rangle_2$  denote the standard inner product on the Hilbert space  $L^2(D)$ . Only the first part of the following proposition is verified. The last statement follows because  $\mathcal{D}(\overline{D})$  is dense, and because the trace theorem above allows for well-defined integration on the boundary  $\Gamma$ .

**Proposition 3.2.2** *Let  $-\Delta$  be the Laplacian operator, and let  $(u, Bu)$  be the first order boundary system defined by the mapping in Theorem 3.2.1. Then, for all  $u, v \in \mathcal{D}(\overline{D})$ ,  $\langle \nabla u, \nabla v \rangle_2 = \langle -\Delta u, v \rangle_2$ . Moreover, this formula extends by continuity to all functions  $u, v \in H_B^2(D)$ .*

*Proof:* Let  $u, v \in \mathcal{D}(\overline{D})$ , and note that  $\frac{\partial u}{\partial r}(r_o) = \frac{\partial v}{\partial r}(r_o) = 0$ . Then

$$\begin{aligned} \langle -\Delta u, v \rangle_2 &= \int_D (-\Delta u) \overline{v} \, dx = \int_D - \left( \frac{1}{r} \frac{\partial u}{\partial r} + \frac{\partial^2 u}{\partial r^2} + \frac{1}{r^2} \frac{\partial^2 u}{\partial \theta^2} \right) \overline{v} \, dx \\ &= \int_0^{2\pi} \int_0^{r_o} - \left( \frac{1}{r} \frac{\partial u}{\partial r} + \frac{\partial^2 u}{\partial r^2} + \frac{1}{r^2} \frac{\partial^2 u}{\partial \theta^2} \right) \overline{v} \, r \, dr \, d\theta. \end{aligned}$$

Evaluating each term, note that

$$\int_D \left( -\frac{1}{r} \frac{\partial u}{\partial r} \right) \overline{v} \, dx = \int_0^{2\pi} \{ \overline{v}(0)u(0) - \overline{v}(r_o)u(r_o) \} \, d\theta + \int_0^{2\pi} \int_0^{r_o} u \frac{\partial \overline{v}}{\partial r} \, dr \, d\theta,$$

$$\int_D \left( -\frac{\partial^2 u}{\partial r^2} \right) \overline{v} \, dx = \int_0^{2\pi} \int_0^{r_o} \frac{\partial u}{\partial r} \overline{v} \, dr \, d\theta + \int_D \frac{\partial u}{\partial r} \frac{\partial \overline{v}}{\partial r} \, dx,$$

and

$$\int_D \left( -\frac{1}{r^2} \frac{\partial^2 u}{\partial \theta^2} \right) \overline{v} \, dx = \int_D \frac{1}{r^2} \frac{\partial u}{\partial \theta} \frac{\partial \overline{v}}{\partial \theta} \, dx.$$

But, after using the formula

$$\int_0^{2\pi} \int_0^{r_o} u \frac{\partial u}{\partial r} \bar{v} dr d\theta = - \left[ \int_0^{2\pi} \{ \bar{v}(0)u(0) - \bar{v}(r_o)u(r_o) \} d\theta + \int_0^{2\pi} \int_0^{r_o} u \frac{\partial \bar{v}}{\partial r} dr d\theta \right],$$

the result follows.  $\square$

A calculation shows that when replacing  $\mathcal{L}$  for  $-\Delta$  in Proposition 3.2.2, the formula

$$\int_D \left( -i u \frac{\partial \bar{v}}{\partial \theta} \right) dx = \int_D \left( i \frac{\partial u}{\partial \theta} \bar{v} \right) dx$$

is valid under the same assumptions. Thus, for all  $u, v \in H_B^2(D)$ ,

$$\langle (i\nabla + r\hat{\theta})u, (i\nabla + r\hat{\theta})v \rangle_2 = \langle (i\nabla + r\hat{\theta})^2 u, v \rangle_2. \quad (3.8)$$

The well-known Sobolev imbedding  $H^2(D) \rightarrow C(\bar{D})$  deserves mention along with these computational results; that is, the functions sought by the estimation method are equal a.e. to bounded, uniformly continuous functions on  $D$ . The tools needed to adapt a variational method to the problem are now in place.

### 3.3 Equivalence of the Variational Problem

A specific relationship between the PDE problem in (1.1) and the functional  $J$  is next formulated. At this stage the functional  $\langle \cdot, \cdot \rangle$ , given in terms of the standard  $L^2(D)$  inner product  $\langle \cdot, \cdot \rangle_2$ , is introduced.

**Lemma 3.3.1** *Let  $\langle \cdot, \cdot \rangle$  mapping  $(L^2(D))^2 \rightarrow \mathbb{R}$  be defined by  $(u, v) \mapsto \langle u, v \rangle = \langle u, v \rangle_2 + \langle v, u \rangle_2$ .*

- i. The relation  $\langle u, v \rangle_2 = (\langle u, v \rangle + i\langle u, iv \rangle)/2$  holds for all  $u, v \in L^2(D)$ .*
- ii. The norm induced by  $\langle \cdot, \cdot \rangle$  is equivalent to the standard norm  $\|u\|_2 = \langle u, u \rangle_2^{1/2} = \left( \int_D |u(x)|^2 dx \right)^{1/2}$  on  $L^2(D)$ .*
- iii.  $L^2(D)$  is a **real inner product space** with respect to the product  $\langle u, v \rangle$ .*

*Proof:* For (i.), let  $u, v \in L^2(D)$ . Using known definitions, one finds that

$$\langle u, v \rangle + i\langle u, iv \rangle = \langle u, v \rangle_2 + \langle v, u \rangle_2 + i(\langle u, iv \rangle_2 + \langle iv, u \rangle_2)$$

and

$$i(\langle u, iv \rangle_2 + \langle iv, u \rangle_2) = \langle u, v \rangle_2 - \langle v, u \rangle_2,$$

so that

$$\langle u, v \rangle + i\langle u, iv \rangle = 2\langle u, v \rangle_2.$$

For (ii.), the relation

$$\|u\|_2^2 = \langle u, u \rangle_2 = \frac{1}{2}(\langle u, u \rangle_2 + \langle u, u \rangle_2) = \langle u, u \rangle / 2$$

demonstrates the necessary equivalence. For result (iii.), let  $a, b \in \mathbb{R}$  and let  $w \in L^2(D)$ . Since  $\bar{a} = a$  and  $\bar{b} = b$ , it follows that

$$\begin{aligned} \langle au + bv, w \rangle &= \langle au + bv, w \rangle_2 + \langle w, au + bv \rangle_2 \\ &= a\langle u, w \rangle_2 + b\langle v, w \rangle_2 + a\langle w, u \rangle_2 + b\langle w, v \rangle_2 \\ &= a(\langle u, w \rangle_2 + \langle w, u \rangle_2) + b(\langle v, w \rangle_2 + \langle w, v \rangle_2) \end{aligned}$$

and thus

$$\langle au + bv, w \rangle = a\langle u, w \rangle + b\langle v, w \rangle.$$

□

It is this *real* inner product that will be most frequently used for the estimation method. Indeed, it is in terms of  $\langle \cdot, \cdot \rangle$  that the Euler-Lagrange derivative of  $J$  is specified.

**Proposition 3.3.2** *Let  $J : H_B^1(D) \rightarrow \mathbb{R}$  be given by (2.10), and let  $u \in H_B^2(D)$ . Then  $J$  is Gateaux differentiable at  $u$ , and the Gateau derivative of  $J$  at  $u$  is  $J'(u)(v) = \langle \mathcal{L}u + au + |u|^2u, v \rangle$ .*

*Proof:* According to the standard definition, it suffices to show that the limit of the difference quotient  $(J(u + tv) - J(u))/t$  exists in  $\mathbb{C}$  as  $t \rightarrow 0$ , whenever  $(u + tv)$  is an element of any given neighborhood of  $u$ . The imbedding and integrability results from Theorems 2.3.1 and 2.3.2 allow the use of the linearity properties of the integral. Thus, if  $U$  is any neighborhood of  $u \in H_B^2(D)$ , then for all  $v \in H_B^2(D)$  and  $t \in \mathbb{R}$  such that  $(u + tv) \in U$ , it follows that

$$\lim_{t \rightarrow 0} \frac{J(u + tv) - J(u)}{t} = \int_D \{a(u\bar{v} + \bar{u}v) + |u|^2u\bar{v} + |u|^2\bar{u}v\} dx$$

$$+ \int_D \left\{ (i\nabla + r\hat{\theta})u \cdot (-i\nabla + r\hat{\theta})\bar{v} + (-i\nabla + r\hat{\theta})\bar{u} \cdot (i\nabla + r\hat{\theta})v \right\} dx,$$

where the second term is recognized as

$$\langle (i\nabla + r\hat{\theta})u, (i\nabla + r\hat{\theta})v \rangle = \langle (i\nabla + r\hat{\theta})^2 u, v \rangle,$$

after extending the result obtained from Proposition 3.2.2, given in Equation (3.8), in the natural way. Similarly, the remaining terms may be expressed in terms of  $\langle \cdot, \cdot \rangle$  to obtain

$$J'(u)(v) = \langle au + |u|^2 u, v \rangle + \langle (i\nabla + r\hat{\theta})^2 u, v \rangle = \langle \mathcal{L}u + au + |u|^2 u, v \rangle,$$

as needed. Since by hypothesis  $u \in H_B^2(D)$ , it follows that  $\mathcal{L}u + au + |u|^2 u \in L^2(D)$ , whence the right side makes sense.  $\square$

Notice that  $J'(u)(v)$  is linear in  $v$ . Assuming that for all  $u \in H_B^2(D)$ , the mapping  $u \mapsto J'(u)(v)$  is continuous whenever  $v \in H_B^2(D)$  is fixed, then  $J$  is *Fréchet differentiable* on  $H_B^2(D)$ . The Fréchet derivative is denoted by  $DJ$ , and one writes  $J'(u)(v) = \langle DJ(u), v \rangle$ . *Critical points* of  $J$  are defined in the standard way; note that the following definition is specified for functions in the domain of  $J$  at which  $J$  is Fréchet differentiable.

**Definition 3.3.3** *Let  $J : H^1(D) \rightarrow \mathbb{R}$  be defined by (2.10). Then,  $u \in H^1(D)$  is called a **critical point** (of  $J$ ) if  $J$  is Fréchet differentiable at  $u$ , and  $J'(u)(v) = 0$  for all  $v \in H^1(D)$ .*

The term *solution* also applies to functions  $u$  from the domain of  $J$  for which  $DJ(u)$  is defined.

**Definition 3.3.4** *A function  $u \in H^1(D)$  at which  $J$  is Fréchet differentiable is called a **solution** if  $DJ(u) = 0$  a.e.*

These definitions lead naturally to the following important proposition:

**Proposition 3.3.5** *Let  $u \in H_B^2(D)$ . Then  $u$  is a critical point of  $J$  if and only if  $u$  is a solution to the PDE problem (1.1).*

*Proof:* This result is clear, by Proposition 3.3.2 and the condition  $u \in H_B^2(D)$ .  $\square$

An immediate result is the existence of such critical points for all parameter values  $a \in \mathbb{R}$ , since we always have the existence of the *trivial solution*  $u = 0$ .

Developments in the following section will allow for the expansion of functions  $u \in H_B^2(D)$  as infinite series that are equal a.e. to (and thus identified with)  $u$  on  $D$ . A complete orthonormal system is then specified, and used in the standard way to produce finite-dimensional approximations to arbitrary accuracy for the elements of  $L^2(D)$ .

### 3.4 The Eigenspace of $\mathcal{L}$ as a Basis for $L^2(D)$ .

The fact that the differential operator  $\mathcal{L}$  is naturally defined on the space  $H_B^2(D)$  yields many useful and well-documented results. These results are referenced next, and several extensions of particular importance are discussed.

Returning first to equations (3.1) and (3.2), it is easy to verify that the operator  $\mathcal{L}$  is equal to its *formal adjoint*  $\mathcal{L}^*$ , defined by

$$\mathcal{L}^*u = \sum_{|p|,|q|\leq 1} (-1)^{|p|} D^p(\overline{a_{qp}}D^q u). \quad (3.9)$$

As in [16], the *realization* of  $\mathcal{L}$  in  $L^2(D)$  is then defined by restricting the domain of  $\mathcal{L}$  to  $H_B^2(D)$ . Similarly, the realization of the operator  $\mathcal{L}^*$  is specified in terms of a corresponding formal adjoint boundary value problem. The regularity properties of  $D$  and those of the elliptic problem itself then allow the next theorem.

**Theorem 3.4.1** *The realization of  $\mathcal{L}^*$  is the adjoint of the realization of  $\mathcal{L}$ , in the sense of unbounded operators in  $L^2(D)$ .*

*Proof:* As detailed in [16], both operators are closed and densely defined in  $L^2(D)$ . After demonstrating that in fact their corresponding domains agree setwise, the result is implied.  $\square$

References to the operator  $\mathcal{L}$  are henceforward to be understood in the context of its  $L^2(D)$  realization on the domain  $H_B^2(D)$ , and  $\mathcal{L}$  is therefore said to be *self-adjoint*. Next, the properties of  $D$  imply that the imbedding

$$H^2(D) \rightarrow L^2(D)$$

is compact, and therefore there is an compact imbedding  $H_B^2(D) \rightarrow L^2(D)$  formed by the obvious restriction. Recall that the composition of a compact operator with a continuous operator (in either order) is compact, thus it

follows that  $\mathcal{L}$  is compact. These properties, along with the fact that  $H_B^2(D)$  is a Hilbert space, lead to the next theorem. This result, provided in [13], constitutes the foundation of the numerical estimation methods presented in the chapters that follow.

**Theorem 3.4.2** *There exists a complete orthonormal basis  $\{\psi_k\}$  of  $H_B^2(D)$  consisting of eigenfunctions of  $\mathcal{L}$ .*

Of course, the term *eigenfunction* is used when describing the members of the collection  $\{\psi_k\}$  to indicate the property that for each index  $k$ ,  $\psi_k$  satisfies

$$\mathcal{L}\psi_k = \lambda_k\psi_k$$

for some  $\lambda_k \in \mathbb{C}$ . The term *basis* is understood to mean that  $\{\psi_k\}$  is a maximal orthonormal set with respect to the standard inner product  $\langle \cdot, \cdot \rangle_{H^2}$  in  $H_B^2(D)$ . Further, an expansion  $\sum_{k=1}^{\infty} \langle u, \psi_k \rangle_{H^2} \psi_k$  in  $\{\psi_k\}$  exists for each  $u \in H_B^2(D)$ , and satisfies

$$u = \sum_{k=1}^{\infty} \langle u, \psi_k \rangle_{H^2} \psi_k \quad \text{a.e. in } D \quad (3.10)$$

and

$$Bu = B \left( \sum_{k=1}^{\infty} \langle u, \psi_k \rangle_{H^2} \psi_k \right) \quad \text{a.e. in } \Gamma. \quad (3.11)$$

The orthonormal basis is *complete* in the sense that for each  $u \in H_B^2(D)$

$$\lim_{N \rightarrow \infty} \left\| u - \sum_{k=1}^N \langle u, \psi_k \rangle_{H^2} \psi_k \right\|_{H^2} = 0, \quad (3.12)$$

where  $\|\cdot\|_{H^2}$  denotes the standard norm on  $H_B^2(D)$ . Moreover, for any  $N$ -dimensional subspace of  $H_B^2(D)$  spanned (for example) by the functions  $\{\psi_k\}_{k=1}^N$ , the real number

$$\left\| u - \sum_{k=1}^N c_k \psi_k \right\|_{H^2} \quad c_k \in \mathbb{C} \quad (3.13)$$

is minimized by setting  $c_k = \langle u, \psi_k \rangle_{H^2}$  for each  $k \in \{1, 2, \dots, N\}$ .

The numerical method relies upon the use of finite-dimensional best estimates provided by eigenfunction expansions for arbitrary elements  $u \in$

$H_B^2(D) \subseteq L^2(D)$ , and the corresponding Fréchet derivative of  $J$  at  $u$ . Next, the *spectrum* and the collection  $\{\psi_k\}$  of eigenfunctions for  $\mathcal{L}$  is determined explicitly, and the properties of this system as they apply to the application of the GNGA algorithm are more carefully studied.

### 3.5 The Eigenfunctions and Spectrum of $\mathcal{L}$

The results from the preceding section demonstrate the importance of both the spectrum and the collection of eigenfunctions for  $\mathcal{L}$ . A closer study of the properties of this operator allow for several useful generalizations regarding these objects. Ultimately, a closed-form formulation for both is available.

The theoretical developments continue after first recalling a standard definition.

**Definition 3.5.1** *The **spectrum**  $\sigma(\mathcal{L})$  of the operator  $\mathcal{L}$  is the set of all points  $\lambda \in \mathbb{C}$  such that the operator  $\mathcal{L} - \lambda$  is singular.*

In the above notation,  $\lambda$  is written in place of  $\lambda \cdot 1_{H_B^2(D)}$ , for simplicity. Also,  $\sigma$  is written for  $\sigma(\mathcal{L})$  whenever it is unambiguous to do so. The first generalization regarding the spectrum is obtained by recalling the analysis provided in the proof for Proposition 3.3.2. The operator  $\mathcal{L}$  is *positive* in the sense that for all  $u \in H_B^2(D)$ , the product  $\langle \mathcal{L}u, u \rangle_2$  is real and nonnegative. As demonstrated in [13], this implies that  $\sigma \subseteq [0, \infty)$ . The fact that  $\mathcal{L}$  is compact means that  $\sigma = \{0\} \cup P\sigma(\mathcal{L})$ , where

$$P\sigma(\mathcal{L}) = \{\lambda \in \mathbb{C} \mid \mathcal{L} - \lambda \text{ is not injective}\}.$$

The set  $P\sigma(\mathcal{L})$  is also countable, each  $\lambda \in P\sigma(\mathcal{L})$  is isolated, and the properties of  $\mathcal{L}$  then imply that each such  $\lambda$  is in fact an eigenvalue. Therefore,  $\sigma$  is a countable subset of  $[0, \infty)$  whose nonzero elements are the eigenvalues for  $\mathcal{L}$ . If eigenfunctions exist, then the next result from [9] allows for a strong conclusion regarding the space to which they must belong.

**Theorem 3.5.2** *Let  $\lambda \in \sigma$ . If  $u \in H_B^2(D)$  is a solution to the equation  $(\mathcal{L} - \lambda)u = 0$ , then  $u \in C^\infty(D)$ .*

The theorem applies, since  $\mathcal{L} - \lambda$  is strongly elliptic and has coefficients with derivatives of arbitrary order in  $\overline{D}$ . Thus, if eigenfunctions  $\psi_k \in H_B^2(D)$  exist, they satisfy the linear equation given by

$$\mathcal{L}u = \lambda u \text{ in } D, \quad Bu = 0 \text{ on } \Gamma \tag{3.14}$$

for some  $\lambda \in [0, \infty)$  and must also be elements of  $C^\infty(D)$ . The most general solution to equation (3.14) is known in a closed form; its derivation is available from several sources, including [3]. For *winding number*  $L \in \mathbb{Z}$ , the doubly-indexed eigenfunctions are written as

$$\psi_{L,j}(r, \theta) = e^{iL\theta} e^{-r^2/2} r^{|L|} M(-n_{|L|,j}, |L| + 1, r^2), \quad (3.15)$$

where

$$M(x, y, z) = 1 + \frac{x}{y}z + \frac{x(x+1)}{y(y+1)}\frac{z^2}{2!} + \frac{x(x+1)(x+2)}{y(y+1)(y+2)}\frac{z^3}{3!} + \dots$$

is the confluent hypergeometric function of the first kind. The corresponding eigenvalues are given by

$$\lambda_{L,j} = 2(1 + L + |L| + 2n_{|L|,j}). \quad (3.16)$$

For each  $(|L|, j) \in (\{0\} \cup \mathbb{N}) \times \mathbb{N}$ , the numbers  $n_{|L|,j}$  are chosen so that

$$\frac{\partial \psi_{L,j}}{\partial r}(r_o, \theta) = 0, \quad (3.17)$$

in order to satisfy the necessary requirement that  $\psi_{L,j} \in H_B^2(D)$  for every possible index combination. By Theorem 3.4.2, after normalizing the collection  $\{\psi_{L,j}\}$  with respect to  $\langle \cdot, \cdot \rangle_{H^2}$ , the resulting collection is a complete orthonormal basis for  $H_B^2(D)$ . Furthermore, since  $P\sigma(\mathcal{L})$  is countable and  $H_B^2(D)$  is a separable Hilbert space, there are only countably many elements in the collection. The next result implies that  $\{\psi_{L,j}\}$  is an orthogonal set in the space  $L^2(D)$ .

**Proposition 3.5.3** *The set  $\{\psi_{L,j}\}$  is orthogonal in  $L^2(D)$ .*

*Proof:* For convenience, first index the collections  $\{\psi_{L,j}\}$  and  $\{\lambda_{L,j}\}$  singly in the natural number  $k$ . For any  $k$ , the linear problem (3.14) reads

$$-\Delta \psi_k + i2 \frac{\partial \psi_k}{\partial \theta} + r^2 u = \lambda \psi_k,$$

and therefore

$$-\frac{1}{r} \frac{\partial}{\partial r} \left( r \frac{\partial \psi_k}{\partial r} \right) - \frac{1}{r^2} \frac{\partial^2 \psi_k}{\partial \theta^2} + i2 \frac{\partial \psi_k}{\partial \theta} + r^2 \psi_k = \lambda_k \psi_k.$$

Let  $k_1, k_2 \in \mathbb{N}$ , and let  $L_1, L_2 \in \mathbb{Z}$  be the winding numbers for the functions  $\psi_{k_1}$  and  $\psi_{k_2}$ . First, suppose that  $k_1 \neq k_2$ . If  $L_1 \neq L_2$ , it is clear that  $\langle \psi_{k_1}, \psi_{k_2} \rangle_2 = 0$ , since it is well-known that  $\int_0^{2\pi} f(r)e^{i\ell\theta} d\theta = 0$  whenever  $\ell$  is a nonzero integer. If instead  $L_1 = L_2$ , after computing the partial derivatives with respect to  $\theta$ , it follows that  $\psi_{k_1}, \psi_{k_2}$  satisfy the Sturm-Liouville equations

$$\frac{\partial}{\partial r} \left( r \frac{\partial \psi_{k_1}}{\partial r} \right) + \left( \lambda_{k_1} r + 2L_1 - \frac{L_1^2}{r} - r^3 \right) \psi_{k_1} = 0$$

and

$$\frac{\partial}{\partial r} \left( r \frac{\partial \psi_{k_2}}{\partial r} \right) + \left( \lambda_{k_2} r + 2L_2 - \frac{L_2^2}{r} - r^3 \right) \psi_{k_2} = 0.$$

Using the standard method, since the winding numbers are equal it follows that

$$(\lambda_{k_2} - \lambda_{k_1}) \int_0^{r_o} r \psi_{k_1} \psi_{k_2} dr = r_o \left[ \frac{\partial \psi_{k_1}}{\partial r}(r_o) \psi_{k_2}(r_o) - \frac{\partial \psi_{k_2}}{\partial r}(r_o) \psi_{k_1}(r_o) \right].$$

The boundary conditions allow that the right hand side is zero, and since the numbers  $\lambda_{k_1}, \lambda_{k_2}$  are distinct, it follows that

$$\int_0^{r_o} r \psi_{k_1} \psi_{k_2} dr = 0.$$

Thus,  $k_1 \neq k_2$  implies that  $\langle \psi_{k_1}, \psi_{k_2} \rangle_2 = 0$ . When  $k_1 = k_2$ , since  $\psi_{k_1}$  is not the zero function it follows that  $0 \neq \|\psi_{k_1}\|_2^2 = \langle \psi_{k_1}, \psi_{k_2} \rangle_2$ . The conclusion follows.  $\square$

If one normalizes  $\{\psi_k\}$  with respect to  $\langle \cdot, \cdot \rangle_2$ , of course a basis for the space  $L^2(D)$  is recovered.

**Theorem 3.5.4** *After normalizing the set  $\{\psi_k\}$  from Proposition 3.5.3 with respect to  $\langle \cdot, \cdot \rangle_2$ , the resulting collection is a complete orthonormal basis for the space  $L^2(D)$ .*

*Proof:* The proof is discussed in [10]. Since  $H_B^2(D)$  is dense in  $L^2(D)$ , each  $u \in L^2(D)$  has an expansion of the form in Equation (3.10). If one normalizes  $\{\psi_k\}$  with respect to  $\langle \cdot, \cdot \rangle_2$ , the terms of the  $\langle \cdot, \cdot \rangle_{H^2}$  expansion are exactly those of the summation

$$\sum_{k=1}^{\infty} \langle u, \psi_k \rangle_2 \psi_k.$$

Since  $u \in L^2(D)$  was selected arbitrarily, the conclusion holds.  $\square$

The eigenfunction expansion and finite estimation results provided in equations (3.10) through (3.13) may therefore be formulated equivalently by normalizing  $\{\psi_k\}$  with respect to the  $L^2(D)$  inner product, then replacing  $\langle \cdot, \cdot \rangle_{H^2}$  with  $\langle \cdot, \cdot \rangle_2$ . Furthermore, the  $L^2(D)$  expansion formulas may instead be written with respect to the collection  $\{\psi_k\} \cup \{i\psi_k\}$ . Using Lemma 3.3.1, this collection also forms a complete orthonormal system for  $L^2(D)$  as a real inner product space with respect to  $\langle \cdot, \cdot \rangle$ .

Figure 3.1 shows estimates for each number  $n_{|L|,j}$  such that Equation (3.17) holds at each  $(L, j) \in \mathbb{Z} \times \mathbb{N}$  when  $r_o = 4$ . The data indicates that all eigenvalues are positive, since each  $n_{|L|,j} \in (-1/2, \infty)$ . The values  $n_{|L|,j}$  are

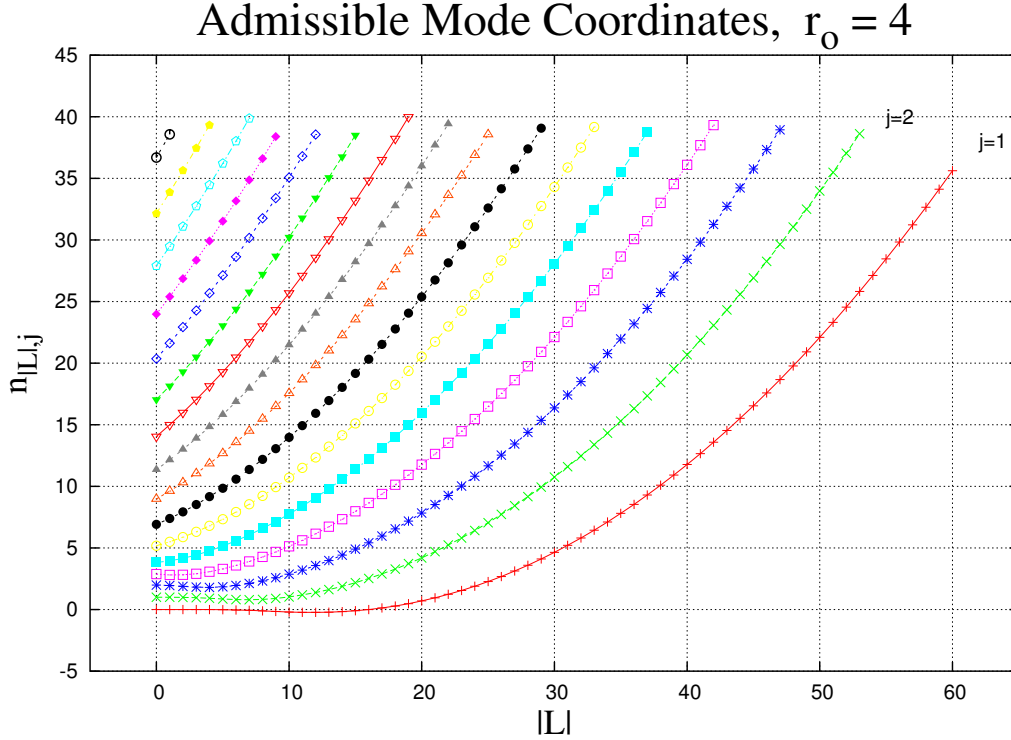


Figure 3.1: Estimated values for  $n_{|L|,j}$  when  $r_o = 4$ . Each corresponding eigenfunction  $\psi_{L,j}$  approximately satisfies Equation (3.17). After normalizing with respect to  $\langle \cdot, \cdot \rangle_{H^2}$ , the resulting collection  $\{\psi_{L,j}\}$  for  $(L, j) \in \mathbb{Z} \times \mathbb{N}$  approximates a complete orthonormal basis for the space  $H_B^2(D)$ .

ordered so that for fixed  $|L|$ , increasing  $j$  corresponds to increasing  $n_{|L|,j}$ , and therefore also to increasing  $\lambda_{L,j}$ . Finite expansions of dimension  $N$  (when considering  $L^2(D)$  as a complex Hilbert space) are calculated by using the first  $N$  elements  $(L, j)$  that yield the smallest  $N$  eigenvalues. This effectively imposes a constraint of the form  $L_{min} \leq L \leq L_{max}$ , where  $L_{min} < 0$ ,  $L_{max} > 0$ ; as well as an upper indexing limit  $t_L$  on  $j$  for each such  $L$ . The resulting coordinate combinations are referred to as the *admissible modes* corresponding to the dimension  $N$ . It is then convenient to allow for the indexing of the admissible eigenfunctions and eigenvalues in the natural number  $k$ . To accomplish this, the first  $N$  natural numbers are assigned to each admissible mode after ordering these first by  $|L|$ , then by  $j$ , and lastly (if necessary) by the sign of  $L$ ; the mode with  $L < 0$  is assigned the larger index. Of course, the choice of indexing notation may depend on the context; the use of either should not cause confusion. To normalize  $\{\psi_k\}$  with respect to  $\langle \cdot, \cdot \rangle$ , each normalized function  $\psi_k$  in the standard  $L^2(D)$  inner product space is divided by  $\sqrt{2}$ . Finally, by setting

$$\lambda_k = \begin{cases} \lambda_k & \text{if } 1 \leq k \leq N \\ \lambda_{k-N} & \text{if } N < k \leq 2N \end{cases} \quad (3.18)$$

and

$$\Psi_k = \begin{cases} \psi_k & \text{if } 1 \leq k \leq N \\ i\psi_{k-N} & \text{if } N < k \leq 2N, \end{cases} \quad (3.19)$$

any  $u \in L^2(D)$  may be approximated by the expansion

$$u \approx \sum_{k=1}^{2N} \langle u, \Psi_k \rangle \Psi_k. \quad (3.20)$$

Sums formed in the orthonormal collection  $\{\Psi_k\}_{k=1}^{2N}$  will provide the necessary  $L^2(D)$  estimates. The space

$$G^{2N} = \text{span}\{\Psi_1, \Psi_2, \dots, \Psi_{2N}\} \quad (3.21)$$

is referred to as the *Galerkin space of dimension  $N$* , and the elements of the collection  $\{\Psi_k\}_{k=1}^{2N}$  are called *basis functions* or *mode functions*. At times it will be useful to consider the space

$$G = \text{span}\{\Psi_1, \Psi_2, \dots\},$$

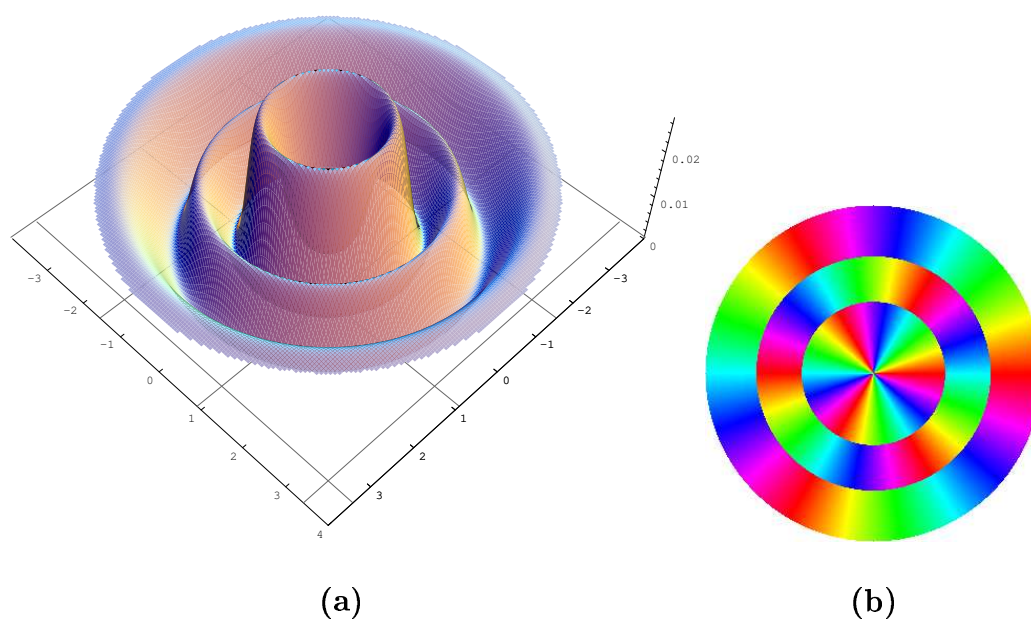


Figure 3.2: (a) The squared modulus plot of the eigenfunction  $\psi_{-3,3}$  on  $D$ . Note that the number of local maxima corresponds to 3, the index for  $j$ . (b) The phase plot for the same function. For fixed  $\theta$ , the function changes sign twice as  $r$  ranges from 0 to  $r_o = 4$ .

obtained by considering all coordinate combinations as being admissible, and to write  $G$  for  $H_B^2(D)$ . A visualization of a typical basis function is provided in Figure 3.2; both  $|\psi_{-3,3}|^2$  and  $\text{Arg}(\psi_{-3,3})$  on  $D$  are plotted for the choice  $r_o = 4$ .

Note that the expansion in (3.20) provides estimates in accordance with those obtained in the previous section. Since

$$\begin{aligned}
\sum_{k=1}^{2N} \langle u, \Psi_k \rangle \Psi_k &= \sum_{k=1}^N \langle u, \psi_k \rangle \psi_k + \sum_{k=N+1}^{2N} \langle u, i\psi_{k-N} \rangle (i\psi_{k-N}) \\
&= \sum_{k=1}^N (\langle u, \psi_k \rangle + i\langle u, i\psi_k \rangle) \psi_k \\
&= \sum_{k=1}^N \frac{1}{2} \left( \langle u, \sqrt{2}\psi_k \rangle + i\langle u, i\sqrt{2}\psi_k \rangle \right) \sqrt{2}\psi_k \\
&= \sum_{k=1}^N \langle u, \sqrt{2}\psi_k \rangle_2 (\sqrt{2}\psi_k),
\end{aligned}$$

actually  $\sum_{k=1}^{2N} \langle u, \Psi_k \rangle \Psi_k$  corresponds to an  $N$ -dimensional approximation of  $u$  with respect to the standard inner product  $\langle \cdot, \cdot \rangle_2$  in the complex inner product space  $L^2(D)$ .

The GNGA numerical algorithm may now be applied to produce and study solution estimates for (1.1). In addition to the descriptions of the algorithms involved and their implementations, there are several computational details that require specific attention. The next chapter proceeds by summarizing and discussing the many aspects of this remarkable method.

# Chapter 4

## Newton's Method and GNGA

The fact that solutions to (1.1) are exactly the zeros of the function  $DJ$  motivates the choice of a Newton's method when seeking numerical estimates. Provided with a reasonably chosen initial guess, the Newton method is well-known to be a powerful tool for generating sequences convergent to the zeros of differentiable functions in many theoretical contexts. The GNGA algorithm employed in this research is essentially an extension of the classical Newton's method; the attending complications may be summarized by the fact that the iteration is applied to the *estimates* of objects in the form of finite-dimensional eigenfunction expansions, rather than the functions themselves. The use of orthogonal systems of functions in Galerkin space will allow the Newton computations to be performed in familiar vector spaces that are *isometrically isomorphic* to the finite-dimensional subspaces of  $L^2(D)$  to which the estimates themselves belong.

There are in fact two types of Newton mappings implemented by the simulation software; the use of either naturally depends on the output required. A generalized definition describing both types is available for the theoretical presentations that follow, allowing for a thorough and efficient treatment of the concepts inherent to all estimation methods. First, a necessary extension of the preceding theory is provided; then a general rule to be used when computing Newton iterations is discussed.

## 4.1 The Newton Map and $J''(u)(v, w)$

Although the algorithms used for the computations that follow make use of finite-dimensional estimates of functions rather than the functions themselves, the objects that are the building blocks of the Newton map may nevertheless be defined on the entire solution space.

To apply the method, the Gateaux derivative of  $DJ$  at  $u$  in an arbitrary direction  $v \in H_B^2(D)$  is calculated. To establish the existence of this function, the method from Proposition 3.3.2 is again used.

**Proposition 4.1.1** *Let  $J : H_B^2(D) \rightarrow \mathbb{R}$  be given by (2.10), and let  $u \in H_B^2(D)$ . Then  $J$  is twice Gateaux differentiable at  $u$ , and the second Gateau derivative of  $J$  at  $u$  is  $J''(u)(v, w) = \langle \mathcal{L}v + av + 2|u|^2v + u^2\bar{v}, w \rangle$ .*

*Proof:* It is shown that the limit of the difference quotient  $(J'(u + tw)(v) - J'(u)(v))/t$  exists in  $\mathbb{C}$  as  $t \rightarrow 0$ , whenever  $(u + tw)$  is an element of any given neighborhood of  $u$ . As in the computation for  $J'(u)(v)$ , the imbedding and integrability results from Theorems 2.3.1 and 2.3.2 will imply the existence of the resulting integrals, and allow use of the usual integral linearity properties. Let  $u, v \in H_B^2(D)$ , let  $U$  be any neighborhood  $u$ , and let  $w \in H_B^2(D)$  and  $t \in \mathbb{R}$  such that  $(u + tw) \in U$ . Then,

$$\begin{aligned} \lim_{t \rightarrow 0} \frac{J'(u + tw)(v) - J'(u)(v)}{t} &= \int_D a(w\bar{v} + \bar{w}v) dx \\ &+ \int_D 2|u|^2(w\bar{v} + \bar{w}v) dx + \int_D u^2(wv + \bar{w}\bar{v}) dx \\ &+ \int_D \left\{ (i\nabla + r\hat{\theta})w \cdot (-i\nabla + r\hat{\theta})\bar{v} + (-i\nabla + r\hat{\theta})\bar{w} \cdot (i\nabla + r\hat{\theta})v \right\} dx. \end{aligned}$$

These terms are conveniently expressed in terms of the product  $\langle \cdot, \cdot \rangle$ . The relation  $\langle (i\nabla + r\hat{\theta})w, (i\nabla + r\hat{\theta})v \rangle = \langle (i\nabla + r\hat{\theta})^2w, v \rangle$  applies, and it then follows that

$$J''(u)(w, v) = \langle aw, v \rangle + \langle 2|u|^2w, v \rangle + \langle u^2\bar{w}, v \rangle + \langle (i\nabla + r\hat{\theta})^2w, v \rangle.$$

Using the properties of  $\langle \cdot, \cdot \rangle$ , and after noting the symmetry relation  $J''(u)(w, v) = J''(u)(v, w)$ , one may finally write

$$J''(u)(v, w) = \langle \mathcal{L}v + av + 2|u|^2v + u^2\bar{v}, w \rangle,$$

as required.  $\square$

At times, it will be convenient to express this result as  $J''(u)(v, w) = \langle D^2 J(u)v, w \rangle$ , where  $D^2 J(u)v = \mathcal{L}v + av + 2|u|^2v + u^2\bar{v}$ . Also, it is clear that  $D^2 J(u)v \in L^2(D)$  whenever  $u, v \in H_B^2(D)$ .

Next, a generalized Newton map  $\mathcal{N}$  is defined. This map is specified only for domains in the class of dimension  $N$  Galerkin spaces, defined in (3.21), as this will suffice for the estimation algorithms. For  $N \in \mathbb{N}$ , let  $\mathcal{N} : G^{2N} \rightarrow G^{2N}$  be given by  $u \mapsto \mathcal{N}(u) = u - s$ , where  $s \in G^{2N}$  is a *search direction* function that depends on  $u$ . Considering all functions in terms of their unique  $G^{2N}$  expansion, for an input function  $u$ , the numerical method seeks a function  $s$  that minimizes the standard  $L^2(D)$  norm of the function  $D^2 J(u)s - DJ(u)$ . This is equivalent to selecting  $s$  such that the real number

$$\sum_{k=1}^N |\langle D^2 J(u)s - DJ(u), \psi_k \rangle_2|^2 \quad (4.1)$$

is minimized. Equation (4.1) may be formulated in terms of the basis functions  $\{\Psi_k\}_{k=1}^{2N}$ , and the inner product  $\langle \cdot, \cdot \rangle$ . For each  $k$ , it follows that

$$\begin{aligned} 4 |\langle D^2 J(u)s - DJ(u), \psi_k \rangle_2|^2 &= \\ &= |\langle D^2 J(u)s - DJ(u), \psi_k \rangle + i \langle D^2 J(u)s - DJ(u), i\psi_k \rangle|^2 \\ &= \langle D^2 J(u)s - DJ(u), \psi_k \rangle^2 + \langle D^2 J(u)s - DJ(u), i\psi_k \rangle^2. \end{aligned}$$

Therefore, after recalling the symmetry of the second Gateaux derivative of  $J$ , Equation (4.1) is rewritten as

$$4 \sum_{k=1}^N |\langle D^2 J(u)s - DJ(u), \psi_k \rangle_2|^2 = \sum_{k=1}^{2N} (\langle D^2 J(u)\Psi_k, s \rangle - \langle DJ(u), \Psi_k \rangle)^2. \quad (4.2)$$

Of course, the factor of “4” is irrelevant to this discussion. This result allows for the computation of  $s$  at each Newton step by means of the familiar methods of linear algebra. This fact is verified after first defining an important mapping.

## 4.2 Newton’s Method in $\mathbb{R}^{2N}$

The functions  $DJ(u)$  and  $D^2 J(u)\Psi_k$  for any  $k \in \mathbb{N}$  and  $u \in H_B^2(D) = G$  are both elements of  $L^2(D)$ , and therefore each possesses a unique expansion in

the Galerkin space  $G^{2N}$ . Recall that these expansions, given by

$$DJ(u) \approx \sum_{m=1}^{2N} \langle DJ(u), \Psi_m \rangle \Psi_m \quad (4.3)$$

and

$$D^2 J(u) \Psi_k \approx \sum_{m=1}^{2N} \langle D^2 J(u) \Psi_k, \Psi_m \rangle \Psi_m, \quad (4.4)$$

provide the best  $L^2(D)$  estimates for each function in the sense of (3.13). The mapping  $P : G^{2N} \rightarrow \mathbb{R}^{2N}$ , defined by

$$u \mapsto Pu = (\langle u, \Psi_1 \rangle, \langle u, \Psi_2 \rangle, \dots, \langle u, \Psi_{2N} \rangle), \quad (4.5)$$

is clearly an *isometric isomorphism* from the  $N$ -dimensional Hilbert space  $G^{2N}$  to  $\mathbb{R}^{2N}$ , since it is continuous and

$$\|u\|_2 = \left( \sum_{m=1}^{2N} \langle u, \Psi_m \rangle^2 \right)^{1/2} = \|Pu\|_{\mathbb{R}^{2N}}. \quad (4.6)$$

In the standard way, the symmetric *Hessian matrix* is formed by applying the mapping  $P$  above to  $D^2 J(u) \Psi_k$ , for each  $k \in \{1, 2, \dots, 2N\}$ . The mapping  $(G^{2N})^{2N} \rightarrow M^{2N \times 2N}(\mathbb{R})$  given by

$$(D^2 J(u) \Psi_1, \dots, D^2 J(u) \Psi_{2N}) \mapsto (PD^2 J(u) \Psi_1, \dots, PD^2 J(u) \Psi_{2N})$$

is an isomorphism. The right-hand side, denoted by  $\Lambda_u$ , is written as

$$\begin{pmatrix} \langle D^2 J(u) \Psi_1, \Psi_1 \rangle & \langle D^2 J(u) \Psi_1, \Psi_2 \rangle & \cdots & \langle D^2 J(u) \Psi_1, \Psi_{2N} \rangle \\ \langle D^2 J(u) \Psi_2, \Psi_1 \rangle & \langle D^2 J(u) \Psi_2, \Psi_2 \rangle & \cdots & \langle D^2 J(u) \Psi_2, \Psi_{2N} \rangle \\ \vdots & \vdots & \ddots & \vdots \\ \langle D^2 J(u) \Psi_{2N}, \Psi_1 \rangle & \langle D^2 J(u) \Psi_{2N}, \Psi_2 \rangle & \cdots & \langle D^2 J(u) \Psi_{2N}, \Psi_{2N} \rangle \end{pmatrix}. \quad (4.7)$$

If  $(s_1, s_2, \dots, s_{2N}) \in \mathbb{R}^{2N}$  is a least-squares solution for the system

$$(\Lambda_u)(Ps)^T = (PDJ(u))^T, \quad (4.8)$$

then according to Equation (4.2), the best estimate in  $G^{2N}$  for the search direction function  $s$  is

$$s = \sum_{m=1}^{2N} s_m \Psi_m.$$

The vector  $(s_1, s_2, \dots, s_{2N})$  may be obtained by use of a least-squares LAPACK linear algebra routine at each Newton step. If  $u = \sum_{k=1}^{2N} c_k \Psi_k$  where  $c_k \langle u, \Psi_k \rangle$  for  $k = 1, 2, \dots, 2N$ , then the object  $PDJ(u)$  is constructed by using the computation

$$\begin{aligned}
\langle DJ(u), \Psi_m \rangle &= \langle (i\nabla + r\theta)^2 u, \Psi_m \rangle + \langle au, \Psi_m \rangle + \langle |u|^2 u, \Psi_m \rangle \\
&= \left\langle \sum_{k=1}^{2N} c_k \lambda_k \Psi_k, \Psi_m \right\rangle + a \left\langle \sum_{k=1}^{2N} c_k \Psi_k, \Psi_m \right\rangle + \langle |u|^2 u, \Psi_m \rangle \\
&= \sum_{k=1}^{2N} c_k \lambda_k \langle \Psi_k, \Psi_m \rangle + a \sum_{k=1}^{2N} c_k \langle \Psi_k, \Psi_m \rangle + \langle |u|^2 u, \Psi_m \rangle \\
&= (\lambda_m + a) c_m + \langle |u|^2 u, \Psi_m \rangle.
\end{aligned} \tag{4.9}$$

The last term must be numerically integrated, according to the formula

$$\langle |u|^2 u, \Psi_m \rangle = \int_D |u|^2 u \bar{\Psi}_m dx + \int_D |u|^2 \bar{u} \Psi_m dx,$$

so that

$$\langle |u|^2 u, \Psi_m \rangle = \begin{cases} 2 \operatorname{Re} \int_D |u|^2 u \bar{\psi}_m dx & \text{if } 1 \leq m \leq N \\ 2 \operatorname{Im} \int_D |u|^2 u \bar{\psi}_{m-N} dx & \text{if } N < m \leq 2N. \end{cases} \tag{4.10}$$

The matrix entries for  $\Lambda_u$  are computed by use of the formula

$$\begin{aligned}
\langle D^2 J(u) \Psi_k, \Psi_m \rangle &= \langle (i\nabla + r\theta)^2 \Psi_k, \Psi_m \rangle + \langle a \Psi_k, \Psi_m \rangle + \langle 2|u|^2 \Psi_k + u^2 \bar{\Psi}_k, \Psi_m \rangle \\
&= \langle \lambda_k \Psi_k, \Psi_m \rangle + a \langle \Psi_k, \Psi_m \rangle + \langle 2|u|^2 \Psi_k + u^2 \bar{\Psi}_k, \Psi_m \rangle \\
&= (\lambda_k + a) \delta_{k,m} + \langle 2|u|^2 \Psi_k, \Psi_m \rangle + \langle u^2 \bar{\Psi}_k, \Psi_m \rangle.
\end{aligned} \tag{4.11}$$

Again, the terms containing  $u$  require numerical integration. For  $1 \leq k, m \leq 2N$ ,  $\langle D^2 J(u) \Psi_k, \Psi_m \rangle$  is given by

$$\left\{ \begin{array}{ll} (\lambda_k + a) \delta_{k,m} + 2(\operatorname{Re} I_{k,m} + \operatorname{Re} \tilde{I}_{k,m}) & \text{if } 1 \leq k, m \leq N \\ 2(\operatorname{Im} \tilde{I}_{k,m-N} - \operatorname{Im} I_{k,m-N}) & \text{if } 1 \leq k \leq N, N < m \leq 2N \\ 2(\operatorname{Im} I_{k-N,m} + \operatorname{Im} \tilde{I}_{k-N,m}) & \text{if } N < k \leq 2N, 1 \leq m \leq N \\ (\lambda_k + a) \delta_{k,m} + 2(\operatorname{Re} I_{k-N,m-N} - \operatorname{Re} \tilde{I}_{k-N,m-N}) & \text{if } N < k, m \leq 2N. \end{array} \right. \tag{4.12}$$

Here  $\delta_{k,m}$  denotes the Kronecker delta, and  $I_{k,m}, \tilde{I}_{k,m}$  represent the integrals

$$\begin{aligned} I_{k,m} &= \int_D 2|u|^2 \bar{\psi}_k \psi_m dx \\ \tilde{I}_{k,m} &= \int_D u^2 \bar{\psi}_k \bar{\psi}_m dx, \end{aligned} \quad (4.13)$$

given in terms of the functions  $\{\psi_k\}_{k=1}^N$ , using Equation (3.19). Numerical integration algorithms will be required to estimate the integrals appearing in Equations (4.10) and (4.13). In the next section, the means by which these estimates are made is considered in some detail.

### 4.3 Numerical Integration on $D$

The choice of numerical integration technique should be made only after careful consideration. In addition to the obvious questions regarding accuracy and precision, there is the more important question regarding simulation run time: how might the computational rules be chosen so that real-time execution is kept to a minimum level? When attempting to formulate a reasonable method, one first examines the all-important characteristics of the eigenfunctions  $\{\psi_k\}_{k=1}^N$ , whose span is the space of estimates  $G^{2N}$ .

When integrating the products of elements in Galerkin space, it seems most convenient (although not strictly necessary) to integrate first in  $\theta$ , then in  $r$ . Thus, let  $r \in (0, r_o]$  be fixed, and consider integrals of the form

$$\int_0^{2\pi} f(\theta) d\theta \quad (4.14)$$

where

$$f(\theta) = \sum_{\ell=4L_{min}}^{4L_{max}} c_\ell e^{i\ell\theta}, \quad c_\ell \in \mathbb{C}. \quad (4.15)$$

According to the specification of  $G^{2N}$  previously provided, note that  $L_{max} > 0$ ,  $L_{min} < 0$ , and also  $|L_{min}| \geq |L_{max}|$ . Naturally, these numbers specify the range of integer winding numbers that are present in arbitrary expansions for typical elements of  $G$  used by the numerical method. The limits in Equation (4.15) are multiplied by “4” in order to consider the integration of functions that are comprised in general of a product of four finite dimensional Galerkin

functions; note the form of the integrals in Equations (4.10) and (4.13) from the previous section. Immediately the relation

$$\int_0^{2\pi} f(\theta) d\theta = 2\pi c_0 \quad (4.16)$$

is recoverable, and the integral from (4.15) reduces to the problem of computing the appropriate coefficient function at each fixed  $r$ . In practice, this approach can be cumbersome. When considering the integrals in Equation (4.10), note the fact that only one basis function  $\psi_m$  appears as a factor in each integrand. Thus, when considering a fixed integer  $m$  at each  $r$ , to determine  $c_0$  one must consider all solutions some integer equation  $z_1 + z_2 + z_3 = m$ , calculating a term of the coefficient at each. Even for the integrals in Equation (4.13), whose integrands have instead two basis functions  $\psi_k$  and  $\psi_m$  (or their conjugates) as factors, one must solve integer equations in two variables. Although in this case there are far fewer solutions to consider, nevertheless a classical trapezoid numerical integration in an optimally selected rule will produce an *exact* result without requiring additional computation time. This rule is determined from the number  $|L_{min}|$ , according to the next proposition regarding the integral of any term  $c_\ell e^{i\ell\theta}$  of  $f(\theta)$  with  $\ell \neq 0$ .

**Proposition 4.3.1** *Let  $g : [0, 2\pi]$  be defined as  $\theta \mapsto g(\theta) = ce^{ik\theta}$  for  $c \in \mathbb{C}$ . Let  $k \in \{1, 2, \dots, N-1\}$ . Then,*

$$\int_0^{2\pi} g(\theta) d\theta = \sum_{j=1}^N \left( ce^{i\frac{2\pi k}{N}j} \right) = 0.$$

*That is, the trapezoid rule for the integral is **exact**, provided that  $N \geq k+1$ .*

*Proof:* Since  $g(\theta)$  is periodic,  $g(0) = g(2\pi)$  and the sum on the right is in fact the well-known trapezoidal rule. Next, recall that the complex number  $e^{i\frac{2\pi k}{N}j}$  is a root of the polynomial  $(1 + z + z^2 + \dots + z^{N-2} + z^{N-1})$  for each  $k$  satisfying  $1 \leq k \leq N-1$ . With  $z = e^{i\frac{2\pi k}{N}j}$ , a calculation shows that

$$\sum_{j=1}^N \left( ce^{i\frac{2\pi k}{N}j} \right) = c \sum_{j=1}^N \left( e^{i\frac{2\pi k}{N}j} \right)^j = cz(1 + z + z^2 + \dots + z^{N-2} + z^{N-1}) = 0,$$

as needed. □

Note that a similar result holds for  $k \in \{-1, -2, \dots, -(N-1)\}$ . Using the linearity of the integral, for  $N \geq 4|L_{min}| + 1$  it therefore follows that the trapezoidal rule applied to the integral from Equations (4.14) and (4.15) allows for an exact computation of the needed integral.

As mentioned, use of the trapezoid rule requires no more computations per fixed  $r$  value than would a more methodical computation using Equation (4.16), on average. Since it is simpler to implement and verify, it is therefore the preferable choice. Integrations in the  $r$  direction are then performed by use of the well-known Simpson rule. Before discussing several higher level computational rules that are used at each Newton step to form the objects  $\Lambda_u$  and  $PDJ(u)$  of Equation (4.8), a generalization of the Newton algorithm as it applies to this research is first introduced.

## 4.4 A Newton Map for Branch Following

The practical goal is to produce estimates for solution “branches” for the problem in (1.1) versus the parameter  $a$ , in Galerkin space. For present purposes, a *solution branch* is defined to be a parameterized solution curve  $(a, f(a, u))$ . The pair  $(a, u)$  indicates a solution estimate  $u \in G^{2N}$  for the PDE problem at  $a$ , and the function  $f(a, u)$  may be any one of several functions on the space  $\mathbb{R} \times G^{2N}$ ; perhaps the  $L^2(D)$  norm of  $u$ , for example. Often, it is particularly convenient to consider  $f$  as the mapping  $(a, u) \mapsto u$ , so that the pair  $(a, u)$  itself represents a type of solution branch. In seeking to estimate solution branches, first consider how the mapping  $\mathcal{N}$  is classically implemented into a larger algorithm designed for this purpose.

If the map  $\mathcal{N}$  is to be used as part of a branch following routine, then a new guess for both  $u$  and  $a$  must be supplied upon convergence to each solution estimate  $(a, u)$ . The procedure of supplying the “next guess” is typically automated by using the last solution  $u$  obtained by  $\mathcal{N}$ , along with an incremented or decremented value of the previous parameter value  $a$  as the starting point for the next recursion. The principle drawback of this classical approach is that the next parameter must be supplied without knowing for certain in which direction (with respect to  $a$ ) the current solution branch may be turning. That is, it is generally not known if the parameter should be incremented or decremented from the current solution estimate. Since the parameter  $a$  is held fixed while a new solution estimate is produced by  $\mathcal{N}$ , this generally results in difficulties. However a remarkable method, provided

by Neuberger, Swift and Sieben [19], is available to address this problem. Only a minor modification to the classical mapping  $\mathcal{N}$  is required.

It is desirable to allow the Newton iteration itself to indicate how the parameter should be varied; that is, a mapping which treats  $a$  as an independent variable is needed. Therefore, the map  $\mathcal{N} : \mathbb{R} \times G^{2N} \rightarrow \mathbb{R} \times G^{2N}$  given by the rule  $(a, u) \mapsto (a, u) - (\Delta a, s)$  is defined by regarding the pair  $(a, u)$  as the variable of interest. When considering the function  $DJ(u)$  as instead  $DJ(a, u)$ , one may recover an augmented Gateaux derivative by computing the limit

$$\lim_{t \rightarrow 0} \frac{DJ((a, u) + t(\Delta a, v)) - DJ(a, u)}{t}. \quad (4.17)$$

This derivative is denoted by  $D^2J(a, u)(\Delta a, v)$ , and a simple computation establishes that

$$D^2J(a, u)(\Delta a, v) = D^2J(u)v + \Delta a u, \quad (4.18)$$

where  $D^2J(u)v$  is exactly that from Proposition 4.1.1. The requirement analogous to that stated in Equation (4.1) is then to determine the pair  $(\Delta a, s)$  such that the number

$$\sum_{k=1}^N |\langle D^2J(a, u)(\Delta a, s) - DJ(a, u), \psi_k \rangle_2|^2 \quad (4.19)$$

is a minimum. After appropriately rewriting this requirement in a form comparable to that in Equation (4.2), it is clear that the number

$$\sum_{k=1}^{2N} (\langle D^2J(u)\Psi_k, s \rangle + \langle u, \Psi_k \rangle \Delta a - \langle DJ(a, u), \Psi_k \rangle)^2 \quad (4.20)$$

should be minimized. To specify an intelligent guess for  $u$  that estimates the progression of the current solution branch, let  $v$  be the function formed by the difference between the two immediately preceding solution estimates. A good starting point for the next Newton iteration is provided by weighting the function  $v$ , then adding this result to the last solution estimate. In addition to the requirement stated in Equation (4.20), the function  $s$  is forced to be orthogonal to  $v$  in  $G^{2N}$ . Thus, the condition that

$$\langle v, s \rangle = 0 \quad (4.21)$$

should be imposed as well; primarily this condition will ensure that some progress along the branch is made between consecutive solution estimates. Therefore, determining the pair  $(\Delta a, s)$  needed at each Newton step is equivalent to finding a least-squares solution to the augmented system

$$(\tilde{\Lambda}_u)(Ps, \Delta a)^T = (PDJ(a, u), 0)^T, \quad (4.22)$$

where

$$\tilde{\Lambda}_u = \left( \begin{array}{ccc|c} & & & \langle u, \Psi_1 \rangle \\ & \Lambda u & & \vdots \\ & & & \langle u, \Psi_{2N} \rangle \\ \hline \langle v, \Psi_1 \rangle & \cdots & \langle v, \Psi_{2N} \rangle & 0 \end{array} \right). \quad (4.23)$$

It is the mapping  $\tilde{\mathcal{N}}$  that is to be recursively called by the branch following algorithms. Before completely describing these, first the behavior of this map on the space  $\mathbb{R} \times G^{2N}$  is studied more carefully.

## 4.5 Computational Rules for Newton's Method

At this stage, the general form for an important subspace of  $G$  is specified, and several computational simplifications to be used when calculating Newton iterations are derived. It is convenient in this section to consider expansions for  $u \in G$  in the form

$$u = \sum_{\ell=-\infty}^{\infty} \sum_{j=1}^{\infty} c_{\ell,j} \psi_{\ell,j}, \quad (4.24)$$

where  $c_{\ell,j} \in \mathbb{C}$  for every indexing pair. Let  $L_1, L_2$  be integers such that  $L_1 \leq L_2$ . If  $L_1 = L_2$  then set  $n = 1$ , and otherwise let  $n \in \mathbb{N}$  be a divisor of  $L_2 - L_1$ . Let  $\ell = L_1 + nz$  for  $z \in \mathbb{Z}$ . The subspace  $G(L_1, L_2, n)$  is defined as

$$G(L_1, L_2, n) \doteq \{u \in G \mid c_{\ell,j} = 0 \text{ for } z \notin \{0, 1, 2, \dots, (L_2 - L_1)/n\}\}. \quad (4.25)$$

Clearly, if  $u \in G(L_1, L_2, n)$ , then  $c_{\ell,j} \neq 0$  only when  $z = 0, 1, 2, \dots, (L_2 - L_1)/n$ . If  $L_1 = L_2$ , then  $c_{\ell,j} \neq 0$  only when  $\ell = L_1 = L_2$ . Note that  $G(L_1, L_2, n) \subseteq G^{2N}$  if and only if  $L_{min} \leq L_1 \leq L_2 \leq L_{max}$ , and  $j \leq t_\ell$  for every  $\ell = L_1 + nz$  given by some  $z \in \{0, 1, 2, \dots, (L_2 - L_1)/n\}$ .

To derive useful computational rules, the subspaces  $G(L_1, L_2, n)$  that are *maximal* subspaces of  $G^{2N}$  are of primary interest. This terminology is used

to indicate that whenever  $L_1 \neq L_2$ , for the space  $G(L_1, L_2, n) \subseteq G^{2N}$  it is assumed that  $L_1 < L_{min} + n$ ,  $L_2 > L_{max} - n$  and  $j = 1, 2, \dots, t_\ell$  for each mode indexed by  $\ell$  in the space. Henceforth, it will be assumed that the space  $G(L_1, L_2, n) \subseteq G^{2N}$  is always maximal in this sense. To simplify the required integrations, it is helpful to first determine to which Galerkin spaces the functions  $|u|^2$ ,  $u^2$  and  $|u|^2u$  must belong whenever  $u \in G(L_1, L_2, n)$ . If  $n$  is some nonnegative integer and  $u \in G(L_1, L_2, n)$ , then it follows that  $\bar{u} \in G(-L_2, -L_1, n)$ , and

$$|u|^2 \in G(L_1 - L_2, L_2 - L_1, n). \quad (4.26)$$

Since  $(L_2 - L_1) - (L_1 - L_2) = 2(L_2 - L_1)$ , the allowable range for  $z$  indexing the maximal subspace of the form in (4.25) that contains  $|u|^2$  has increased by a factor of 2. For  $z$  such that  $nz = L_2 - L_1$ , since  $L_1 - L_2 + nz = 0$  it is clear that Galerkin expansions for  $|u|^2$  generally admit the modes corresponding to  $\ell = 0$ . Clearly, it follows that  $u^2 \in G(2L_1, 2L_2, n)$ . Forming another product, also

$$|u|^2u \in G(2L_1 - L_2, 2L_2 - L_1, n). \quad (4.27)$$

Notice that  $(2L_2 - L_1) - (2L_1 - L_2) = 3(L_2 - L_1)$ , and thus the allowable range for  $z$  has increased by a factor of 3. Furthermore, with  $z$  such that  $nz = L_2 - L_1$ , note that  $2L_1 - L_2 + nz = L_1$ . Therefore, the best estimate of the function  $|u|^2u$  in  $G^{2N}$  is in the subspace  $G(L_1, L_2, n)$  itself, the space from which  $u$  was originally taken.

Equations (4.26) and (4.27) allow for several computational simplifications, as well as an important intermediate result. Consider first the integral expressions in Equation (4.10). The function  $\psi_m$  is a single basis function, let  $L_m$  denote its winding number. Since  $L_{min} \leq L_m \leq L_{max}$ , the terms in the expansion of  $|u|^2u$  that are not in  $G^{2N}$  will not effect the integration. Dismissing these, for uniquely determined  $c_{\ell,j} \in \mathbb{C}$  the integrand may be expanded as

$$|u|^2u\bar{\psi}_m \approx \sum_{\ell=L_1-L_m}^{L_2-L_m} \left( \sum_{j=1}^{t_\ell} c_{\ell,j} \psi_{\ell,j} \right),$$

where  $t_\ell$  is the maximum number of modes in winding number  $\ell$ , according to the construction of  $G^{2N}$ . From this expression, it is clear that the only terms having a nonzero integral on  $D$  are those for which  $\ell = L_1 - L_m + nz = 0$ . Therefore, the  $m^{th}$  entry of  $PDJ(a, u)$  should be computed numerically only when

$$L_m = L_1 + nz. \quad (4.28)$$

From this, an intermediate result is obtained.

**Proposition 4.5.1** *Let  $u \in G(L_1, L_2, n)$ , where  $G(L_1, L_2, n) \subseteq G^{2N}$  is maximal. Then, the best approximation for  $DJ(u)$  in  $G^{2N}$  is contained in  $G(L_1, L_2, n)$ .*

*Proof:* The result represented by Equation (4.28) implies the conclusion. The only nonzero entries for the  $G^{2N}$  expansion of  $DJ(u)$  are those for which  $\ell = L_1 + nz$ , for some appropriate nonnegative integer  $z$ .  $\square$

Next, consider the integral expressions in Equation (4.13). Let  $L_m$  and  $L_k$  denote the winding number of the functions  $\psi_m$  and  $\psi_k$ , respectively. Then, the first integrand  $|u|^2 \bar{\psi}_k \psi_m$  is an element of the subspace

$$G(L_1 - L_2 - L_k + L_m, L_2 - L_1 - L_k + L_m, n).$$

The integral  $I_{k,m}$  is therefore calculated only when  $\ell = L_1 - L_2 - L_k + L_m + nz = 0$  for some nonnegative  $z$ ; that is, when

$$L_k - L_m = L_1 - L_2 + nz \quad (I_{k,m}). \quad (4.29)$$

The second integrand,  $u^2 \bar{\psi}_k \bar{\psi}_m$ , belongs to the subspace

$$G(2L_1 - L_k - L_m, 2L_2 - L_k - L_m, n),$$

and thus  $\tilde{I}_{k,m}$  is to be computed only when

$$L_k + L_m = 2L_1 + nz \quad (\tilde{I}_{k,m}). \quad (4.30)$$

These integration rules are useful in many practical computational situations, since every solution estimate is strictly an element of  $G(L_1, L_2, n)$  for some suitable combination of  $L_1, L_2$  and  $n$ .

The implications of Equations (4.28), (4.29) and (4.30) extend beyond just a computational convenience. In fact, they are next used to demonstrate two useful consequences for the mapping  $\mathcal{N}$  on the subspaces  $G(L_1, L_2, n)$ . The first states that  $\mathcal{N}$  is an invariant mapping with respect to such spaces.

**Proposition 4.5.2** *Let  $u \in G(L_1, L_2, n)$ , where  $G(L_1, L_2, n) \subseteq G^{2N}$  is maximal. Then, the best approximation for  $\mathcal{N}(u)$  in  $G^{2N}$  is obtained in  $G(L_1, L_2, n)$ .*

*Proof:* Since  $\mathcal{N}(u) = u - s$ , it suffices to show that  $s \in G(L_1, L_2, n)$ . Fix any suitable  $z_1$  such that  $L_k = L_1 + nz_1$ . By the above results, an entry to  $\Lambda_u$  is nonzero only when  $L_m = L_2 + n(z_1 - z)$  or  $L_m = L_1 + n(z - z_1)$  for some nonnegative integer  $z \geq z_1$ . Thus, if  $PDJ(u)$  in (4.8) has a nonzero entry, the corresponding row in  $\Lambda_u$  is an image under  $P$  from the space  $G(L_1, L_2, n)$ . Therefore, in obtaining the least-squares solution  $Ps$  to the linear system, the conclusion  $s \in G(L_1, L_2, n)$  is clear.  $\square$

Of course, this result applies in the natural way if one considers instead the augmented Newton map  $\tilde{\mathcal{N}}$ .

The second result allows for a further computational simplification, applicable during iteration of the Newton maps. By referring to the analysis in Proposition 4.5.2, it is clear that when solving the linear system (4.8) for  $Ps$ , only those entries  $\langle D^2J(u)\Psi_k, \Psi_m \rangle$  of  $\Lambda_u$  are required for which  $\Psi_k, \Psi_m \in G(L_1, L_2, n)$ . After computing these entries, the algorithm replaces every diagonal entry that is zero with one, so that  $\Lambda_u$  is not forced to be a singular matrix. This type of procedure is termed a *minimal* computation of the matrix  $\Lambda_u$ .

Knowing how to efficiently compute Newton steps and the invariant behavior of the Newton mappings, the next obvious task is to construct algorithms and evaluate the results. In the next section, the “core” GNGA algorithm is described. Also, a general algorithm that is used to follow an arbitrary solution branch (given a reasonable solution estimate on that branch) is discussed.

## 4.6 A Generalized Algorithm and GNGA

The computational algorithms presented in this section are the building blocks for all of the simulation methods used in this research. The GNGA algorithm itself generalizes to allow the use of either the classical Newton map  $\mathcal{N}$ , or the augmented map  $\tilde{\mathcal{N}}$ . The branch following algorithm repeatedly executes GNGA typically with the augmented Newton map (although either may be used), and is used to follow all types of branch estimates that are observed.

Before specifying these algorithms, a definition of fundamental importance is first needed.

**Definition 4.6.1** For  $u \in G^{2N}$ , the number of eigenvalues of  $\Lambda_u$  that are less than zero is the **signature** of  $\Lambda_u$ .

Sometimes it is convenient also to refer to the signature of  $u$  itself, in which case the role of  $\Lambda_u$  is understood. Note that since  $\Lambda_u$  is symmetric and has only real number entries, each of its eigenvalues are real and the definition makes sense.

The GNGA algorithm stops when  $\|DJ(u)\|_2$  for the current iterate  $u$  is sufficiently small, then the signature of  $u$  is recorded. As discussed in the following chapter, this information is used by other algorithms to estimate points of bifurcation along solution branches.

The **GNGA Algorithm** is as follows:

```

Obtain the initial vector  $Pu \in \mathbb{R}^{2N}$  and  $a$ .
If  $\tilde{\mathcal{N}}$  is selected, obtain the initial vector  $Pv \in \mathbb{R}^{2N}$ .
Initialize the iteration counter.
LOOP:
  Compute the current iterate  $u$  on  $D$ .
  Compute the vector  $PDJ(u)$ .
  Compute  $\|DJ(u)\|_2$  and evaluate the STOP condition.
  Compute the minimal matrix  $\Lambda_u$  or  $\tilde{\Lambda}_u$ ; increment counter.
  Solve the system for  $Ps$  or  $(Ps, \Delta a)$ .
  Compute the next iterate:
     $Pu = Pu - Ps$  (classical algorithm with  $\mathcal{N}$ )
     $(Pu, a) = (Pu - Ps, a - \Delta a)$  (augmented algorithm with  $\tilde{\mathcal{N}}$ ).
STOP:
  Compute the matrix  $\Lambda_u$  and the signature of  $u$ .
  Output solution estimate information.

```

Standard LAPACK routines are used to obtain least-squares solutions and the signature of the estimate. The minimal matrix  $\Lambda_u$  ( $\tilde{\Lambda}_u$ ) has only those entries needed to find the search direction vector. Throughout the entire procedure, only those numbers in the matrix which may be nonzero are calculated.

The branch following algorithm typically is used with  $\tilde{\mathcal{N}}$ , although the simulation software allows for the classical method as well. For the classical

algorithm, the current branch estimate is used as the next guess, then the parameter is decremented, and the GNGA algorithm above is used with  $\mathcal{N}$ . Sometimes  $a$  is observed to be non-monotonic along a branch, in which case the classical method will fail. As in the GNGA algorithm, the input required depends upon which Newton map is to be used. If  $Pv$  is specified, it should be such that the sum  $u + v \in G^{2N}$  provides a good estimate for a nearby solution on the branch to follow. Once a solution estimate on the branch is determined, the vector  $Pv$  to be used next is formed as the difference between the current and previous solution estimates. The **STOP** condition depends on the expected results; generally the parameter  $a$  is checked for a range condition.

The **Branch Algorithm** is as follows:

```

Obtain a branch solution estimate  $Pu \in \mathbb{R}^{2N}$  and  $a$ .
If  $\tilde{\mathcal{N}}$  is selected, obtain the initial vector  $Pv \in \mathbb{R}^{2N}$ .
Obtain the parameter  $\epsilon > 0$  and initialize the loop counter.
LOOP:
  Increment the loop counter.
  Store the current solution estimate information.
  Set GNGA initial guess to:
     $Pu$  and  $a = a - \epsilon$  (classical algorithm)
     $Pu + \epsilon Pv$  (augmented algorithm).
  Execute GNGA; check  $(Pu, a)$  for the STOP condition.
  Compute the next vector  $Pv$  (augmented algorithm).

```

Among the many strengths of the augmented algorithm is that it allows the use of critical eigenfunctions for  $\Lambda_u$  in place of  $v$  when estimating the start of a bifurcating branch of estimates.

The algorithms above are used to estimate the solutions at which bifurcations occur, and then also to follow the corresponding new solution branches which are expected to exist based upon analytical considerations. The interplay between observations obtained by simulation and corresponding theoretical considerations allow for an abundance of insight into the characteristics of this particular GL problem.

# Chapter 5

## Equivalence, Equivariance and Invariance in $G^{2N}$

According to the variational method that is applied, of principal interest is the evolution of solution energy along the branch estimates. That is, the study will proceed by examining solution branches expressed in the form  $(a, J(u))$ ; where  $u$  is a solution estimate at a parameter value of  $a$ . One important way to distinguish two solution estimates at some  $a$  is to check if they have a different (nondimensionalized) energy. Since all estimations are made in some finite-dimensional Galerkin space  $G^{2N}$ , an expression for  $J(u)$  given  $u \in G^{2N}$  is therefore needed. After defining a concept of equivalence in  $J$  and studying its implications, the behavior of the Newton mappings used in the numerical algorithms with respect to this equivalence must be determined, and any related properties need to be extracted. First, several notational conveniences for Galerkin expansions to be used for the remaining discussions are presented.

### 5.1 Notations for $G^{2N}$ Expansions

Recall the expansion for  $u$  in Equation (3.20). For  $u \in G^{2N}$ , a convenient notation to use is to let

$$\gamma_k = \langle u, \Psi_k \rangle \quad \text{for } 1 \leq k \leq 2N$$

and

$$\begin{aligned} \alpha_k &= \gamma_k && \text{for } 1 \leq k \leq N \\ \beta_{k-N} &= \gamma_k && \text{for } N < k \leq 2N. \end{aligned}$$

Then,  $u$  can be expanded using real coefficients as

$$\begin{aligned}
u &= \sum_{k=1}^{2N} \langle u, \Psi_k \rangle \Psi_k = \sum_{k=1}^{2N} \gamma_k \Psi_k \\
&= \sum_{k=1}^N \alpha_k \Psi_k + \sum_{k=N+1}^{2N} \beta_{k-N} \Psi_k \\
&= \sum_{k=1}^N (\alpha_k \Psi_k + \beta_k \Psi_{k+N}).
\end{aligned} \tag{5.1}$$

Each notation might at times be convenient. When it is instead preferable to consider the expansion in terms of  $\{\psi_k\}_{k=1}^N$ , then for complex coefficients  $\{c_k\}$  satisfying  $c_k = \langle u, \psi_k \rangle + i\langle u, i\psi_k \rangle$  for  $k = 1, 2, \dots, N$ , note that

$$\begin{aligned}
\sum_{k=1}^N c_k \psi_k &= \sum_{k=1}^N (\langle u, \psi_k \rangle + i\langle u, i\psi_k \rangle) \psi_k \\
&= \sum_{k=1}^N (\langle u, \Psi_k \rangle + i\langle u, \Psi_{k+N} \rangle) \psi_k \\
&= \sum_{k=1}^N \langle u, \Psi_k \rangle \Psi_k + \sum_{k=1}^N \langle u, \Psi_{k+N} \rangle \Psi_{k+N} \\
&= \sum_{k=1}^N (\operatorname{Re} c_k) \Psi_k + \sum_{k=1}^N (\operatorname{Im} c_k) \Psi_{k+N}.
\end{aligned} \tag{5.2}$$

Now, it is clear that since  $u = \sum_{k=1}^N c_k \psi_k$ , it must be that  $\alpha_k = \operatorname{Re} c_k$  and  $\beta_k = \operatorname{Im} c_k$  for  $k = 1, 2, \dots, N$ . Note also that whenever it is more illustrative to incorporate the double-indexing scheme for expansions in  $\{\psi_k\}_{k=1}^N$  (as in Equation (4.24), for example), the relation

$$c_{\ell,j} = \alpha_{\ell,j} + i\beta_{\ell,j}$$

holds for each admissible double index  $(\ell, j)$  as well. For  $u \in G^{2N}$ , the energy functional  $J(u)$  is most easily expressed by use of the complex coefficients  $\{c_k\}$ .

## 5.2 The Energy Functional on Galerkin Space

Recall the expression for  $J(u)$  provided in Equation (2.10), and let  $u$  be a  $G^{2N}$  approximation for some  $H_B^2(D)$  function given by its equivalent expansions of Equations (5.1) and (5.2) above. Using the linearity of the integral, it follows that

$$J(u) = \int_D a|u|^2 dx + \int_D \frac{1}{2}|u|^4 dx + \int_D |(i\nabla + r\hat{\theta})u|^2 dx. \quad (5.3)$$

The first term may be computed in terms of the coefficients of its expansion, since

$$\int_D a|u|^2 dx = a \int_D |u|^2 dx = a\|u\|_2^2 = \frac{a}{2}\langle u, u \rangle = \frac{a}{2} \sum_{k=1}^N |c_k|^2 \quad (5.4)$$

by Parseval's formula and previous results. For the third term, the integral is calculated similarly with the use of Equation (3.8) to be

$$\begin{aligned} \int_D |(i\nabla + r\hat{\theta})u|^2 dx &= \langle (i\nabla + r\hat{\theta})u, (i\nabla + r\hat{\theta})u \rangle_2 = \langle (i\nabla + r\hat{\theta})^2 u, u \rangle_2 \\ &= \left\langle \sum_{k=1}^N \lambda_k c_k \psi_k, u \right\rangle_2 = \sum_{k=1}^N \lambda_k |c_k|^2 \|\psi_k, \psi_k\|_2^2 \\ &= \sum_{k=1}^N \frac{\lambda_k}{2} |c_k|^2 \langle \psi_k, \psi_k \rangle = \sum_{k=1}^N \frac{\lambda_k}{2} |c_k|^2. \end{aligned} \quad (5.5)$$

Generally, the second term is numerically integrated on  $D$ . This term is discussed in a more detailed fashion in the next section.

## 5.3 $J$ -Equivalence and the Group $\mathbb{T}^2$ .

A concept of equivalence in energy is next needed, in order to provide a means of classifying solution estimates and distinguishing between simulated solution branches. Several equivalence results are then demonstrated.

**Definition 5.3.1** *Let  $u, v \in H_B^2(D)$ , and fix the parameter  $a \in \mathbb{R}$ . Then,  $u$  and  $v$  are called  **$J$ -equivalent** if  $J(u) = J(v)$  and  $\|DJ(u)\|_2 = \|DJ(v)\|_2$ . In this case, the relation is denoted by  $u \sim v$ .*

It is clear that  $J$ -equivalence is an equivalence relation. A useful extension of Theorem 2.5.4 now follows.

**Proposition 5.3.2** *Let  $u \in H_B^2(D)$ , and fix  $a \in \mathbb{R}$ . Then for any  $c \in \mathbb{R}$ ,  $u \sim ue^{ic}$ .*

*Proof:* Let  $u \in H_B^2(D)$  and  $a, c \in \mathbb{R}$ . First, note that

$$\|DJ(u)\|_2 = |e^{ic}| \|DJ(u)\|_2 = \|e^{ic} DJ(u)\|_2 = \|DJ(e^{ic}u)\|_2,$$

and thus  $\|DJ(u)\|_2 = \|DJ(e^{ic}u)\|_2$ . For the second result, recall Theorem 2.5.4. For the particular GL problem posed by the functional  $J$  and Equation (1.1) on the space  $H_B^2(D)$ , the theorem implies that  $J(ue^{ic}) = J(u)$  for all  $c \in \mathbb{R}$ .  $\square$

To summarize this result; the gauge equivalence class of  $u$  is contained in its  $J$ -equivalence class at each parameter value  $a$ . This motivates the definition of function spaces of the form

$$G(L_1, L_2, n, \xi) \doteq \{u \in G(L_1, L_2, n) \mid \text{Arg}(c_{\ell,j}) = \xi + y_j\pi, y_j \in \mathbb{Z}\}, \quad (5.6)$$

for  $\xi \in \mathbb{R}$ . Here  $\ell = L_1 + nz$  for  $z = 0, 1, 2, \dots, (L_2 - L_1)/n$  as in Equation (4.25). If  $u \in G(L_1, L_2, n, \xi)$ , it is clear that  $e^{-i\xi}u \in G(L_1, L_2, n, 0)$ . Thus, with the use of Proposition 5.3.2, every such  $u$  is  $J$ -equivalent to a Galerkin function whose expansion coefficients are real numbers that agree in modulus with those for  $u$ .

The definition of  $J$ -equivalence will often be useful in cases where  $u \in G^{2N}$  only estimates a solution. In these situations, it is required that  $J(u) = J(v)$  and that the second condition holds for the best  $G^{2N}$  estimates of  $DJ(u)$  and  $DJ(v)$ . This convention should be understood whenever appropriate in the current context.

There is at least one other obvious equivalence to consider, based upon the cylindrically symmetric geometry of the domain  $D$ . Extending (5.6) above, Galerkin subspaces of the form  $G(L_1, L_2, n, \xi, \varphi) \subseteq G(L_1, L_2, n)$  for  $\varphi \in \mathbb{R}$  are defined as

$$G(L_1, L_2, n, \xi, \varphi) \doteq \{u \in G(L_1, L_2, n) \mid \text{Arg}(c_{L_1+nz,j}) = \xi + z\varphi + y_j\pi, y_j \in \mathbb{Z}\}. \quad (5.7)$$

Functions whose expansions are of this form represent a large class of solution estimates produced by the numerical algorithms. Clearly if  $u \in$

$G(L_1, L_2, n, \xi, \varphi)$  for some  $\xi, \varphi \in \mathbb{R}$ , then  $e^{-i\xi}u \in G(L_1, L_2, n, 0, \varphi)$ . If  $u \in G(L_1, L_2, n, 0, \varphi)$ , then the  $G^{2N}$  expansion for  $u$  takes the form

$$u(r, \theta) = \sum_{z=0}^{\tilde{z}} f_{\ell_z}(r) e^{iz\varphi} e^{i\ell_z\theta}, \quad (5.8)$$

where  $\tilde{z} = (L_2 - L_1)/n$ ,  $\ell_z = L_1 + nz$ , and  $f_{\ell_z}$  maps into  $\mathbb{R}$ . When  $u$  is a solution estimate, then  $u(r, \theta)e^{iL_1\frac{\varphi}{n}}$  is as well, and

$$\begin{aligned} u(r, \theta) &\sim \sum_{z=0}^{\tilde{z}} (f_{\ell_z}(r) e^{iz\varphi} e^{i\ell_z\theta}) e^{iL_1\frac{\varphi}{n}} \\ &= \sum_{z=0}^{\tilde{z}} f_{\ell_z}(r) e^{i\ell_z\theta} e^{izn(\frac{\varphi}{n})} e^{iL_1\frac{\varphi}{n}}. \\ &= \sum_{z=0}^{\tilde{z}} f_{\ell_z}(r) e^{i\ell_z(\theta + \frac{\varphi}{n})} \end{aligned} \quad (5.9)$$

This means that each such  $u$  is  $J$ -equivalent to an element  $v \in G(L_1, L_2, n, 0, 0)$  that is rotated clockwise about the  $z$ -axis through  $\frac{\varphi}{n}$  radians. That the last function in Equation (5.9) is in fact  $J$ -equivalent to such  $v$  is the subject of the next proposition.

**Proposition 5.3.3** *Let  $u \in G(L_1, L_2, n, 0, \varphi) \subseteq G^{2N}$  for some parameter  $a \in \mathbb{R}$ , and let  $\varphi \in \mathbb{R}$ . Let  $\tilde{u}(r, \theta) = u(r, \theta - \frac{\varphi}{n})$ . Then,  $u(r, \theta) \sim \tilde{u}(r, \theta)$ . That is,  $J(u) = J(\tilde{u})$  and  $\|DJ(u)\|_2 = \|DJ(\tilde{u})\|_2$ .*

*Proof:* Let  $a, \varphi \in \mathbb{R}$  and  $u \in G(L_1, L_2, n, 0, \varphi)$ . First, the equality regarding  $J$  is shown. According to Equations (5.4) and (5.5), the first and third term of  $J$  are the same number at both functions; indeed the phase of the Galerkin coefficients is irrelevant to these computations. The integrand of the second term must be formed for both functions. One may expand  $u$  as

$$u(r, \theta) = \sum_{z=0}^{\tilde{z}} f_{\ell_z}(r) e^{iz\varphi} e^{i\ell_z\theta},$$

as in Equation (5.8) above. Also, since

$$\tilde{u}(r, \theta) = u\left(r, \theta - \frac{\varphi}{n}\right) \sim \sum_{z=0}^{\tilde{z}} f_{\ell_z}(r) e^{i\ell_z\theta} = v(r, \theta)$$

according to Equation (5.9), by the transitivity of  $\sim$  it suffices to compare the Galerkin terms in  $G^{2N}$  of  $|u|^4$  and  $|v|^4$  that have a zero winding number. Clearly  $|u|^2 \in G(L_1 - L_2, L_2 - L_1, n)$ , and its expansion may be written as

$$|u(r, \theta)|^2 = \sum_{z=0}^{2\tilde{z}} g_{L_1 - L_2 + nz}(r) e^{i(L_1 - L_2 + nz)\theta} = \sum_{z=0}^{2\tilde{z}} g_{\lambda_z}(r) e^{i\lambda_z\theta},$$

where  $L_1 - L_2 + nz$  is denoted by  $\lambda_z$  for  $z = 0, 1, 2, \dots, 2\tilde{z}$ . A computation shows that

$$\begin{aligned} g_{\lambda_z} &= \sum_{y=0}^z f_{\ell_y} f_{\ell_{y+\tilde{z}-z}} e^{-i(\tilde{z}-z)\varphi} & \text{for } 0 \leq z < \tilde{z} \\ g_{\lambda_z} &= \sum_{y=0}^{2\tilde{z}-z} f_{\ell_y} f_{\ell_{y+z-\tilde{z}}} e^{-i(\tilde{z}-z)\varphi} & \text{for } \tilde{z} < z \leq 2\tilde{z} \\ g_{\lambda_z} &= \sum_{y=0}^{\tilde{z}} f_{\ell_y}^2 & \text{for } z = \tilde{z}. \end{aligned}$$

The term of  $|u|^4$  with zero winding number is therefore

$$\sum_{y=0}^{2\tilde{z}} g_{\lambda_y} g_{\lambda_{2\tilde{z}-y}},$$

since  $\lambda_z = -\lambda_{2\tilde{z}-z}$  for  $z = 0, 1, 2, \dots, 2\tilde{z}$ . The argument to the complex exponential factor of the  $y^{\text{th}}$  term is just

$$-(\tilde{z} - y)\varphi - (\tilde{z} - (2\tilde{z} - y))\varphi = -\tilde{z}\varphi + y\varphi + \tilde{z}\varphi - y\varphi = 0.$$

Thus, the zero winding number term in the integrand is the same for both  $|u|^4$  and  $|v|^4$ . This implies that  $\int_D |u|^4 dx = \int_D |v|^4 dx$ ,  $J(u) = J(v)$  and by transitivity  $J(u) = J(\tilde{u})$ .

Next, it is shown that  $\|DJ(u)\|_2 = \|DJ(v)\|_2$  in  $G^{2N}$ . The formula for  $DJ(u)$  allows an expansion as

$$DJ(u) = \sum_{z=0}^{\tilde{z}} h_{\ell_z}(r) e^{i\ell_z\theta},$$

here the functions  $h_{\ell_z}$  depend only on  $r$  and are generally complex valued. Since the eigenvalues of  $\mathcal{L}$  are real, the function  $\tilde{f}_{\ell_z} = \mathcal{L}f_{\ell_z}$  is a real valued function of  $r$ . Thus

$$h_{\ell_z} = \left( \tilde{f}_{\ell_z} + af_{\ell_z} \right) e^{iz\varphi} + \sum_{y=0}^{\tilde{z}} (f_{\ell_y} e^{iy\varphi}) g_{\lambda_{\tilde{z}+z-y}},$$

for  $z = 0, 1, 2, \dots, \tilde{z}$ . According to the analysis above, the argument to the complex exponential factor of the third term is just

$$y\varphi - (\tilde{z} - (\tilde{z} + z - y))\varphi = y\varphi + z\varphi - y\varphi = z\varphi,$$

so that  $u \in G(L_1, L_2, n, 0, \varphi)$  implies that  $DJ(u) \in G(L_1, L_2, n, 0, \varphi)$ . Next, since  $\|DJ(u)\|_2 = \int_D |DJ(u)|^2 dx$ , the term of zero winding number in the product  $|DJ(u)|^2$  must be formed. It follows that

$$\|DJ(u)\|_2 = \sum_{z=0}^{\tilde{z}} |h_{\ell_z}|^2 = \|DJ(v)\|_2,$$

hence the value of  $\varphi$  is not relevant. By transitivity,  $\|DJ(u)\|_2 = \|DJ(\tilde{u})\|_2$  and the result is shown.  $\square$

It should be noted that the results of Proposition 5.3.3 hold equally well when instead the coefficient functions  $f_{\ell_z}$  are complex-valued; the proof requires only minor modifications.

In summary, the proposition above implies that for each  $u \in G^{2N}$ , the  $J$ -equivalences  $u(r, \theta) \sim u(r, \theta - \varphi)$  and  $u \sim e^{i\xi}u$  follow, for every pair  $\xi, \varphi \in \mathbb{R}$ . This motivates the specification of the action of the well-known compact Lie group  $\mathbb{T}^2 = \mathbb{S}^1 \times \mathbb{S}^1$  on  $G$  and its subspaces. Thus, for  $(\xi, \varphi) \in \mathbb{T}^2$  and  $u \in G$ , let

$$u(r, \theta) \cdot (\xi, \varphi) = e^{i\xi}u(r, \theta - \varphi). \quad (5.10)$$

Note (for example) that if  $u \in G(L_1, L_2, n, \xi, \varphi)$ , then  $u \cdot (-\xi + L_1 \frac{\phi}{n}, \frac{\varphi}{n}) \in G(L_1, L_2, n, 0, 0)$ . Next, the results of Propositions 5.3.2 and 5.3.3 are extended to provide several equivariance results.

## 5.4 $\mathbb{T}^2$ –Equivariance and Invariances of $\mathcal{N}$ .

Some of the most useful properties lending insight into the numerical results that follow are now available. In the normal way, if  $\Gamma$  is a group acting on  $G$ ,

then a map  $A$  on  $G$  is called  $\Gamma$ -Equivariant if  $A(u \cdot \tau) = A(u) \cdot \tau$  for all  $\tau \in \Gamma$  and  $u \in G$ . Of course, the same definition is also used with regard to the finite-dimensional subspaces of  $G$ ; the case where  $u \in G(L_1, L_2, n) \subseteq G^{2N}$  will be of primary interest. As has already been noted, often the map under consideration is not  $G^{2N}$ -Invariant. However, all functions are regarded in this section in terms of their best estimate in  $G^{2N}$ . Therefore, the analysis proceeds by demonstrating the needed results with respect to the  $G^{2N}$  projections of the images under  $A$  of the current domain of interest. Unless otherwise specified, this should be understood according to the current context. First, a result that follows from the previous two propositions is available.

**Proposition 5.4.1** *For each  $N \in \mathbb{N}$ , the map  $DJ$  on  $G^{2N}$  is  $\mathbb{T}^2$ -Equivariant.*

*Proof:* Let  $N \in \mathbb{N}$ . It will be shown that the result holds on an arbitrary subspace  $G(L_1, L_2, n) \subseteq G^{2N}$  for any suitable numbers  $L_1, L_2$  and  $n$ . Thus, let  $u \in G(L_1, L_2, n)$  and let  $(\xi, \varphi) \in \mathbb{T}^2$ . For complex-valued functions  $f_{\ell_z}$ , one may expand  $u$  as

$$u(r, \theta) = \sum_{z=0}^{\tilde{z}} f_{\ell_z}(r) e^{i\ell_z \theta}.$$

Similarly to Proposition 5.3.3,

$$|u(r, \theta)|^2 = \sum_{z=0}^{2\tilde{z}} g_{\lambda_z}(r) e^{i\lambda_z \theta}$$

where  $L_1 - L_2 + nz$  is denoted by  $\lambda_z$  for  $z = 0, 1, 2, \dots, 2\tilde{z}$ . Here

$$\begin{aligned} g_{\lambda_z} &= \sum_{y=0}^z f_{\ell_y} \bar{f}_{\ell_{y+\tilde{z}-z}} & \text{for } 0 \leq z < \tilde{z} \\ g_{\lambda_z} &= \sum_{y=0}^{2\tilde{z}-z} \bar{f}_{\ell_y} f_{\ell_{y+z-\tilde{z}}} & \text{for } \tilde{z} < z \leq 2\tilde{z} \\ g_{\lambda_z} &= \sum_{y=0}^{\tilde{z}} |f_{\ell_y}|^2 & \text{for } z = \tilde{z}. \end{aligned}$$

Using expansions for  $DJ(u)$  as in Proposition 5.3.3, it follows first that

$$DJ(u) \cdot (\xi, \varphi) = e^{i\xi} \sum_{z=0}^{\tilde{z}} h_{\ell_z}(r) e^{i\ell_z(\theta-\varphi)} = \sum_{z=0}^{\tilde{z}} (e^{i\xi} e^{-i\ell_z \varphi}) h_{\ell_z}(r) e^{i\ell_z \theta}.$$

The coefficient functions are complex-valued, and

$$\begin{aligned} (e^{i\xi} e^{-il_z \varphi}) h_{\ell_z} &= (e^{i\xi} e^{-il_z \varphi}) \left[ \left( \tilde{f}_{\ell_z} + a f_{\ell_z} \right) + \sum_{y=0}^{\tilde{z}} f_{\ell_y} g_{\lambda_{\tilde{z}+z-y}} \right] \\ &= \mathcal{L} \left( e^{i\xi} f_{\ell_z} e^{-il_z \varphi} \right) + a \left( e^{i\xi} f_{\ell_z} e^{-il_z \varphi} \right) + (e^{i\xi} e^{-il_z \varphi}) \sum_{y=0}^{\tilde{z}} f_{\ell_y} g_{\lambda_{\tilde{z}+z-y}}. \end{aligned}$$

The factor  $g_{\lambda_{\tilde{z}+z-y}}$  in the last summation is evaluated according to the current index  $z$ . Thus, its terms are expressed differently at each  $y$ , according to the above expressions. For  $y > z$ ,

$$(e^{i\xi} e^{-il_z \varphi}) f_{\ell_y} g_{\lambda_{\tilde{z}+z-y}} = (e^{i\xi} f_{\ell_y} e^{-il_y \varphi}) \sum_{x=0}^{\tilde{z}+z-y} (e^{i\xi} f_{\ell_x} e^{-il_x \varphi}) \left( \overline{e^{i\xi} f_{\ell_{x-z+y}} e^{-il_{x-z+y} \varphi}} \right).$$

For  $y < z$ , it follows that

$$(e^{i\xi} e^{-il_z \varphi}) f_{\ell_y} g_{\lambda_{\tilde{z}+z-y}} = (e^{i\xi} f_{\ell_y} e^{-il_y \varphi}) \sum_{x=0}^{\tilde{z}-z+y} \left( \overline{e^{i\xi} f_{\ell_x} e^{-il_x \varphi}} \right) (e^{i\xi} f_{\ell_{x+z-y}} e^{-il_{x+z-y} \varphi}).$$

Lastly, when  $y = z$ ,

$$(e^{i\xi} e^{-il_z \varphi}) f_{\ell_y} g_{\lambda_{\tilde{z}+z-y}} = (e^{i\xi} f_{\ell_y} e^{-il_y \varphi}) \sum_{x=0}^{\tilde{z}} (e^{i\xi} f_{\ell_x} e^{-il_x \varphi}) \left( \overline{e^{i\xi} f_{\ell_x} e^{-il_x \varphi}} \right).$$

Since

$$u(r, \theta) \cdot (\xi, \varphi) = \sum_{z=0}^{\tilde{z}} (e^{i\xi} e^{-il_z \varphi} f_{\ell_z}(r)) e^{il_z \theta},$$

the above computation implies that the  $z^{\text{th}}$  coefficient function of  $DJ(u) \cdot (\xi, \varphi)$  is exactly that for  $DJ(u \cdot (\xi, \varphi))$ , for  $z = 0, 1, 2, \dots, \tilde{z}$ . Therefore, the result follows.  $\square$

An important corollary now follows from the proof above. Notice that if the coefficient functions  $f_{\ell_z}$  are real-valued in the expansion for  $u$ , then the functions  $h_{\ell_z}$  must be real as well (take  $(\xi, \varphi) = (0, 0)$ , for example). Therefore, the invariance property

$$DJ[G(L_1, L_2, n, 0, 0)] \subseteq G(L_1, L_2, n, 0, 0)$$

in  $G^{2N}$  is established. This result is sharpened by the following:

**Corollary 5.4.2** For each  $N \in \mathbb{N}$  and  $G(L_1, L_2, n, \xi, \varphi) \subseteq G^{2N}$ , it follows that  $DJ[G(L_1, L_2, n, \xi, \varphi)] \subseteq G(L_1, L_2, n, \xi, \varphi)$  in  $G^{2N}$ .

*Proof:* Let  $G(L_1, L_2, n, \xi, \varphi) \subseteq G^{2N}$ , and let  $u \in G(L_1, L_2, n, \xi, \varphi)$ . Then if  $\tau = (-\xi + L_1 \frac{\phi}{n}, \frac{\varphi}{n})$ , it follows that  $u \cdot \tau \in G(L_1, L_2, n, 0, 0)$  and also that  $DJ(u \cdot \tau) = DJ(u) \cdot \tau$ . Since  $DJ(u \cdot \tau) \in G(L_1, L_2, n, 0, 0)$ , the result follows.  $\square$

Similar arguments apply for the operator  $D^2J$ .

**Proposition 5.4.3** For each  $N \in \mathbb{N}$ , the map  $D^2J$  on  $G^{2N} \times G^{2N}$  is  $\mathbb{T}^2$ -Equivariant.

*Proof:* Let  $N \in \mathbb{N}$ . It will be shown that the result holds on an arbitrary subspace  $G(L_1, L_2, n) \times G(L_1, L_2, n) \subseteq G^{2N} \times G^{2N}$ , for any suitable numbers  $L_1, L_2$  and  $n$ . Thus, let  $u, v \in G(L_1, L_2, n)$  and let  $(\xi, \varphi) \in \mathbb{T}^2$ . It suffices to show that  $D^2(u \cdot (\xi, \varphi))(v \cdot (\xi, \varphi)) = D^2(u)v \cdot (\xi, \varphi)$ . The needed expansions are

$$u(r, \theta) = \sum_{z=0}^{\tilde{z}} f_{\ell_z}(r) e^{i\ell_z \theta} \quad \text{and} \quad v(r, \theta) = \sum_{z=0}^{\tilde{z}} p_{\ell_z}(r) e^{i\ell_z \theta},$$

where  $\tilde{z} = (L_2 - L_1)/n$ , and the coefficient functions are complex-valued. The product  $u^2$  will be required. If

$$u(r, \theta)^2 = \sum_{z=0}^{2\tilde{z}} q_{\kappa_z}(r) e^{i\kappa_z \theta}$$

where  $\kappa_z = 2L_1 + nz$  for  $z = 0, 1, \dots, 2\tilde{z}$ , then

$$\begin{aligned} q_{\kappa_z} &= \sum_{y=0}^z f_{\ell_y} f_{\ell_{z-y}} && \text{for } 0 \leq z < \tilde{z} \\ q_{\kappa_z} &= \sum_{y=0}^{2\tilde{z}-z} f_{\ell_{z-y}} f_{\ell_{z-(z-y)}} && \text{for } \tilde{z} < z \leq 2\tilde{z} \\ q_{\kappa_z} &= \sum_{y=0}^{\tilde{z}} f_{\ell_y} f_{\ell_{z-y}} && \text{for } z = \tilde{z}. \end{aligned}$$

The expansion for  $D^2J(u)(v) \cdot (\xi, \varphi)$  has the form of

$$D^2J(u)v \cdot (\xi, \varphi) = (e^{i\xi} e^{-i\ell_z \varphi}) \sum_{z=0}^{\tilde{z}} k_{\ell_z} e^{i\ell_z \theta},$$

where

$$k_{\ell_z} = \tilde{p}_{\ell_z} + ap_{\ell_z} + 2 \sum_{y=0}^{\tilde{z}} p_{\ell_y} g_{\lambda_{\tilde{z}+z-y}} + \sum_{y=0}^{\tilde{z}} \bar{p}_{\ell_y} q_{\kappa_{y+z}}$$

is a function of  $r$  into  $\mathbb{C}$ , for  $z = 0, 1, 2, \dots, \tilde{z}$ . Recall the expressions for the coefficient functions  $g_{\lambda_z}$  above, and note that  $\mathcal{L}p_{\ell_z} = \tilde{p}_{\ell_z}$ . Thus

$$\begin{aligned} (e^{i\xi} e^{-il_z \varphi}) k_{\ell_z} &= (e^{i\xi} e^{-il_z \varphi}) \left[ \tilde{p}_{\ell_z} + ap_{\ell_z} + 2 \sum_{y=0}^{\tilde{z}} p_{\ell_y} g_{\lambda_{\tilde{z}+z-y}} + \sum_{y=0}^{\tilde{z}} \bar{p}_{\ell_y} q_{\kappa_{y+z}} \right] \\ &= \mathcal{L} (e^{i\xi} p_{\ell_z} e^{-il_z \varphi}) + a (e^{i\xi} p_{\ell_z} e^{-il_z \varphi}) \\ &\quad + 2 (e^{i\xi} e^{-il_z \varphi}) \sum_{y=0}^{\tilde{z}} p_{\ell_y} g_{\lambda_{\tilde{z}+z-y}} + (e^{i\xi} e^{-il_z \varphi}) \sum_{y=0}^{\tilde{z}} \bar{p}_{\ell_y} q_{\kappa_{y+z}}. \end{aligned}$$

As is Propostion 5.4.1, the terms of the last two summations depend on the current coefficient function and the index  $y$ . Consider the summation  $2 (e^{i\xi} e^{-il_z \varphi}) \sum_{y=0}^{\tilde{z}} p_{\ell_y} g_{\lambda_{\tilde{z}+z-y}}$ . For  $y > z$ ,

$$(e^{i\xi} e^{-il_z \varphi}) p_{\ell_y} g_{\lambda_{\tilde{z}+z-y}} = (e^{i\xi} p_{\ell_y} e^{-il_y \varphi}) \sum_{x=0}^{\tilde{z}+z-y} (e^{i\xi} f_{\ell_x} e^{-il_x \varphi}) \left( \overline{e^{i\xi} f_{\ell_{x-z+y}} e^{-il_{x-z+y} \varphi}} \right).$$

For  $y < z$ , it follows that

$$(e^{i\xi} e^{-il_z \varphi}) p_{\ell_y} g_{\lambda_{\tilde{z}+z-y}} = (e^{i\xi} p_{\ell_y} e^{-il_y \varphi}) \sum_{x=0}^{\tilde{z}-z+y} \left( \overline{e^{i\xi} f_{\ell_x} e^{-il_x \varphi}} \right) (e^{i\xi} f_{\ell_{x+z-y}} e^{-il_{x+z-y} \varphi}).$$

When  $y = z$ ,

$$(e^{i\xi} e^{-il_z \varphi}) p_{\ell_y} g_{\lambda_{\tilde{z}+z-y}} = (e^{i\xi} p_{\ell_y} e^{-il_y \varphi}) \sum_{x=0}^{\tilde{z}} (e^{i\xi} f_{\ell_x} e^{-il_x \varphi}) \left( \overline{e^{i\xi} f_{\ell_x} e^{-il_x \varphi}} \right).$$

Considering now the second summation  $(e^{i\xi} e^{-il_z \varphi}) \sum_{y=0}^{\tilde{z}} \bar{p}_{\ell_y} q_{\kappa_{y+z}}$ , for  $y < \tilde{z} - z$ ,

$$(e^{i\xi} e^{-il_z \varphi}) \bar{p}_{\ell_y} q_{\kappa_{y+z}} = \left( \overline{e^{i\xi} p_{\ell_y} e^{-il_y \varphi}} \right) \sum_{x=0}^{y+z} (e^{i\xi} f_{\ell_x} e^{-il_x \varphi}) (e^{i\xi} f_{\ell_{y+z-x}} e^{-il_{y+z-x} \varphi}).$$

For  $y > \tilde{z} - z$ , it follows that

$$\begin{aligned} (e^{i\xi} e^{-il_z \varphi}) \bar{p}_{\ell_y} q_{\kappa_{y+z}} &= \\ &= \left( \overline{e^{i\xi} p_{\ell_y} e^{-il_y \varphi}} \right) \sum_{x=0}^{2\tilde{z}-y-z} (e^{i\xi} f_{\ell_{\tilde{z}-x}} e^{-il_{\tilde{z}-x} \varphi}) (e^{i\xi} f_{\ell_{x+y+z-\tilde{z}}} e^{-il_{x+y+z-\tilde{z}} \varphi}). \end{aligned}$$

When  $y = \tilde{z} - z$ ,

$$(e^{i\xi} e^{-il_z \varphi}) \bar{p}_{\ell_y} q_{\kappa_{y+z}} = \left( \overline{e^{i\xi} p_{\ell_y} e^{-il_y \varphi}} \right) \sum_{x=0}^{\tilde{z}} (e^{i\xi} f_{\ell_x} e^{-il_x \varphi}) (e^{i\xi} f_{\ell_{\tilde{z}-x}} e^{-il_{\tilde{z}-x} \varphi}).$$

Since

$$u(r, \theta) \cdot (\xi, \varphi) = \sum_{z=0}^{\tilde{z}} (e^{i\xi} e^{-il_z \varphi} f_{\ell_z}(r)) e^{il_z \theta}$$

and

$$v(r, \theta) \cdot (\xi, \varphi) = \sum_{z=0}^{\tilde{z}} (e^{i\xi} e^{-il_z \varphi} p_{\ell_z}(r)) e^{il_z \theta},$$

the result follows.  $\square$

Again, there is an important corollary to consider. If the functions  $f_{\ell_z}$  and  $p_{\ell_z}$  are real-valued, then it is obvious from the above discussion that the coefficient functions  $k_{\ell_z}$  in the expansion of  $D^2 J(u)v$  must be real as well. Therefore, if  $u \in G(L_1, L_2, n, 0, 0)$  then it must be that

$$D^2 J(u) [G(L_1, L_2, n, 0, 0)] \subseteq G(L_1, L_2, n, 0, 0)$$

in  $G^{2N}$ . The corollary below provides the natural extension.

**Corollary 5.4.4** *For each  $N \in \mathbb{N}$  and  $u \in G(L_1, L_2, n, \xi, \varphi) \subseteq G^{2N}$ , it follows that  $D^2 J(u) [G(L_1, L_2, n, \xi, \varphi)] \subseteq G(L_1, L_2, n, \xi, \varphi)$  in  $G^{2N}$ .*

*Proof:* Let  $G(L_1, L_2, n, \xi, \varphi) \subseteq G^{2N}$ , and let  $u, v \in G(L_1, L_2, n, \xi, \varphi)$ . Then if  $\tau = (-\xi + L_1 \frac{\phi}{n}, \frac{\varphi}{n})$ , it follows that  $u \cdot \tau, v \cdot \tau \in G(L_1, L_2, n, 0, 0)$  and also that  $D^2 J(u \cdot \tau)(v \cdot \tau) = D^2 J(u)v \cdot \tau$ . Since  $D^2 J(u \cdot \tau)(v \cdot \tau) \in G(L_1, L_2, n, 0, 0)$ , the conclusion is implied.  $\square$

These propositions may be combined to show the analogous results for the Newton mapping  $\mathcal{N}$ . At each  $u \in G^{2N}$ , there exists a Moore-Penrose generalized inverse  $(D^2 J(u))^\dagger$  for the linear operator  $D^2 J(u)$  in  $G^{2N}$ . Furthermore,

since the search direction function  $s$  is obtained by least-squares approximation, it follows that

$$\mathcal{N}(u) = u - (D^2J(u))^\dagger DJ(u).$$

A well-known corollary of Proposition 5.4.3 may be obtained after recalling that the generalized inverse satisfies the same equivariance conditions as the original transformation does.

**Corollary 5.4.5** *For each  $N \in \mathbb{N}$ , the Newton map  $\mathcal{N}$  on  $G^{2N}$  is  $\mathbb{T}^2$ -Equivariant.*

*Proof:* The previous two propositions, along with the fact that  $(u + v) \cdot \tau = u \cdot \tau + v \cdot \tau$  for all  $\tau \in \mathbb{T}^2$ , imply the conclusion.  $\square$

A similar result holds for the augmented map  $\tilde{\mathcal{N}}$ . Furthermore, the invariance of the Newton maps with regard to the spaces  $G(L_1, L_2, n, \xi, \varphi) \subseteq G^{2N}$  may be shown. If  $u \in G(L_1, L_2, n, \xi, \varphi)$ , then by restricting the  $D^2J(u)$  map to the orthogonal complement  $K_u^\perp$  of its kernel  $K_u$  at  $u$ , it is clear that

$$D^2(u) [G(L_1, L_2, n, 0, 0) \cap K_u^\perp] \subseteq G(L_1, L_2, n, 0, 0) \cap K_u^\perp \subseteq G(L_1, L_2, n, 0, 0),$$

which can only mean that

$$(D^2J(u))^\dagger [G(L_1, L_2, n, 0, 0)] \subseteq G(L_1, L_2, n, 0, 0).$$

But since  $(D^2J(u))^\dagger$  is  $\mathbb{T}^2$ -Equivariant, it is now a simple matter to conclude that

$$(D^2J(u))^\dagger [G(L_1, L_2, n, \xi, \varphi)] \subseteq G(L_1, L_2, n, \xi, \varphi)$$

whenever  $u \in G(L_1, L_2, n, \xi, \varphi)$ , using Corollary 5.4.4. From this analysis, the proof of the next result is obvious.

**Corollary 5.4.6** *For each  $N \in \mathbb{N}$  and  $G(L_1, L_2, n, \xi, \varphi) \subseteq G^{2N}$ , it follows that  $\mathcal{N} [G(L_1, L_2, n, \xi, \varphi)] \subseteq G(L_1, L_2, n, \xi, \varphi)$ .*

Again, the analogous result for the augmented Newton mapping is clear.

There are examples of solution estimates not in subspaces of the form  $G(L_1, L_2, n, \xi, \varphi)$ . In these cases, it nevertheless may be possible to obtain  $J$ -Equivalent estimates by means of one or more well-defined action(s) that cannot be expressed in terms of  $\mathbb{T}^2$  group elements alone. For these situations, an additional action, defined by Dr. James Swift, is needed. Fortunately, the results of the previous two sections may be naturally extended to accommodate this complication.

## 5.5 The “Conjugate-Reflection” Action $C$ .

Typically, observed solution estimates are elements of some subspace  $G(L_1, L_2, n, \xi, \varphi)$  of  $G^{2N}$ , and the  $J$ -Equivalence classes of a solution are adequately described in terms of the action of the group  $\mathbb{T}^2$  alone. However, this is not always the case. Thus, the action

$$u \cdot C \doteq \overline{u(r, -\theta)} \quad (5.11)$$

for  $u \in H_B^2(D)$  is defined. First, the needed extensions of Propositions 5.3.2 and 5.3.3 are discussed.

**Proposition 5.5.1** *Let  $u \in G^{2N}$  and fix  $a \in \mathbb{R}$ . Then,  $u \sim u \cdot C$ .*

*Proof:* First, it is shown that  $J(u) = J(u \cdot C)$ . Expand  $u \in G(L_1, L_2, n)$  as in Proposition 5.4.1, and note that

$$\overline{u(r, -\theta)} = \sum_{z=0}^{\tilde{z}} \overline{f_{\ell_z}}(r) e^{i\ell_z \theta},$$

and

$$|\overline{u(r, -\theta)}|^2 = \sum_{z=0}^{2\tilde{z}} \overline{g_{\lambda_z}}(r) e^{i\lambda_z \theta}.$$

Here

$$\begin{aligned} \overline{g_{\lambda_z}} &= \overline{\sum_{y=0}^z f_{\ell_y} \overline{f_{\ell_{y+\tilde{z}-z}}} } = \sum_{y=0}^z \overline{f_{\ell_y}} f_{\ell_{y+\tilde{z}-z}} & \text{for } 0 \leq z < \tilde{z} \\ \overline{g_{\lambda_z}} &= \overline{\sum_{y=0}^{2\tilde{z}-z} \overline{f_{\ell_y}} f_{\ell_{y+z-\tilde{z}}} } = \sum_{y=0}^{2\tilde{z}-z} f_{\ell_y} \overline{f_{\ell_{y+z-\tilde{z}}} } & \text{for } \tilde{z} < z \leq 2\tilde{z} \\ \overline{g_{\lambda_z}} &= \sum_{y=0}^{\tilde{z}} |f_{\ell_y}|^2 & \text{for } z = \tilde{z}, \end{aligned}$$

hence when replacing  $z$  with  $2\tilde{z} - z$  above, it follows that  $\overline{g_{\lambda_{2\tilde{z}-z}}} = g_{\lambda_z}$  and  $\overline{g_{\lambda_z}} = g_{\lambda_{2\tilde{z}-z}}$  for  $z = 0, 1, 2, \dots, 2\tilde{z}$ . The remaining computations mimic those in Proposition 5.3.2. Concentrating upon the quartic term in the functional

$J$ , it follows that

$$\begin{aligned} \int_D |u|^4 dx &= \int_D \left( \sum_{y=0}^{2\bar{z}} g_{\lambda_y} g_{\lambda_{2\bar{z}-y}} \right) dx = \int_D \left( \sum_{y=0}^{2\bar{z}} |g_{\lambda_y}|^2 \right) dx \\ &= \int_D \left( \sum_{y=0}^{2\bar{z}} |\bar{g}_{\lambda_y}|^2 \right) dx = \int_D \left( \sum_{y=0}^{2\bar{z}} \bar{g}_{\lambda_y} \bar{g}_{\lambda_{2\bar{z}-y}} \right) dx \\ &= \int_D |u \cdot C|^4 dx. \end{aligned}$$

Thus,  $J(u) = J(u \cdot C)$ . The fact that  $\|DJ(u)\|_2 = \|DJ(u \cdot C)\|_2$  follows in a similar way, since each norm may be expressed in terms of the modulus of  $r$ -dependent coefficient functions.  $\square$

The natural extensions of the equivariance results in Propositions 5.4.1 and 5.4.3 are obtained by reproducing each corresponding proof with the action of  $(\xi, \varphi)$  replaced with that of  $C$ . For this reason, the proof of the following proposition is omitted.

**Proposition 5.5.2** *Let  $u, v \in G^{2N}$ . Then, the mappings  $DJ$ ,  $D^2J$  and  $\mathcal{N}$  are equivariant with respect to the action of  $C$ . That is,  $DJ(u \cdot C) = DJ(u) \cdot C$ ,  $D^2J(u \cdot C)(v \cdot C) = D^2J(u)v \cdot C$ , and  $\mathcal{N}(u \cdot C) = \mathcal{N}(u) \cdot C$ .*

The results of this chapter have far-reaching implications throughout the remainder of this study. In several cases, the results will allow the conclusion that several types of bifurcating solution branches estimated by the numerical algorithms consist of a single  $J$ -equivalence class. Furthermore, whenever a collection of elements whose action fixes a given solution may be specified, additional insight into the types of bifurcating solution branches that can exist is obtained. Next, simulation results are presented along with the related procedures and supporting theory necessary to clarify the observations.

# Chapter 6

## Solution Branch Estimation and Analysis

The GNGA and Branch simulation algorithms previously described are next applied and extended to simulate solution branches that pass through several points of *bifurcation*. This terminology is defined in the usual way: A solution estimate  $u$  on a branch at a parameter value of  $a$  is called a point of *bifurcation* if there is more than one branch of solution estimates beginning at the point  $(a, u)$ . Recall that two branches are to be distinguished if the solution estimates at any parameter at which the branch exists are not  $J$ -Equivalent in the sense of Definition 5.3.1. Additionally, it might occur that two branch estimates are  $J$ -Equivalent, although there is no known group action mapping the estimates along one branch to the other. In this case, one also regards the solution branches as being distinct. This observation makes the definition of another well-known type of equivalence relation useful. It provides another means of distinguishing functions from  $G^{2N}$ , and the estimated solution branches that they compose.

**Definition 6.0.3** *Let  $u, v \in G$ , and let  $\mathcal{G}$  denote an abstract group acting on the space  $G$ . Then,  $u$  and  $v$  are called  $\mathcal{G}$ -Equivalent if there exists  $\xi \in \mathcal{G}$  such that  $u = v \cdot \xi$ .*

It is convenient to denote the  $\mathbb{T}^2$ -Equivalence relation by  $\sim_2$ . Previous propositions have demonstrated that  $\mathbb{T}^2$ -Equivalence implies  $J$ -Equivalence, however the converse might not always follow.

Along a given solution branch, an invariance of the Newton map of the form  $\mathcal{N}[G_1] \subseteq G_1$  is typically observed, where  $G_1$  is some subspace of the

form  $G(L_1, L_2, n)$  (for appropriately selected integers  $L_1, L_2$  and  $n$ ) of minimal dimension in  $L^2(D)$  such that the containment condition holds. For example, take  $G_1 = \{0\}$  along the trivial branch, otherwise one selects  $L_1, L_2$  according to the maximality criteria and  $n$  as large as possible. Whenever an invariance of this form holds, additional insight into the properties of solutions along the corresponding branch is available.

Many classes of solution estimates always have known null eigenfunctions corresponding to the infinitesimal actions of elements from  $\mathbb{T}^2$ ; indeed arbitrary actions in this infinite group always produce a function that is  $J$ -Equivalent to the original. Thus, when studying the *critical eigenspace* of  $D^2J(u)$  (the kernel) at a given solution estimate  $u \in G^{2N}$  for the purpose of detecting a new solution branch, these *default* null functions should be disregarded. Then, one expects that a new solution branch may begin near a given point  $(a, u)$  provided that an estimate of an eigenspace contained in the kernel of the operator  $D^2J(u)$  and properly containing the default eigenspace can be made. This eigenspace, less the collection of nonzero default eigenfunctions, is termed “branch critical,” and a branch critical eigenfunction is often called a branch eigenfunction. The sum of each branch eigenfunction and  $u$  are then regarded as candidate initial guesses for the Branch Algorithm to produce new estimates on distinct solution branches.

In the standard way, one assumes that a bifurcation point may exist between two estimates along a given branch if the signatures of  $\Lambda_u$  at each estimate  $u$  are not the same. Such an observation suggests an increase in the dimension of the kernel of  $D^2J(u)$  at some intermediate point estimate  $(a, u)$ , and thus the existence of a branch eigenspace near the same point that may contain the building blocks of suitable initial guesses for the Branch Algorithm. To specify the presumed bifurcation points themselves requires an additional algorithm that produces an estimate of the corresponding branch eigenspace. As will be shown, it sometimes follows that every branch eigenfunction of  $D^2J(u)$  near a bifurcation point estimate  $(a, u)$  forms no better an initial guess when added to  $u$  than does any other. However, this conclusion is not always valid; there are cases in which the branch eigenspace must be analyzed more carefully. To begin, the bifurcations from the trivial solution are examined, and related analysis is provided.

## 6.1 Bifurcations from the Trivial Branch

It is convenient to refer to the solution branch estimates that begin from the trivial solution as *primary* branches. The line  $u = 0$  for all  $a \in \mathbb{R}$  is called the *trivial branch* of solutions. Knowledge of the properties of the Newton maps provided in the previous chapter allows for a complete characterization of the primary branch approximations that can possibly be produced by the numerical algorithms. In fact, since the critical eigenspace near any trivial bifurcation point always takes a known form, a complete qualitative description of primary branches is available. Note that when  $u = 0$ , critical eigenfunctions are branch eigenfunctions.

When considering Equation (4.12), if  $u$  is a trivial solution then the only nonzero entries of  $\Lambda_u$  are the diagonal entries. Moreover, it follows that the  $k^{\text{th}}$  diagonal entry is zero if and only if  $a = -\lambda_k$ . Thus, the kernel of the estimate  $\Lambda_u$  of  $D^2J(0)$  is nontrivial if and only if  $a = -\lambda_k$  for some  $k \in \{1, 2, \dots, N\}$ , in which case the corresponding critical eigenspace must be exactly

$$E_k = \{c_k \psi_k \mid c_k \in \mathbb{C}\}. \quad (6.1)$$

It is clear that for every pair of eigenfunctions  $e_1, e_2 \in E_k$  such that  $|e_1| = |e_2|$ , there exist  $\xi, \varphi \in \mathbb{R}$  such that the relations  $e_1 = e_2 \cdot (\xi, 0)$  and  $e_1 = e_2 \cdot (0, \varphi)$  hold. To clarify this statement, note that it must therefore follow that for every such pair, only a single element from the abstract group  $\mathbb{S}^1$  is necessary to find an action sending  $e_1$  to  $e_2$ , or vice-versa. Here the action of  $\mathbb{S}^1$  on  $G$  may be defined either as that of gauge transformation or as rotation; the former will be used for simplicity. In this way, the orbit of any eigenfunction under the abstract group  $\mathbb{S}^1$  is contained in its  $J$ -Equivalence class. Since the index  $k$  corresponds to exactly one admissible  $(L, j)$  combination obtained in the construction of  $G^{2N}$ , it should also be noted that for each  $\xi \in \mathbb{R}$  and  $e \in E_k$ , the action of the element  $(L\xi, \xi)$  fixes the function  $e$ ; that is  $e \cdot \xi = e$ . Also, generally it is clear that  $E_k \subseteq G(L, L, 1)$ . Often, it is convenient to refer to the  $k^{\text{th}}$  branch by its corresponding combination  $(L, j)$ ; the use of either type of reference should be clear from the context. The next result maintains that there can be only one primary branch estimated by the numerical algorithms up to  $J$ -Equivalence beginning at each point  $(-\lambda_k, 0)$ .

**Proposition 6.1.1** *Let  $(-\lambda_k, 0)$  denote a bifurcation point estimate on the trivial branch, for some  $k \in \{1, 2, \dots, N\}$ . Then, there is a primary branch estimate  $(a, v)$  obtained by the Branch Algorithm beginning at  $(-\lambda_k, 0)$  and*

having solution estimates  $v \in G(L, L, 1, 0)$  at each parameter value  $a$  for which it is defined. This branch is unique up to a change in sign of each function  $v$ . Furthermore, if  $(a, u)$  denotes any other primary branch estimate beginning at  $(-\lambda_k, 0)$  obtained by the Branch Algorithm, then at each parameter value  $a$  for which the branch is defined,  $u \in G(L, L, 1, \xi)$  for some  $\xi \in \mathbb{S}^1$ . Lastly, it follows that  $u \sim v$  at each parameter value  $a$  for which both branches are defined, and therefore that  $(a, J(v))$  uniquely describes the energy versus parameter dependence of every primary branch estimate beginning at  $(-\lambda_k, 0)$ .

*Proof:* The proof presumes the existence of a suitable guess in the critical eigenspace that generates any arbitrary primary branch beginning at  $(-\lambda_k, 0)$ . The observed behavior of the numerical simulations indicates that this is a reasonable assumption. Let  $k \in \{1, 2, \dots, N\}$ , and let  $e = c\psi_k$  for some suitable real number  $c$  so that  $e \in G(L, L, 1, 0)$ . Using either type of Newton mapping, the result of each successive Newton iteration performed during the Branch Algorithm is an element of  $G(L, L, 1, 0)$  as well, according to Corollary 5.4.6. Note that the sign of the function estimate  $v$  obtained at each parameter value  $a$  can depend only upon the sign of  $c$ , thus each such function is unique up to a change in sign. Now, let  $(a, u)$  denote any other primary branch estimate beginning at  $(-\lambda_k, 0)$ , and let  $e_u \in E_k$  represent the critical eigenvector supplied to the Branch Algorithm in obtaining the primary branch estimate  $(a, u)$ . First, it is shown that  $u \in G(L, L, 1, \xi)$  at each branch parameter value  $a$ , for some  $\xi \in \mathbb{S}^1$ . Since  $e_u \in E_k$ , choose  $\xi \in \mathbb{S}^1$  such that  $e_u \in G(L, L, 1, \xi)$ . For either type of Newton mapping, the result of each successive Newton iteration is an element of  $G(L, L, 1, \xi)$ , by Corollary 5.4.6; when using the augmented algorithm, the fact that  $G(L, L, 1, \xi)$  is a vector subspace was used for this conclusion. Therefore, it follows that  $u \in G(L, L, 1, \xi)$  at each  $a$ . Now, starting with the initial guess for each branch at the point  $(-\lambda_k, 0)$ , it is clear that  $\mathcal{N}(e_u) = \mathcal{N}(e \cdot \xi) = \mathcal{N}(e) \cdot \xi$ ; the same result holds when replacing  $\mathcal{N}$  with  $\tilde{\mathcal{N}}$ . By inductively applying Corollary 5.4.5, it must be that  $u \sim_2 v$  and thus  $u \sim v$  at each common parameter value. Since the branch  $(a, u)$  was chosen arbitrarily, it follows that the estimate  $(a, J(v))$  describes the energy vs. parameter relationship of any primary branch estimate.  $\square$

To summarize this theorem, for each  $k = 1, 2, \dots, N$  there is exactly one primary branch up to  $J$ -Equivalence beginning at  $a = -\lambda_k$ .

Primary branch estimates corresponding to the smallest nine eigenvalues

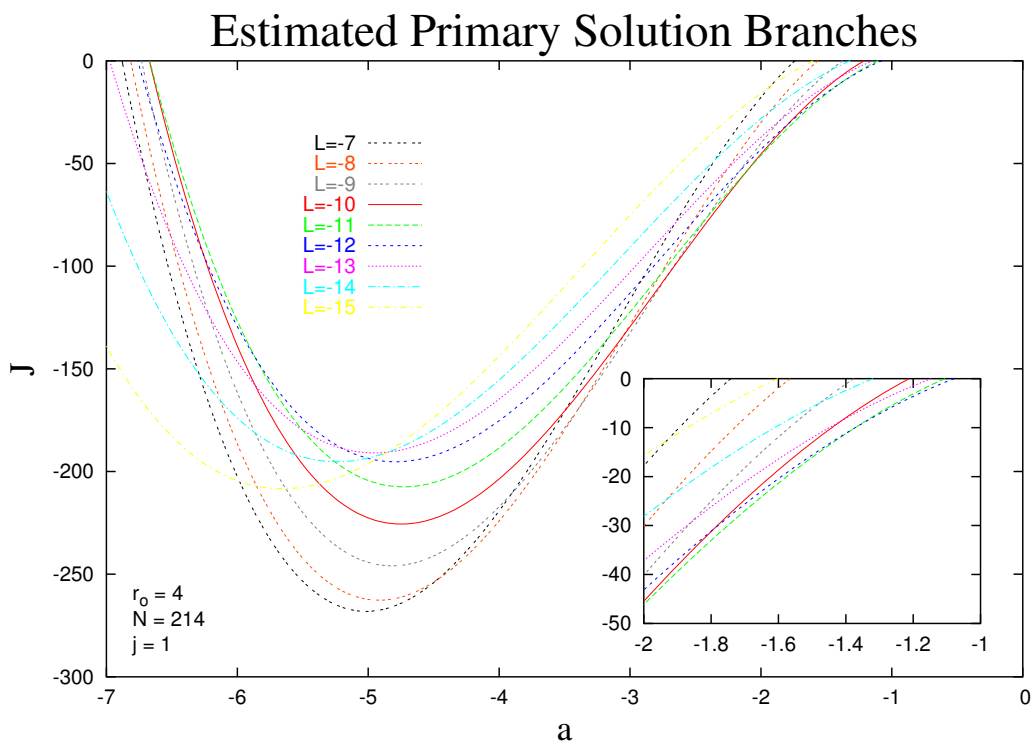


Figure 6.1: Primary branch estimates beginning at  $(-\lambda_{L,1}, 0)$  for  $-15 \leq L \leq -7$ . The branches for which  $-13 \leq L \leq -9$  are signature 0 on parameter intervals contained in  $[-2, -1]$ ; the branch with  $L = -12$  has the largest such interval.

in the spectrum of  $\mathcal{L}$  when  $r_o = 4$  are shown in Figure 6.1. In each case, the estimating functions are elements of  $G(L, L, 1, 0)$ ; that is, each  $L^2(D)$  expansion coefficient  $c_{L,j}$  is a real number. The signature 0 branches with  $L = -11, -12$  and parameter  $a > -2$  are perhaps the best estimate that the numerical method provides for a global minimizer of  $J$  at the onset of superconductivity.

At each primary branch estimate  $(a, u)$ , the function  $u \cdot \xi$  for arbitrary  $\xi \in \mathbb{S}^1$  is an equivalent solution estimate. This suggests that at each such  $u$ , the matrix  $\Lambda_u$  is singular, a condition which is always observed. In forming the difference between  $u$  and  $u \cdot \xi$  as  $\xi \rightarrow 0$ , the null eigenvector  $iu$  is obtained. This result has implications for the computational algorithms, after

reconsidering the implications of Corollary 5.4.6. Suppose that the Branch Algorithm is used to form the particular branch estimate  $(a, v)$  suggested by Proposition 6.1.1, where each  $v \in G(L, L, 1, 0)$  at each parameter value  $a$ . It is clear then that all Newton iterations needed in computing this branch are elements of the same space,  $G(L, L, 1, 0)$ . Hence, in terms of Equation (4.12), one sees that only those entries of  $\Lambda_u$  for which  $1 \leq m \leq N$  are required to compute any Newton step. Since the entries corresponding to when  $N < k \leq 2N$ ,  $1 \leq m \leq N$  are in this case zero, it follows that only those for which  $1 \leq k, m \leq N$  are needed to properly compute each search direction estimate. But, it is clear that the implementation of these rules will have an even greater impact upon computational efficiency when one recalls that for every solution estimate produced by  $\mathcal{N}$ , there is a corresponding null eigenfunction in  $G(L, L, 1, \pi/2)$ . After replacing each zero diagonal entry with one, the resulting minimal matrix  $\Lambda_u$  cannot have an eigenfunction from  $G(L, L, 1, \pi/2)$ . Therefore, the rank of  $\Lambda_u$  is effectively increased, without compromising the integrity of the iterations. The resulting increase in rate of convergence means that fewer Newton iterations are required, hence an improvement in the run-time of the algorithm does result. This type of minimal computation for  $\Lambda_u$  applies when the Galerkin coefficients of the current Newton iterate are real, and will be useful in many instances when producing estimates for solution branches.

Figure 6.2 depicts primary solution estimates on the branches corresponding to  $(L, j) = (-12, 1)$  and  $(L, j) = (-12, 2)$ . The diagram shows an increased superfluid density near the boundary of  $D$ , which is a phenomena that has been documented by several authors (see [3]). It is clear from the figure that any  $\mathbb{S}^1$  action can only result in another solution estimate of the same energy. Furthermore, such action might either be regarded as a gauge adjustment, in which the colors in the phase plot are effectively “cycled,” or as a rotation in the variable  $\theta$ , which produces here the same effect. When  $j = 2$ , the corresponding primary branch begins at  $-\lambda_{-12,2} \approx -7.5$ , and its solution estimates begin with a substantially larger signature given by exactly twice the number of eigenvalues of  $\mathcal{L}$  less than  $\lambda_{-12,2}$ . The observation that the electron-pair density maximizes away from the boundary of  $D$  suggests that this function estimates a saddle point, rather than a minimizer, of  $J$ .

The characteristics of the solutions shown are typical of all primary branch estimates that are produced by the numerical method. In all cases observed, the phase of the solution estimate depends linearly on  $\theta$  according

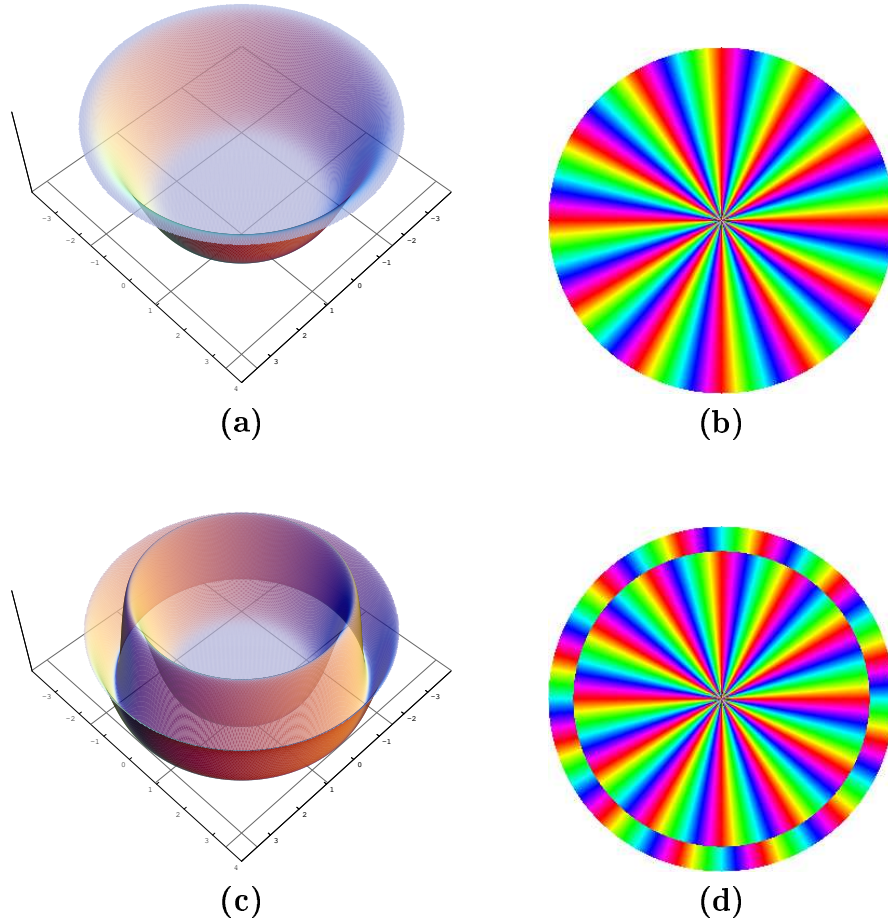


Figure 6.2: (a) Squared modulus plot of a primary solution estimate with  $(L, j) = (-12, 1)$ . The solution pictured corresponds to  $a \approx -2$  and  $J(u) \approx -42$  in Figure 6.1. (b) The phase plot of the  $(-12, 1)$  estimate. There is an apparent factor of 12 between the phase and  $\theta$ , and no dependence on  $r$ . (c) The squared modulus plot of a primary solution estimate with  $(L, j) = (-12, 2)$ . The corresponding branch begins near  $a = -7.5$ , the 36<sup>th</sup> primary branch that occurs when decreasing the parameter from zero. The branch begins with a signature of 72, and the estimate shown has the same signature. (d) The phase plot of the  $(-12, 2)$  estimate indicates a sign change near the boundary of  $D$ . Again, there is no dependence of the phase on  $r$ .

to the winding number, and there is no  $r$  dependence. Also, each estimate has exactly  $j - 1$  concentric circles in  $D$  at which the solution passes through zero. The signature of estimates along the primary branches is studied next, as it applies to the formation of secondary solution branch estimates.

## 6.2 Bifurcations from the Primary Branches

Estimated solution branches that begin at a primary solution estimate are called *secondary* branches. The equivariance and invariance properties of the Newton map are again instrumental in the study of the secondary branch approximations that have been obtained. All of these estimations are found to exhibit several common characteristics, allowing for interesting conclusions and computational rules that motivate further study. In particular, it will be shown that as in the case of primary branch estimates, only one secondary branch begins near each bifurcation point, up to  $J$ -Equivalence.

First, the algorithm used to specify reasonable estimates for bifurcation points on primary branches is introduced. It relies upon the fact that at each primary solution estimate  $(a, u)$ , the matrix  $\Lambda_u$  has at least one eigenvalue of zero corresponding to the null eigenvector  $iu$  discussed in the previous section. The input is two points  $(a_1, u_1)$  and  $(a_2, u_2)$ , with  $a_1 < a_2$ , on a branch between which a single bifurcation point on the branch exists. A detected change in solution signature along a branch can only correspond to the change in sign of one or more eigenvalues of  $\Lambda_u$ ; these are called the *branch* eigenvalues. The algorithm works essentially by finding a zero of a branch eigenvalue of  $\Lambda_u$  near  $u$  as a function of parameter  $a$ . It is convenient to use the term *character* when referring to the algebraic multiplicity of a branch eigenvalue. The *character* of a bifurcation point estimate is defined to be the number of branch eigenvalues including multiplicity for that point. Whenever there is only one branch eigenvalue, the character of that eigenvalue and the character of the associated bifurcation point are the same. Also, it is clear that the character of a bifurcation point equals the absolute value of the detected change in the signature of  $\Lambda_u$  that is recorded by the Branch Algorithm when passing that point.

In all simulations to date, it is observed that there is only one branch eigenvalue up to algebraic multiplicity near any approximate bifurcation point, and the design of the Primary Bifurcation Algorithm takes this observation as an assumption. Furthermore, the algorithm was designed for the

cases when the character of a bifurcation point is either 1 or 2; although most often only the latter situation is observed for points along primary branches. The estimate for the branch eigenspace is determined at the initial function  $u_1$  by using the LAPACK routines to store the eigenspace corresponding to the branch eigenvalue for  $\Lambda_{u_1}$ . For this reason, the initial estimates themselves are required to be reasonably good estimates of the bifurcation point.

The **Primary Bifurcation Algorithm** is as follows:

Obtain the initial estimates  $(a_1, Pu_1)$  and  $(a_2, Pu_2)$ .

Store the character of the bifurcation point.

Store the estimated branch eigenspace.

LOOP:

    Verify the character of the bifurcation point.

    Setup indexing rules to evaluate the branch eigenvalue.

    Evaluate the branch eigenvalue at each parameter value.

    Estimate a bifurcation parameter value  $a_*$ .

    Compute a solution estimate and the branch eigenvalue at  $a_*$ .

    Check for indexing changes and the STOP condition.

    Reset the bifurcation point estimates.

STOP:

    Store the bifurcation estimate  $(a_*, u_*)$

This algorithm does not select the eigenvector that should be used when forming an initial guess for the Branch Algorithm, it merely provides a good estimate of the branch eigenspace and the corresponding bifurcation point.

Further study of the properties of  $D^2J(u)$  when  $u$  is a primary bifurcation point estimate allow for significant insight into the types of null eigenspaces that may be observed. First, there is an intermediate result regarding the gauge transformations of critical eigenfunctions.

**Proposition 6.2.1** *Let  $u \in G^{2N}$  be a solution estimate on a primary branch such that  $(a, u)$  is a bifurcation point estimate, and let  $v$  be a critical eigenfunction of  $D^2J(u)$ . Then,  $v \cdot (\xi, 0)$  is also a critical eigenfunction if and only if  $\xi = y\pi$  for  $y \in \mathbb{Z}$ .*

*Proof:* If  $v$  is a critical eigenfunction of  $D^2J(u)$ , then

$$D^2J(u)v + av + 2|u|^2v + u^2\bar{v} = 0.$$

Let  $\xi \in \mathbb{R}$ . Then,  $v \cdot (\xi, 0) = e^{i\xi}v$  is a critical eigenfunction as well if and only if

$$e^{i\xi} (D^2J(u)v + av + 2|u|^2v) + e^{-i\xi} (u^2\bar{v}) = 0.$$

By substituting the first expression into the second, both expressions are zero if and only if

$$(e^{-i\xi} - e^{i\xi}) u^2\bar{v} = 0.$$

The function  $u^2\bar{v}$  is not the zero function, thus it is required that

$$\sin(\xi) = 0,$$

and the result follows.  $\square$

The next result is useful when considering primary bifurcation point estimates with a single corresponding branch eigenvalue (up to multiplicity). First, consider when the coefficients  $c_{L,j}$  of the expansion for  $u$  are real.

**Proposition 6.2.2** *Let  $u \in G(L, L, 1, 0)$  be a solution estimate on a primary branch such that  $(a, u)$  is a bifurcation point estimate. Then, there is a nontrivial estimate for a branch eigenspace of  $D^2J(u)$  as an operator mapping into  $G^{2N}$ . Furthermore, if this branch eigenspace is not contained in  $G(L, L, 1)$ , then  $e_1(r, \theta) = f(r)e^{i(L-n)\theta} + g(r)e^{i(L+n)\theta}$  is a branch eigenfunction of  $D^2J(u)$  for some  $n \in \mathbb{N}$ , and real-valued functions  $f$  and  $g$  of  $r$  such that  $f, g \neq 0$ . In this case  $e_2(r, \theta) = if(r)e^{i(L-n)\theta} - ig(r)e^{i(L+n)\theta}$  is also a branch eigenfunction of the same operator, and the character of the bifurcation estimate is at least 2.*

*Proof:* Since  $(a, u)$  is a bifurcation point estimate, the existence of an estimated branch eigenspace of  $D^2J(u)$  may be assumed. For mode indices  $k, m \in \{1, 2, \dots, 2N\}$ , let  $L_k, L_m$  denote their corresponding winding numbers. First, consider any  $k \in \{1, 2, \dots, N\}$  such that  $L_k \neq L$ , and set  $n = |L_k - L|$ . According to the computational rules provided in Equations (4.29) and (4.30), the  $m^{\text{th}}$  entry in row  $k$  of  $\Lambda_u$  is nonzero only if  $L_m = L_k$  or  $L_m = 2L - L_k$ . If  $L_k < L$ , then since  $L_k = L - (L - L_k) = L - n$  and  $2L - L_k = L + (L - L_k) = L + n$ , it follows that the  $m^{\text{th}}$  entry is nonzero only when  $L_m = L - n$  or  $L_m = L + n$ . The result is the same when  $L_k > L$ , since then  $L_k = L + (L_k - L) = L + n$  and  $2L - L_k = L - (L_k - L) = L - n$ . Since the branch eigenspace is nonempty and not contained in  $G(L, L, 1)$ , choose  $k \in \{1, 2, \dots, N\}$  such that  $L_k \neq L$  and the  $m^{\text{th}}$  entries of row  $k$  described above are not all zero. Since  $u \in G(L, L, 1, 0)$ , when  $N < m \leq 2N$

the corresponding entry to  $\Lambda_u$  is zero, according to Equation (4.12). This means that  $e_1$  has the indicated form for some real-valued functions  $f$  and  $g$  and natural number  $n$ . Next, consider row  $k + N$  of  $\Lambda_u$ . Then, the entries to  $\Lambda_u$  for which  $1 \leq m \leq N$  are zero. Also, when  $N < m \leq 2N$ , similar arguments show that the  $m^{\text{th}}$  entry of the row is nonzero only if  $L_m = L - n$  or  $L_m = L + n$ . Since  $L_{m-N} = L_m$  for each  $m$  satisfying  $N < m \leq 2N$ , there are two possibilities to consider. First, it might be that the entries for which  $L_m = L - n$  are the negative of those for which  $L_{m-N} = L - n$  on row  $k$ , and the entries for which  $L_m = L + n$  are equal to those for which  $L_{m-N} = L + n$  on row  $k$ . Otherwise, only the reverse situation can occur; that is that the entries for which  $L_m = L - n$  are equal to those for which  $L_{m-N} = L - n$  on row  $k$ , and the entries for which  $L_m = L + n$  are the negative of those for which  $L_{m-N} = L + n$  on row  $k$ . Thus,  $e_2$  is an eigenfunction of the indicated form. It remains to show that both functions  $f$  and  $g$  are nonzero. Suppose otherwise, and without loss of generality suppose that  $g = 0$ . Now, for each pair of real numbers  $\alpha_1$  and  $\alpha_2$ , it must follow that  $\alpha_1 P e_1 + \alpha_2 P e_2$  is an eigenvector for  $\Lambda_u$ . In particular, since  $e_1(r, \theta) = f(r)e^{i(L-n)\theta}$ , for each  $\xi \in \mathbb{R}$  it follows then that  $e^{i\xi} e_1$  is an eigenfunction of  $D^2 J(u)$ . Clearly, this contradicts Proposition 6.2.1. Lastly, since the functions  $e_1$  and  $e_2$  are linearly independent and correspond to the single branch eigenvalue of  $D^2 J(u)$ , this eigenvalue must have a minimum character of 2, whence  $u$  itself has a character of at least 2.  $\square$

As mentioned, for the functions  $e_1$  and  $e_2$  in the above proposition,  $P e_1$  and  $P e_2$  are linearly independent in  $\mathbb{R}^{2N}$ . Thus, given the branch eigenfunction estimates  $e_1$  and  $e_2$  of Proposition 6.2.2 near a bifurcation point estimate  $(a, u) \in \mathbb{R} \times G(L, L, 1, 0)$  of character 2, the corresponding branch eigenspace must be spanned over the real numbers by the same functions. In this case, every branch eigenfunction of the operator  $D^2 J(u)$  is a real multiple of the function  $\cos \varphi e_1 + \sin \varphi e_2$ , for some  $\varphi \in \mathbb{R}$ . This analysis motivates the next result. For convenience, the branch eigenspace corresponding to a solution estimate  $u$  near a bifurcation point is denoted by  $E_u$ .

**Proposition 6.2.3** *Let  $u \in G(L, L, 1, 0)$  be a solution estimate on a primary branch such that  $(a, u)$  is a bifurcation point estimate of character 2, and suppose that the branch eigenfunctions  $e_1, e_2 \in E_u$  as in Proposition 6.2.2 are given. Then, every element of  $E_u$  is a real multiple of  $e_1 \cdot (L\varphi, \varphi)$  for some  $\varphi \in \mathbb{R}$ .*

*Proof:* Let  $\tilde{e} \in E_u$ . Given the eigenfunctions  $e_1$  and  $e_2$ , one may choose  $\varphi, c \in \mathbb{R}$  such that

$$\tilde{e} = c [\cos(n\varphi) e_1 + \sin(n\varphi) e_2].$$

If  $\tilde{e}$  is the zero function, then with  $c = 0$  the result holds. Otherwise,  $c \neq 0$  and a calculation shows that

$$\begin{aligned} \frac{1}{c} \tilde{e}(r, \theta) &= \cos(n\varphi) e_1(r, \theta) + \sin(n\varphi) e_2(r, \theta) \\ &= e^{iL\varphi} e^{-iL\varphi} [\cos(n\varphi) (f(r)e^{i(L-n)\theta} + g(r)e^{i(L+n)\theta}) \\ &\quad + \sin(n\varphi) (if(r)e^{i(L-n)\theta} - ig(r)e^{i(L+n)\theta})] \\ &= e^{iL\varphi} e^{-iL\varphi} [(f(r) \cos(n\varphi) + if(r) \sin(n\varphi)) e^{i(L-n)\theta} \\ &\quad + (g(r) \cos(n\varphi) - ig(r) \sin(n\varphi)) e^{i(L+n)\theta}] \\ &= e^{iL\varphi} (f(r)e^{i(L-n)\theta} e^{-iL\varphi} e^{i(n\varphi)} + g(r)e^{i(L+n)\theta} e^{-iL\varphi} e^{-i(n\varphi)}) \\ &= e^{iL\varphi} (f(r)e^{i(L-n)(\theta-\varphi)} + g(r)e^{i(L+n)(\theta-\varphi)}) = e_1 \cdot (L\varphi, \varphi). \end{aligned}$$

□

Thus, in this case every branch eigenfunction is a gauge-adjusted rotation of every other branch eigenfunction. One other intermediate result is needed to provide the necessary framework for the main result of this section.

**Proposition 6.2.4** *Let  $u \in G(L, L, 1, 0)$  be a solution estimate on a primary branch such that  $(a, u)$  is a bifurcation point estimate of character 2, and suppose that the branch eigenfunctions  $e_1, e_2 \in E_u$  as in Proposition 6.2.2 are given. Then, for each  $e \in E_u$ , it follows that  $u + e \in G(L_1, L_2, n, \xi, \varphi)$  for suitable  $L_1, L_2 \in \mathbb{Z}$ ,  $n \in \mathbb{N}$  and some  $(\xi, \varphi) \in \mathbb{T}^2$ .*

*Proof:* Let  $e \in E_u$ . Then, for some  $\varphi, c \in \mathbb{R}$  it follows that  $e = c e_1 \cdot (-L\varphi/n, -\varphi/n)$  by Proposition 6.2.3, where  $e_1$  is as in Proposition 6.2.2.

Here  $n$  is the natural number corresponding to the branch eigenspace  $E_u$ . Note that  $e$  therefore may be written as

$$e(r, \theta) = c \left( e^{-i\varphi} f(r) e^{i(L-n)\theta} + e^{+i\varphi} g(r) e^{i(L+n)\theta} \right),$$

for some real-valued functions  $f$  and  $g$  of  $r$ . Select  $L_1, L_2$  according to the maximality condition, and note then that  $u + e \in G(L_1, L_2, n)$ . Now, choose  $z_* \in \{0, 1, 2, \dots, (L_2 - L_1)/n\}$  such that  $L = L_1 + nz_*$ . Setting  $\xi = -z_*\varphi$ , it follows that  $e \in G(L_1, L_2, n, \xi, \varphi)$ . Since here  $u \in G(L, L, 1, 0)$ , the conclusion follows.  $\square$

By Corollary 5.4.6, it therefore follows that every secondary branch estimate beginning at a primary branch estimate  $u \in G(L, L, 1, 0)$  (with corresponding branch eigenfunctions  $e_1, e_2 \in E_u$  as in Proposition 6.2.2) is an element of some  $G^{2N}$  subspace of the form  $G(L_1, L_2, n, \xi, \varphi)$ . Moreover, if one uses  $u + e_1$  as an initial guess for the Branch Algorithm, the resulting secondary branch will be composed of estimates from  $G(L_1, L_2, n, 0, 0)$ , and will have Galerkin expansion coefficients  $c_{\ell,j} \in \mathbb{R}$ . Now, it must follow that the Branch Algorithm will produce only one secondary branch beginning at each such primary bifurcation point estimate, up to  $J$ -Equivalence.

**Proposition 6.2.5** *Let  $u \in G^{2N}$  be a solution estimate on a primary branch such that  $(a, u)$  is a bifurcation point estimate of character 2. Let  $u_1$  denote the unique function up to sign from  $G(L, L, 1, 0)$  that is  $J$ -Equivalent to  $u$  at  $a$ , and suppose that the branch eigenfunctions  $e_1, e_2 \in E_{u_1}$  as in Proposition 6.2.2 are given. Then, any two secondary branch estimates obtained from the Branch Algorithm beginning at  $(a, u)$  and  $(a, u_1)$  are pointwise  $J$ -Equivalent.*

*Proof:* Let  $(a, v)$  and  $(a, v_1)$  denote any two secondary branch estimates obtained from the Branch Algorithm beginning at  $(a, u)$  and  $(a, u_1)$ , respectively. Let  $e_1, e_2$  denote the branch eigenfunctions for  $D^2J(u_1)$  from Proposition 6.2.2. Choose  $\xi \in \mathbb{R}$  such that  $u = u_1 \cdot \xi$ , and note then that  $E_{u_1} = E_u \cdot (\xi, 0)$ , according to Proposition 5.4.3. Since the branch eigenspace of  $D^2J(u_1)$  must in this case be spanned by  $e_1$  and  $e_2$ , suppose without loss of generality that the initial guesses to the Branch Algorithm producing the branch estimates  $(a, u)$  and  $(a, u_1)$  are  $u + e_1 \cdot (\xi + L\varphi_1, \varphi_1)$  and  $u_1 + e_1 \cdot (L\varphi_2, \varphi_2)$ , respectively, for some real numbers  $\varphi_1, \varphi_2 \in \mathbb{R}$ . Recalling

that  $u, u_1 \in G(L, L, 1)$ , it follows that

$$\begin{aligned} u + e_1 \cdot (\xi + L\varphi_1, \varphi_1) &= u_1 \cdot (\xi, 0) + e_1 \cdot (\xi + L\varphi_1, \varphi_1) \\ &= (u_1 \cdot (L\varphi_1, \varphi_1)) \cdot (\xi, 0) + e_1 \cdot (\xi + L\varphi_1, \varphi_1) \\ &= (u_1 + e_1) \cdot (\xi + L\varphi_1, \varphi_1), \end{aligned}$$

and that

$$\begin{aligned} u_1 + e_1 \cdot (L\varphi_2, \varphi_2) &= u_1 \cdot (L\varphi_2, \varphi_2) + e_1 \cdot (L\varphi_2, \varphi_2) \\ &= (u_1 + e_1) \cdot (L\varphi_2, \varphi_2). \end{aligned}$$

Thus

$$\mathcal{N}(u + e_1 \cdot (\xi + L\varphi_1, \varphi_1)) = \mathcal{N}(u_1 + e_1) \cdot (\xi + L\varphi_1, \varphi_1),$$

and

$$\mathcal{N}(u_1 + e_1 \cdot (L\varphi_2, \varphi_2)) = \mathcal{N}(u_1 + e_1) \cdot (L\varphi_2, \varphi_2),$$

so that  $\mathcal{N}(u + e_1 \cdot (\xi + L\varphi_1, \varphi_1)) \sim \mathcal{N}(u_1 + e_1 \cdot (L\varphi_2, \varphi_2))$ . According to the Branch Algorithm, it follows by induction that each pair of solution estimates  $v$  and  $v_1$  obtained must be  $J$ -Equivalent at each parameter value  $a$ . When considering the augmented algorithm, the fact that the subspaces of the form  $G(L_1, L_2, n, \xi, \varphi)$  are vector spaces was used. Thus, the conclusion follows.  $\square$

The fact that  $u \cdot (L\varphi, \varphi) = u$  for all  $\varphi \in \mathbb{R}$  is needed in showing the above proposition. Notice that if the branch  $(a, v_1)$  is obtained from the Branch Algorithm using the above indicated guess with  $\varphi_2 = 0$ , then  $v_1 \in G(L_1, L_2, n, 0, 0)$  at each parameter value  $a$ . Therefore, as in the case of simulated primary solution branches, each secondary solution branch (of the type considered in Proposition 6.2.5) may be estimated equivalently in terms of functions whose Galerkin coefficients are real numbers.

Several extensions, as they apply to the case when a bifurcation point estimate is observed to be of character 1, may be drawn from the above analysis. First, note that the converse of Proposition 6.2.2 implies that if a primary bifurcation point estimate  $u \in G(L, L, 1, 0)$  is of character 1 and  $e$  is a branch eigenfunction for  $D^2J(u)$ , then  $e \in G(L, L, 1)$  as well. It then follows that either  $e = f(r)e^{iL\theta}$  or  $e = if(r)e^{iL\theta}$ , for some nonzero function  $f$  of  $r$  mapping into  $\mathbb{R}$ . One can see in particular that if  $u + if(r)e^{iL\theta}$  converges under  $\mathcal{N}$  to a new branch estimate  $v$  near  $u$ , then certainly  $v \in G(L, L, 1)$ . However, it could happen that  $v \notin G(L, L, 1, \xi)$  for all  $\xi \in \mathbb{R}$ . The simulation

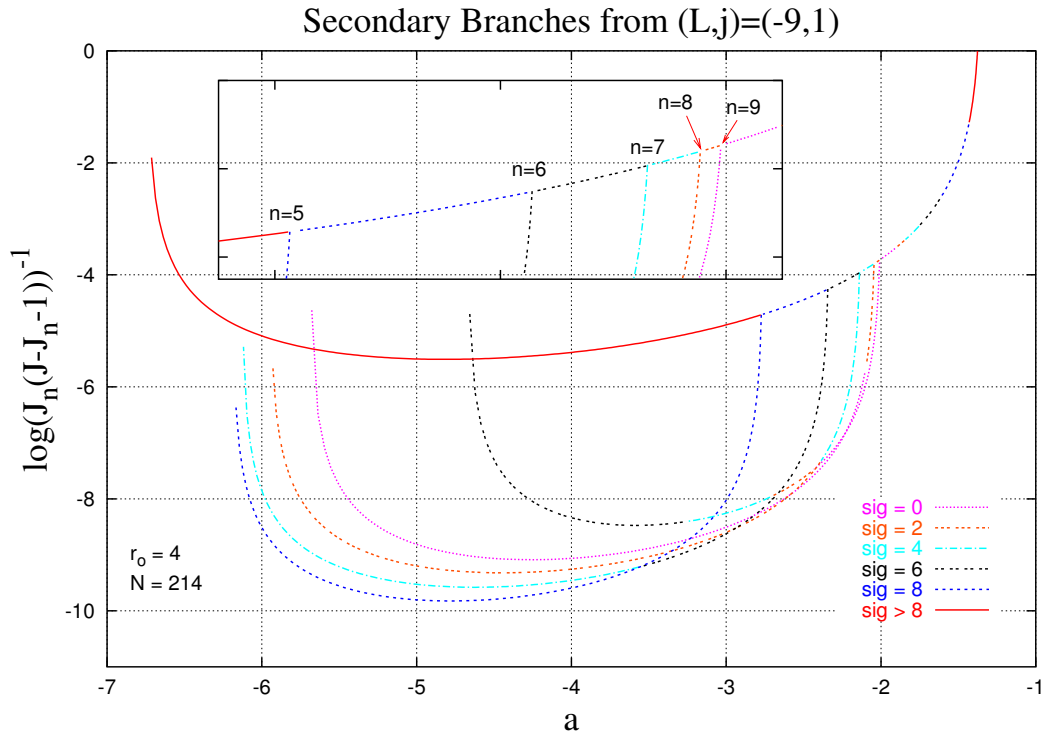


Figure 6.3: Plot of the secondary branch estimates bifurcating from the  $(L, j) = (-9, 1)$  primary branch. The number  $J_n$  for  $5 \leq n \leq 9$  denotes the energy of the corresponding bifurcation point estimate. The trace legend indicates the signature of  $\Lambda_u$  at each estimate  $u$ .

results observed indicate that this situation is rare, although possible; an example solution estimate is available.

All secondary branch estimates bifurcating from the primary branches  $(L, 1)$  for  $-7 \leq L \leq -12$  were simulated with  $N = 99$ , and those which either contained solution estimates of signature 0, or probable estimates for minimizers of  $J$ , were re-simulated with  $N = 214$ . Results for the case with  $L = -9$  are depicted in Figure 6.3. The scaling of each trace, indicated on the vertical axis in the figure, is applied to clarify the display of the signature transitions as  $a$  decreases. These transitions are typical of those observed at primary bifurcation estimates of character 2, when the signature along the primary branch is increasing with decreasing  $a$ . When instead signatures on

Table 6.1: The parameter and energy ranges for which several secondary branch estimates are signature 0. The parameter ranges at which each branch may approximate a minimizer of  $J$  are also shown.

$L$	$n$	Range ( $a$ )	Range ( $J$ )	Minimum $J$ Range
-8	8	-3.31, -2.80	-151.9, -112.51	-
-8	7	< -2.69	-250, -109.09	-
-9	9	-2.45, -2.01	-84.36, -40.88	-
-9	8	< -2.10	-243.1, -50.04	-
-10	10	-2.23, -2.01	-66.44, -45.85	-
-10	9	< -2.06	-232.23, -51.12	-2.55, -2.12
-11	11	-2.13, -2	-57.05, -46.34	-2.03, -2.01
-11	10	-4.04, -2.04	-218.22, -49.33	-2.11, -2.04
-12	12	-2.08, -2	-49.14, -43.25	-
-12	11	-3.47, -2.02	-181.38, -44.91	-

the primary branch decrease with parameter depth, the bifurcating secondary branches often begin with a signature that is an averaged value.

Table 6.1 provides a summary of several simulated secondary branches that achieve a signature of 0 on the parameter ranges specified. One can see that the process of simulating all secondary solution branches has yielded probable minimizer estimates extending down to at most a parameter value of -2.55. Figure 6.4 depicts several signature 0 secondary solution estimates. The first two, which have approximately the minimum value of  $J(u)$  attained along their respective branches, have a somewhat evenly-distributed vortex configuration that is often observed for low energy solutions of relatively high stability. The phase plots allow for a visual verification of the following fact:

**Proposition 6.2.6** *Let  $u \in G(L_1, L_2, n, \xi, \varphi)$  be a secondary solution estimate. Then,  $u \cdot (\frac{2\pi L_1}{n}k, \frac{2\pi}{n}k) = u$  for all  $k \in \mathbb{Z}$ .*

In fact, one may substitute any  $\ell_z = L_1 + nz$ ,  $z \in \{1, 2, \dots, \tilde{z}\}$  for  $L_1$  and the results still holds. The proof of the proposition is only a simple computation.

Figure 6.5 shows the phase plot of a secondary solution estimate originating from the  $(L, j) = (4, 0)$  primary branch, from a primary bifurcation estimate of character 1. The phase of the function exhibits  $r$ -dependence, which can only mean that it is not an element of any subspace  $G(L, L, 1, \xi) \subseteq G^{2N}$ .

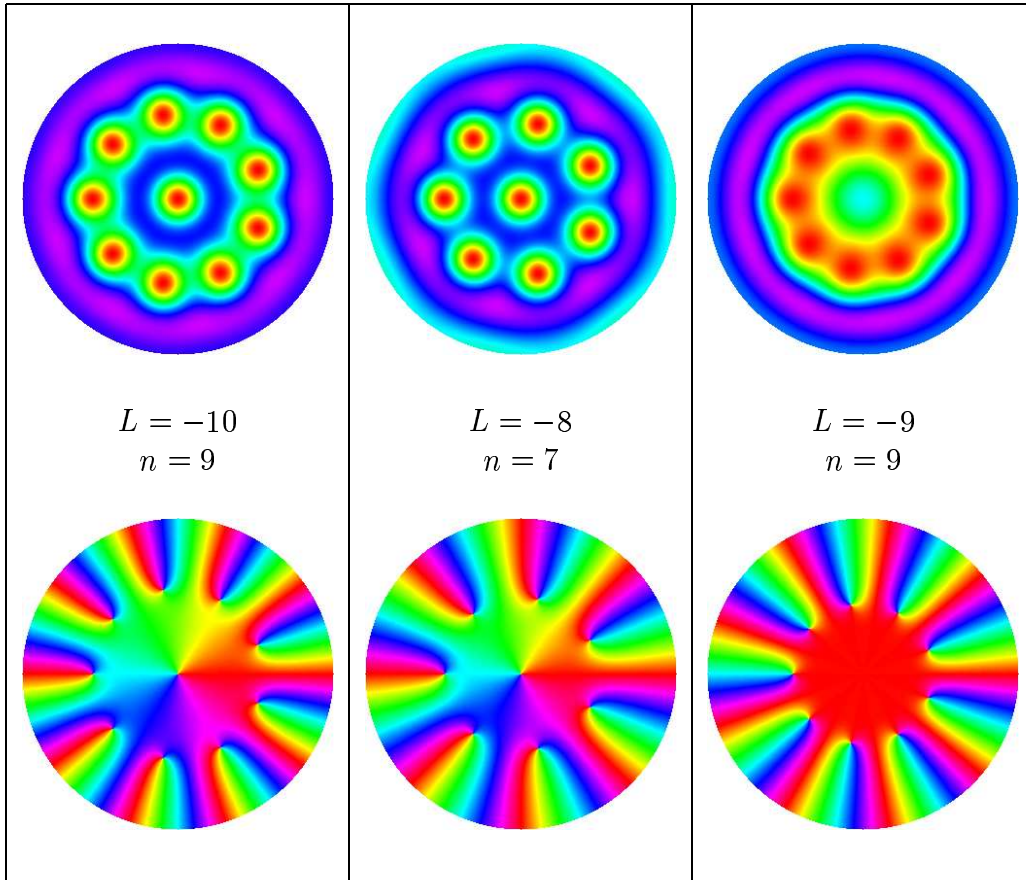


Figure 6.4: Squared modulus plots (above) and phase plots (below) of selected signature 0 secondary solution estimates. The first and second from the left have minimum energy on their corresponding branches. From the phase plots, it is clear that the action  $(\frac{2\pi L}{n}k, \frac{2\pi}{n}k) \in \mathbb{T}^2$  fixes each estimate whenever  $k \in \mathbb{Z}$ ; note that a rotation without gauge adjustment through any multiple of  $\frac{2\pi}{9}$  radians fixes the rightmost estimate.

The two solution estimates were produced by using the single eigenfunction estimate  $e$  returned by the Primary Bifurcation Algorithm, and its additive inverse  $-e$ . It is clear that while these solutions must be  $J$ -Equivalent, there is no  $\mathbb{T}^2$  action relating the two. However, the conjugate-reflection action of  $C$  does map between the two estimates. While solutions of this type are found to be quite rare, they may exist, and are only associated with

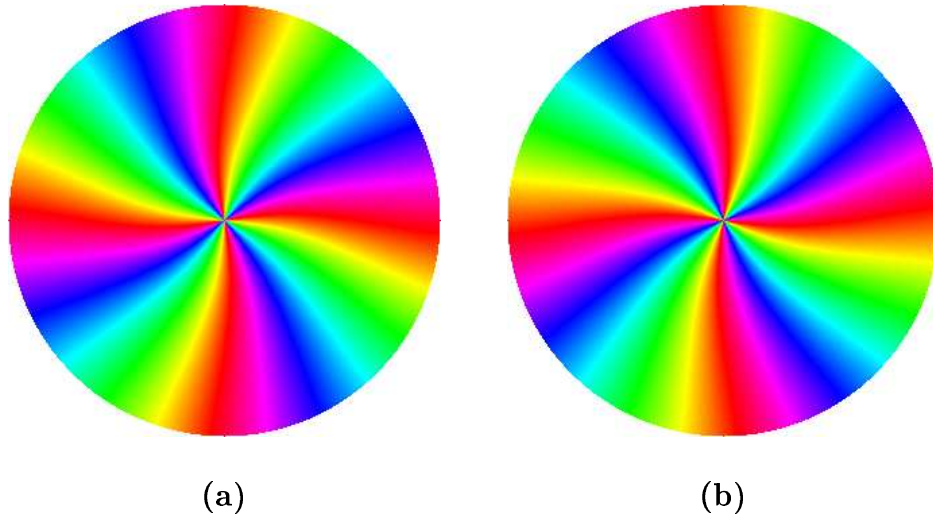


Figure 6.5: (a) Phase plot of a secondary solution estimate along a branch emanating from the primary branch  $(L, j) = (4, 0)$ . The estimate pictured belongs to  $G(4, 4, 1)$ , but is not in  $G(4, 4, 1, \xi)$  for any  $\xi \in \mathbb{R}$ . The base solution is in  $G(4, 4, 1, 0)$ , and the eigenfunction  $e$  used to produce the branch belongs to  $G(4, 4, 1, \pi/2)$ . (b) Phase plot for a secondary solution estimate at the same parameter and energy value as that on the left, but on the branch obtained by using instead  $-e$  to form the initial guess for the Branch Algorithm. The action of  $C$  maps one solution to the other, there is no action of an element from  $\mathbb{T}^2$  relating the two solutions.

bifurcations of character 1.

Before proceeding to study the many types of bifurcating branches that may next occur, an important property of secondary solution estimates first is introduced. Recall that when  $u$  is a primary solution estimate, a null eigenfunction of  $D^2J(u)$  always exists corresponding to an infinitesimal rotation action of elements from the group  $\mathbb{S}^1$ . When  $u$  is instead a secondary estimate,  $D^2J(u)$  always has a nontrivial kernel as well, although in this case one observes at least two zero eigenvalues of  $\Lambda_u$  along each corresponding branch. This increase in multiplicity is attributable to the fact that nontrivial actions of gauge rotation and rotation in  $\theta$  are distinguishable when regarding a secondary estimate; there exist gauge rotation actions which can-

not be expressed as a physical rotation, and vice-versa. This fact is taken into account when defining the branch eigenspace of a secondary bifurcation estimate. Further, a modest modification of the Primary Bifurcation Algorithm is needed to specify the base solutions for tertiary branch estimates. The utility and versatility of the numerical algorithms used in this study becomes more apparent in the next chapter, as the number of classes of solution estimates increases.

### 6.3 Bifurcations from the Secondary Branches

In this section, tertiary branch estimates are presented and analyzed. A *tertiary* branch estimate is defined to be a new branch of solutions beginning from a secondary branch estimate. As in the case of primary bifurcation estimates, the character of a secondary bifurcation point is always observed to be either 1 or 2, although the first case occurs now much more frequently. However, a new level of mathematical complexity is apparent when estimating tertiary solution branches, owing primarily to the fact that the subspaces containing typical base solutions are now substantially larger. In addition, when the character of a secondary bifurcation point is 2, the numerical algorithms can estimate two tertiary solution branches beginning from the same point, such that no corresponding  $\mathbb{T}^2$  action maps one to the other.

As in the previous sections, the subspaces of the form  $G(L_1, L_2, n, 0, 0)$  containing functions that are expandable in  $\{\psi_k\}_{k=1}^N$  using only real coefficients are of primary interest; nearly all secondary solution estimates may be equivalently expressed as elements of such spaces. This affords certain computational simplifications, and also allows for increased simulation efficiency in cases where the base secondary solution plus a selected branch eigenfunction is also expandable in the  $L^2(D)$  basis using real numbers. This results because  $\Lambda_u$  at a secondary bifurcation estimate  $u$  always has 0 as an eigenvalue with a multiplicity of 2, and two linearly dependent null eigenfunctions from some appropriate subspace  $G(L_1, L_2, n, \pi/2)$ ; these functions cannot be elements of the kernel of the minimally computed matrix. Thus, in such cases the minimal form of  $\Lambda_u$  is typically nonsingular, resulting in an increased rate of convergence and a significant decrease in execution times.

The properties of the estimated branch eigenspaces are instrumental to the understanding of the bifurcation phenomena that can occur. Recall that the branch eigenspaces corresponding to trivial and primary bifurca-

tion points are (up to a scalar multiple) the orbit of an eigenfunction under some appropriate subgroup of  $\mathbb{T}^2$  that fixes the bifurcation estimate itself; this result allowed the conclusion that only one new branch is simulated at each such point. However, the description of the branch eigenspaces of  $\Lambda_u$  when  $u$  is a secondary estimate near a point of bifurcation is less obvious, and the same conclusion does not hold.

Several considerations regarding secondary branch estimates originating from character 2 primary bifurcation points having solution estimates in subspaces of the form  $G(L_1, L_2, n, 0, 0)$  are necessary. Recall that estimates of this type constitute the vast majority of those observed, and therefore most base solutions for tertiary solution branches may be expressed equivalently by functions from the same type of subspace.

There are at least two complications of note when regarding secondary solution estimates, rather than the somewhat simpler primary variety that have only a single winding number. First, whenever  $u \in G(L, L, 1, 0)$  is a primary solution estimate, it has been shown that the only other function in  $G(L, L, 1, 0)$  within a  $\mathbb{T}^2$  action of  $u$  is  $-u$ . This is not the case when  $u$  lies in a subspace of functions with several winding numbers, along a secondary branch. First, expand  $u \in G(L_1, L_2, n, 0, 0)$  in the familiar way as

$$u(r, \theta) = \sum_{z=0}^{\tilde{z}} f_{\ell_z}(r) e^{i\ell_z\theta},$$

where  $\ell_z = L_1 + nz$  for  $z \in \{0, 1, 2, \dots, \tilde{z}\}$ , and the coefficient functions  $f_{\ell_z}$  are real-valued. Using  $\tilde{z} = (L_2 - L_1)/n$ , clearly the function

$$u \cdot \left( \frac{\pi L_1}{n}, \frac{\pi}{n} \right) = \sum_{z=0}^{\tilde{z}} (-1)^z f_{\ell_z}(r) e^{i\ell_z\theta}$$

is in  $G(L_1, L_2, n, 0, 0)$ ,  $\mathbb{T}^2$ -equivalent to  $u$ , and not the additive opposite of  $u$ . After defining  $u_*$  as the right hand side of the above expression, the relation

$$u_* = u \cdot \left( \frac{\pi L_1}{n} k, \frac{\pi}{n} k \right) \quad \text{for odd } k \in \mathbb{Z} \quad (6.2)$$

follows. If  $k$  is instead even, then  $u$  is fixed by the action. Secondly, recall that whenever  $u \in G(L, L, 1, 0)$  is a primary bifurcation estimate of character 2 with eigenfunctions  $e_1$  and  $e_2$  as given in Proposition 6.2.2, the action of

the element  $(\frac{\pi L}{n}, \frac{\pi}{n})$  fixes  $u$ , and sends any eigenfunction  $e \in \text{span}\{e_1, e_2\}$  to  $-e$ . A similar result does not always hold when instead  $u$  is a secondary estimate from some subspace  $G(L_1, L_2, n, 0, 0)$ . More specifically, it is not always possible to conclude for such  $u$  that  $u + e$  and  $u - e$  are related by a  $\mathbb{T}^2$  action. It is then possible that two tertiary branch estimates emanating from a single bifurcation point (up to  $\mathbb{T}^2$ -Equivalence) are not related at each point by such an action. These facts are central to the the study of the largest class of typical secondary base solutions.

A useful description of the eigenspace of secondary branch estimates is clearly needed. The proof of the next proposition is only a minor modification of that for Proposition 6.2.2, and is based upon the formulas for the entries of  $\Lambda_u$  provided in Equation (4.12).

**Proposition 6.3.1** *Let  $u \in G(L_1, L_2, n, 0, 0)$  be a solution estimate on a secondary branch such that  $(a, u)$  is a bifurcation point estimate. Then, there is a nontrivial estimate for a branch eigenspace of  $D^2J(u)$  as an operator mapping into  $G^{2N}$ . Furthermore, if this branch eigenspace is not contained in  $G(L_1, L_2, n)$ , then*

$$e_1(r, \theta) = \sum_{z=0}^{\tilde{z}} f_z(r) e^{i(\ell_z - p)\theta} + g_z(r) e^{i(\ell_z + p)\theta}$$

*is a branch eigenfunction of  $D^2J(u)$  for some some  $p \in \{1, 2, \dots, n/2\}$  and functions  $f_z$  and  $g_z$  of  $r$  that are real or imaginary valued. If  $p < n/2$ , then each coefficient function  $f_z$  and  $g_z$  may be chosen to be real-valued, in which case*

$$e_2(r, \theta) = \sum_{z=0}^{\tilde{z}} i f_z(r) e^{i(\ell_z - p)\theta} - i g_z(r) e^{i(\ell_z + p)\theta}$$

*is also a branch eigenfunction of the same operator. In this last case, the character of the bifurcation estimate is at least 2.*

The cases when  $p = n/2$ , or when the branch eigenspace lies in  $G(L_1, L_2, n)$ , are both possible; they remain to be discussed in more detail. Presently the case when  $p < n/2$  is of interest. Note that if the functions  $f_z$  and  $g_z$  in the above proposition are taken to be real valued, then both  $u$  and  $e_1$  are elements of the subspace  $G(L_1, L_2, (n, p), 0, 0)$ , where  $(n, p)$  is the greatest common divisor of  $n$  and  $p$ . Also, since in this case  $e_2 \in G(L_1, L_2, (n, p), \pi/2, 0)$ , the smallest invariant subspace containing both  $u$  and  $e_2$  is  $G(L_1, L_2, n)$ . It

will be further assumed that each of the functions  $f_z$  and  $g_z$  are nonzero; this represents the typically observed situation. Whenever the functions  $e_1$  and  $e_2$  are given as the branch eigenfunctions corresponding to a secondary bifurcation estimate  $u$  of character 2, every branch eigenfunction from the space  $E_u$  is a scalar multiple of some function in the span of this pair over the real numbers. Moreover, when  $e \in E_u$ , it follows that

$$e \cdot \left( \frac{\pi L_1}{n} k, \frac{\pi}{n} k \right) \in E_u \quad \text{for even } k \in \mathbb{Z}$$

A similar conclusion can be drawn regarding the branch eigenspace  $E_{u_*}$ , for  $u_*$ . According to the analysis above, it must be that

$$e \cdot \left( \frac{\pi L_1}{n} k, \frac{\pi}{n} k \right) \in E_{u_*} \quad \text{for odd } k \in \mathbb{Z}$$

whenever  $e \in E_u$ . Furthermore, according to the last proposition

$$E_{u_*} = \text{span}\{e_{1_*}, e_{2_*}\},$$

for some branch eigenfunctions  $e_{1_*}$  and  $e_{2_*}$  of  $u_*$ , such that  $e_{1_*} \in G(L_1, L_2, n, 0, 0)$  and  $e_{2_*} \in G(L_1, L_2, n, \pi/2, 0)$ . When considering a secondary bifurcation estimate  $u$  as given in Proposition 6.3.1, it is convenient to use the notation  $e$  for  $e_1$  and  $e_*$  for  $e_{1_*}$ , as those eigenfunctions having expansions in  $\{\psi_k\}_{k=1}^N$  with real-number coefficients are natural choices to consider in the formation of new initial guesses.

One can now establish that there are two tertiary branch estimates, distinct in the sense of  $\sim_2$  and originating from  $u$  or  $u_*$ , that are composed of estimates whose expansions in  $\{\psi\}_{k=1}^N$  have real coefficients. Furthermore, it is shown that these branches are produced using the Branch Algorithm and no more than two of the four functions  $u + e$ ,  $u - e$ ,  $u_* + e_*$  or  $u_* - e_*$  as initial guesses. The selection of the guesses depends only upon the algebraic properties of  $n$  and  $p$ . To simplify the language, the terminology *common divisor* is used always with reference to the natural numbers  $n$  and  $p$  from Proposition 6.3.1.

**Proposition 6.3.2** *Let  $u \in G(L_1, L_2, n, 0, 0)$  be a solution estimate on a secondary branch such that  $(a, u)$  is a bifurcation point estimate. Suppose that the branch eigenspace of  $D^2J(u)$  is not in  $G(L_1, L_2, n)$ , and that  $p < n/2$ . Let  $u_* \in G(L_1, L_2, n, 0, 0)$  be given as in Equation (6.2), and let  $e$  and  $e_*$  denote the eigenfunctions of  $u$  and  $u_*$ , respectively, from  $G(L_1, L_2, (n, p), 0, 0)$  according to Proposition 6.3.1. Then,  $u + e \varrho_2 u - e$  or  $u + e \varrho_2 u_* + e_*$ .*

*Proof:* Since all functions considered are from  $G(L_1, L_2, n, 0, 0)$ , the action of  $C$  is not important in this context. It suffices to show that in any situation, there is no  $\mathbb{T}^2$  action corresponding to at least one of the two relations.

There are several preliminary facts to consider. First, note that a gauge adjustment action alone never fixes  $u$ , nor sends  $u$  to  $u_*$ ; for this reason no such action can possibly correspond to either of the stipulated equivalences. Now, since the expansion of each function under consideration in the basis  $\{\psi_k\}_{k=1}^N$  has only real coefficients, the  $\mathbb{T}^2$  actions that are of interest are those that map functions from some  $G(L_1, L_2, n, 0, 0)$  into  $G(L_1, L_2, (n, p), 0, 0)$ . These have the form  $(L_1\pi/g, \pi/g)$ , where  $g$  is a common divisor. Using such elements, to send  $u$  to itself or to  $-u$  requires some  $(L_1\pi/g, \pi/g)$  with common divisor  $g$  such that  $n/g$  is even. Moreover, mapping  $u$  to  $u_*$  or to  $-u_*$  with such an action requires some  $g$  such that  $n/g$  is odd.

Now, the possible cases are examined separately. Suppose that  $n$  is odd. Then for any common divisor  $g$ , it follows that  $n/g$  is not even. Therefore, no nontrivial  $\mathbb{T}^2$  action to consider fixes  $u$ , and clearly none fixes  $u$  while sending  $e$  to  $-e$ . In this case, it follows that  $u + e \approx_2 u - e$ . Otherwise,  $n$  is even. If for every common divisor  $g$  it follows that  $n/g$  is even, then there is no mapping from  $u$  to  $u_*$  or  $-u_*$  to consider, and it can be concluded that  $u + e \approx_2 u_* + e_*$ . Otherwise, there are common divisors  $g_1, g_2$  with  $n/g_1$  even and  $n/g_2$  odd. Suppose that whenever  $g$  is such that  $n/g$  is even, it follows that  $p/g$  is also even. Then, there is no  $\mathbb{T}^2$  action fixing  $u$  while sending  $e$  to  $-e$  to consider; in this case  $u + e \approx_2 u - e$ . The only other possibility is that  $n/g$  is even and  $p/g$  is odd for some common divisor  $g$ . But then  $2 \mid n/g$  while  $2 \nmid p/g$ , and the largest power of 2 that divides  $n$  is larger than that which divides  $p$ . This means that  $n/g$  is even for every common divisor  $g$ , a situation which was already addressed.  $\square$

These results can be further clarified. When  $n$  is even, then clearly  $n/g$  is even for every common divisor  $g$  if and only if  $n/(n, p)$  is even. Also,  $n$  is odd or  $p/g$  is even whenever  $n/g$  is if and only if  $n/(n, p)$  is odd. Thus,  $n/(n, p)$  even implies that  $u + e \approx_2 u_* + e_*$ ; and  $n/(n, p)$  odd implies that  $u + e \approx_2 u - e$ . One then expects that two tertiary solution branches beginning from a character 2 secondary bifurcation point (that has a two dimensional eigenspace as discussed in Proposition 6.3.1) may be distinct in the sense of  $\approx_2$  only when the two initial guesses used in the Branch Algorithm are as well. According to the above proposition, two such initial guesses always exist at these types of secondary base solutions. Table 6.2 summarizes the

relationship between the initial guess selection and the parity of  $n/(n, p)$ .

Table 6.2: Initial guess rules used when simulating two types of tertiary branches beginning at a character 2 secondary bifurcation estimate using the Branch Algorithm. The resulting branches are composed of estimates from subspaces of the type  $G(L_1, L_2, (n, p), 0, 0)$ .

Case	First Branch	Second Branch
$n/(n, p)$ even	$u + e$	$u_* + e_*$
$n/(n, p)$ odd	$u + e$	$u - e$

The Equivariance property of  $\mathcal{N}$  implies that the tertiary branch estimates obtained according to these rules are composed of solution estimates from  $G(L_1, L_2, (n, p), 0, 0)$ . Furthermore, if  $u$  is as above and the Branch Algorithm is restricted to the four possible initial guesses  $u + e$ ,  $u - e$ ,  $u_* + e_*$  and  $u_* - e_*$ , (the eigenfunctions are specified here up to a positive real scalar multiple of a reasonable size), then with standard convergence assumptions it then follows that the two types of tertiary branches estimated are the only two composed of estimates from  $G(L_1, L_2, (n, p), 0, 0)$ ; up to a sign change of the estimating functions. This can be concluded, since when considering all positive real multiples of the eigenfunctions in each of the four guesses considered, there must exist a resulting collection obtained from the same four that consists of functions from at most two  $\mathbb{T}^2$ -equivalence classes.

Figure 6.6 shows two solution estimates near the minimum of a secondary branch beginning from the  $(-12, 1)$  primary branch with  $n = 12$ . Each is an element of  $G(-36, 36, 12, 0, 0)$ ; the second is exactly the first under the action of  $(0, \pi/12)$ . For every parameter value along this branch, there are two solution estimates from  $G(-36, 36, 12, 0, 0)$  that agree with those pictured in the angular arrangement of the lines through the origin on which vortex pairs are centered. That is, one has two vortices centered on each line  $\theta = \frac{\pi}{12}k$  for  $k = 0, 2, 4, \dots, 10$ , the second has a pair centered on the same lines for when  $k = 1, 3, 5, \dots, 11$ ; each vortex is also the same distance from the origin.

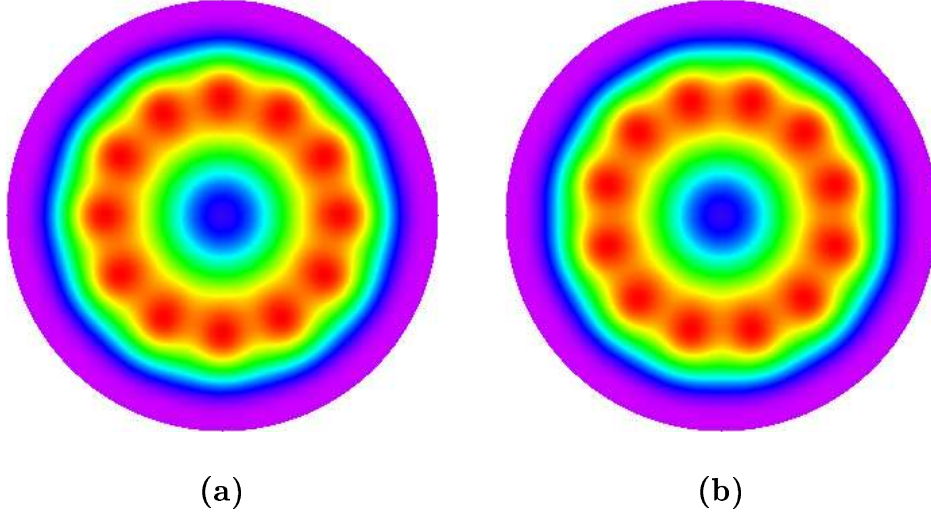


Figure 6.6: Secondary solution estimates near the minimum of the  $(L, j) = (-12, 1)$ ,  $n = 12$  secondary branch. The image in (a) shows the vortex arrangement similar to that for the first type of base estimate from  $G(-36, 36, 12, 0, 0)$ ,  $u$ , used when forming initial guesses for the tertiary branches of either type beginning along the secondary branch. The function plotted in (b),  $u_*$ , results from the  $\mathbb{T}^2$  action  $(0, \pi/12)$ , and represents the second type of base solution used in producing the tertiary solution estimates that follow.

Several pairs of tertiary solution branches beginning at points along the same secondary branch were simulated; in each case the bifurcation point estimates  $u$  and  $u_*$  in  $G(-36, 36, 12, 0, 0)$  used have the expected vortex arrangement. Figure 6.7 shows the modulus squared contour plots for three low-signature tertiary solution estimates near the minimum energy on both types of solution branches. It is always observed that the two types of branch estimates differ in signature by 1 near the secondary bifurcation point; apparently this corresponds to a slight difference in vortex arrangement. Three new values for  $n$  are shown in the figure. Notice that although no action from  $\mathbb{T}^2$  maps a solution of the first type to one of the second type for any of the  $n$  values shown, the action of  $(0, \frac{\pi}{n}k)$  nevertheless fixes both, provided  $k$  is even. Table 6.3 summarizes each solution type, and branch information

near each energy minimum.

Table 6.3: Information for low signature tertiary branches originating from selected character 2 bifurcations of the  $(L, j) = (-12, 1)$ ,  $n = 12$  secondary branch. For each new  $n$  value, the point estimates for the energy minima of the branches are reasonably close. However, near the beginning of each there is a signature difference of 1, and the vortex configurations of the corresponding solution estimates are remarkably different (see Figure 6.7).

$n$ value	Solution Label	$a$ Near Min.	$J$ Near Min.	Signature Near Min.	Signature Near Bifurcation
2	A	-4.18	-226.49	0	1
2	B	-4.18	-227.2	1	2
3	A	-4.05	-215.01	0	2
3	B	-4.05	-214.89	1	3
4	A	-3.88	-192.72	1	4
4	B	-3.87	-194.28	1	5

Solutions on the first type of branch in Figure 6.7 evolve with decreasing parameter somewhat intuitively; one can visualize every  $12/n^{\text{th}}$  vortex traveling inward, along the same line on which it is originally centered at the base solution. However, the estimates on the second type of branch evolve somewhat differently. In this case, a pair of vortices first meets at one point  $(r, \frac{\pi}{n}k)$ , where  $r > 0$ , for each nonnegative integer  $k < 2n$  having parity opposite to that of  $n$ . Then, one from either overlapped pair moves inward along the corresponding line  $\theta = \frac{\pi}{n}k$ . This phenomena results in a somewhat opposed arrangement, in which several zeros of the solution may be centered along these lines.

Although no proof is provided here, the two types of tertiary branches estimated are conjectured to be the only two up to  $\mathbb{T}^2$ -Equivalence beginning at each such secondary bifurcation point. Whenever there is an action  $\xi$  from  $\mathbb{T}^2$  sending an eigenfunction  $e$  of  $\Lambda_u$  to another eigenfunction while fixing  $u$  itself, the corresponding tertiary branch estimated by using  $u + e \cdot \xi$  as an initial guess is  $\mathbb{T}^2$ -Equivalent to that obtained by instead using  $u + e$ . The orbit of such an eigenfunction under the  $\mathbb{T}^2$  subgroup fixing the secondary base solution is not the same as the branch eigenspace itself, and the question of whether or not it is appropriate to use other eigenfunctions in

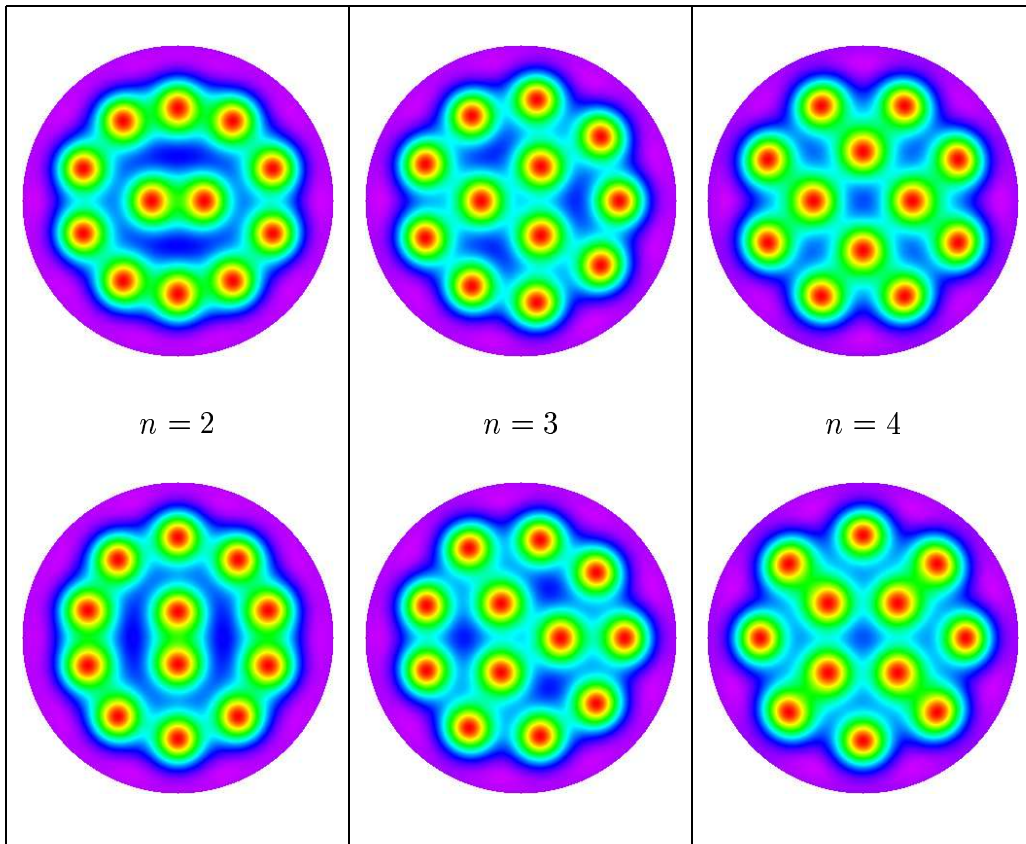


Figure 6.7: Squared modulus plots of selected low signature tertiary solution estimates originating from the  $(L, j) = (-12, 1)$ ,  $n = 12$  secondary branch. For each new  $n$  value, a solution near the energy minimum on the first type of branch (above) and on the second type (below) is pictured. Each estimate is signature 0 or 1, and has exactly the parameter versus energy coordinates as specified in Table 6.3.

forming initial guesses has not been completely answered. However, whenever the base solution is expandable in  $\{\psi_k\}_{k=1}^N$  using only real coefficients, it is natural to make use of the corresponding eigenfunctions of  $\Lambda_u$  which satisfy the same criteria.

Returning to Proposition 6.2.2, there are at least two other types of branch eigenfunctions that may lead to new tertiary branch estimates near a secondary bifurcation point  $u$ . First, it might be observed that  $p = n/2$  when

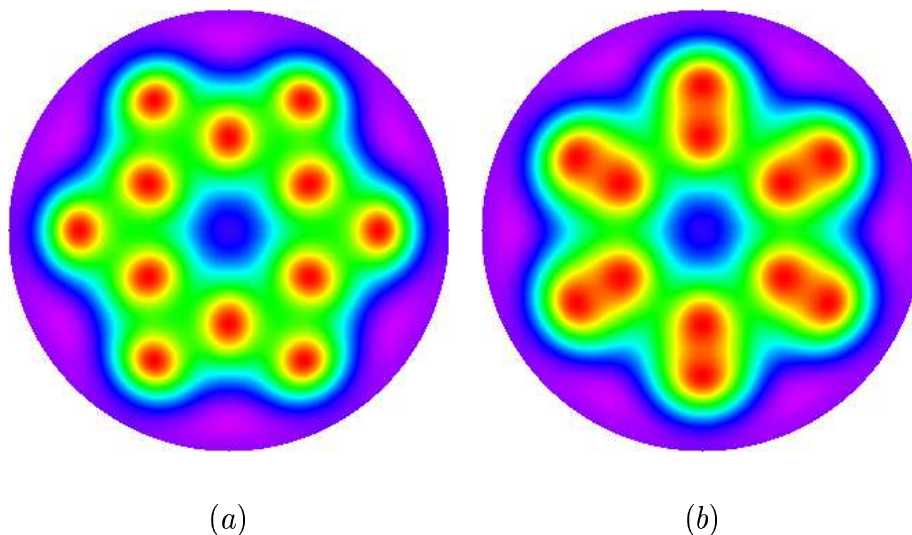


Figure 6.8: Squared modulus plots for tertiary solution estimates originating from two separate character 1 bifurcations of the  $(L, j) = (-12, 1)$ ,  $n = 12$  secondary branch. The  $n$  value has changed from 12 to 6 at each bifurcation; i.e.  $p = n/2$ . The tertiary branch estimate on which (a) exists begins near a larger parameter value than that for (b), and was obtained using the initial guess  $u + e$ . The branch for the estimate in (b) was begun with the initial guess  $u_* + e_*$ . The evolution of the second estimate with decreasing parameter is comparable to those of the second type, depicted in Figure 6.7.

$n$  is even. In this situation, one expects only a single branch eigenfunction corresponding to the branch eigenvalue. This follows according to the formulas from Equation (4.12), since whenever a  $k^{th}$  row of  $\Lambda_u$  has nonzero entries in the  $m^{th}$  columns whose associated winding numbers  $L_m$  equal  $L_1 + nz - n/2$  or  $L_1 + nz + n/2$  for  $z = 1, 2, \dots, \tilde{z}$ , the  $m + N^{th}$  entries of row  $k + N$  will not match, unless the second integral associated with each respective entry is zero. This eigenfunction  $e$  might be in either of the spaces  $G(L_1, L_2, n/2, 0, 0)$  or  $G(L_1, L_2, n/2, \pi/2, 0)$ . In either situation, the  $\mathbb{T}^2$  element  $(L_1 2\pi/n, 2\pi/n)$  fixes the base solution, while mapping  $e$  to  $-e$  (in the second case,  $C$  has the same effect), and therefore only one solution branch up to  $J$ -Equivalence is simulated. As might be expected, the character of such types of bifurcation

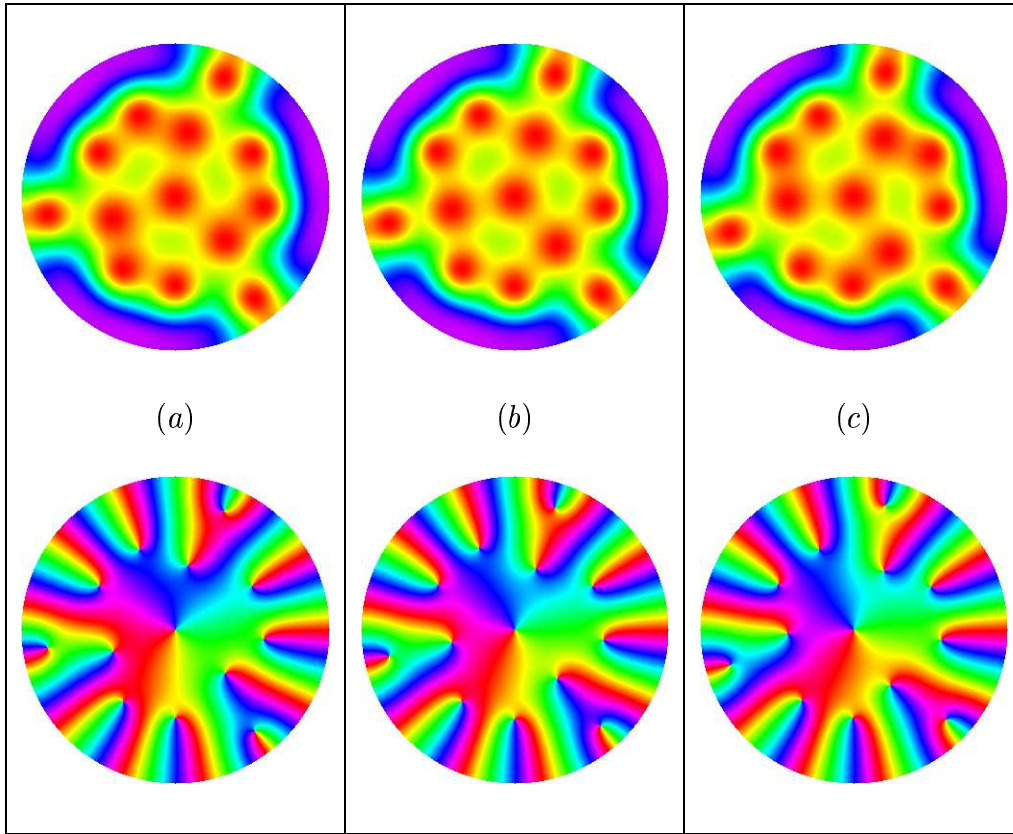


Figure 6.9: Squared modulus (above) and phase (below) plots for tertiary estimates originating from a character 1 secondary estimate. The ‘parent’ secondary branch originated from the  $(L, j) = (-10, 1)$  primary branch. The branch eigenfunction used is an element of  $G(-40, 38, 3, \pi/2, 0)$ , the  $n$  value of 3 incurred no change through the third bifurcation. When following the corresponding branch, the parameter values passed through those corresponding to (a), then changed direction near estimate (b), then proceeded through (c) toward the original bifurcation point as similar energy levels were maintained. It is conjectured that (a) and (c) approximate a single solution up to  $J$ -Equivalence near  $a = -2.27$ ; however there is no  $\mathbb{T}^2$  action mapping one to the other.

estimates is observed to be 1. Figure 6.8 depicts examples of solution estimates resulting from this type of bifurcation. Those shown are on distinct

branches originating from the  $(L, j) = (-12, 1)$ ,  $n = 12$  secondary branch, near parameter values that are somewhat smaller than those at which the branches corresponding to the estimates pictured in Figure 6.7 begin. The two types of bifurcation phenomena previously discussed are again manifest in these examples. The branch corresponding to the estimate in (a) began with the guess  $u + e$ ; in this case  $u$ ,  $e$  (and  $u + e$ ) are elements of  $G(-36, 36, 6, 0, 0)$ . The estimate in (b) is on a second branch that begins at a distinct parameter and energy value. Its corresponding base solution  $u$  originally had a single branch eigenfunction from  $G(-36, 36, 6, \pi/2, 0)$ . Thus, the initial guess  $u_* + e_*$  was instead used, because  $u_*$ ,  $e_*$  and  $u_* + e_*$  must then be elements of  $G(-36, 36, 6, 0, 0)$ . As a result, both of the corresponding branches are composed of solution estimates whose expansions in  $\{\psi_k\}_{k=1}^N$  have real coefficients.

It is also sometimes observed that a branch eigenfunction corresponding to a secondary estimate from  $G(L_1, L_2, n, 0, 0)$  may exist either completely in the same space, or in the space  $G(L_1, L_2, n, \pi/2, 0)$ ; in which case each coefficient function is imaginary. For the related bifurcations in these situations, the  $n$  value of the new branch inherits that of the original secondary branch, and the character of the associated bifurcation estimate  $u$  is observed to be 1. Similarly to the first case, each  $m^{\text{th}}$  entry of a  $k^{\text{th}}$  row of  $\Lambda_u$  having corresponding winding numbers that are  $L_1 + nz$  for suitable  $z$  are composed of both types of integral expressions from Equation (4.12); and therefore the existence of an eigenfunction from either  $G(L_1, L_2, n, 0, 0)$  or  $G(L_1, L_2, n, \pi/2, 0)$  does not imply the existence of the other. Figure 6.9 depicts tertiary solution estimates along a branch that originated from the  $(L, j) = (-10, 1)$ ,  $n = 3$  secondary branch; the new branch also has  $n = 3$ . The estimate shown in (b) is near the parameter turn around point on the branch followed by the algorithm. The estimates in (a) and (c) both correspond to the point  $a \approx -2.27$ ,  $J \approx -59.7$ , although they clearly cannot be  $\mathbb{T}^2$ -Equivalent.

The simulation algorithms may also be programmed to estimate new branches beginning from tertiary bifurcation estimates. These routines are similar, although not presently completed. However, the data obtained from tertiary estimations indicates the presence of numerous new bifurcation estimates along most branches, again either of character 1 or 2.

# Chapter 7

## Problem Extensions and Conclusions

There are questions in several key areas that have implications both for continued research in this specific mathematical problem, as well as for other numerical studies that employ similar methods. The theoretical formalism cited as the foundation of the problem leaves certain questions unanswered, and the aspects of these ideas that are impacted by any desirable geometrical complications of the domain  $D$  should be well understood. The analytic behavior of the Newton map in Galerkin space could be further studied, as surely such knowledge is necessary for a complete understanding of the problem dynamics. There are many interesting extensions that could be made to the GL model that was used; they may be regarded as being either geometrical extensions, or as additional complexities introduced in order to form models that apply at higher ambient temperatures, or that account for the anisotropy or nonhomogeneity of real materials. The simulation algorithms are well developed; nevertheless for each there are many potential improvements worthy of consideration, and higher-level features that could be implemented.

The classical PDE theory and analysis that was outlined as it applies to this problem complicates when the *regularity* conditions on the general domain  $\Omega$  are relaxed. Rigorously obtaining the standard variational result in which the derivative of  $J$  is expressed in terms of the equation solved becomes a problem in its own right whenever such conditions are significantly weakened. Also, there are open questions regarding the regularity of solutions to Equation (1.1). The author has chosen to assume the solution space  $H_B^2(D)$ ,

however a clear proof demonstrating that the Euler-Lagrange derivative (the left hand side of Equation (1.1)) may be expanded in  $G^{2N}$  when  $u$  is any function in the domain of  $J$  itself was elusive. Notwithstanding these complications, it is expected that the GNGA approach does fit within a suitable theoretical context for a large class of choices for  $\Omega$  and types of PDE.

The dynamical behavior of  $\mathcal{N}$  was not studied to a great extent, despite the fact that many results relied upon an assumption of the appropriate or expected convergence of this mapping. Since the Newton guesses are specified “intelligently” throughout the numerical method, this treatment is justified to some extent; however, more knowledge regarding the sensitivity of the iteration to changes (particularly those related to the initial guess in the Branch Algorithm) would certainly be beneficial. It is well-established that there are cases in which Newton’s method can exhibit undesirable or unpredictable dynamics, and even fail to converge. Although this fact is perhaps less of a concern when iterating along a given solution branch, it has been demonstrated that the selection of the first guess used in beginning a branch estimate must be carefully considered. On the other hand, the utility of the algorithms when following branches of estimates that are not necessarily minimizers of  $J$  is remarkable, and offers a unique insight into the mathematics governing the system. Surely, the combination of results that are only readily obtained by using GNGA or a similar method with those obtained via a more classical approach could provide a powerful means in understanding the complexities of specific phenomena that might otherwise be substantially difficult to explain.

The GL model used in this research does represent a highly simplified approach to a complex physical phenomena. However, more complete models are normally given in terms of reasonable extensions of the well-known equations that have been studied herein. Therefore, a useful perspective regarding the most significant challenges that might arise when applying a similar GNGA method in a more complex mathematical setting has been gained. Perhaps the most natural next step is to consider a similar problem instead in three dimensions, in which case the vector potential  $\mathbf{A}$  is also unknown. This represents a considerable complication in many ways. Firstly, it seems obvious that regardless of the approach employed, a marked increase in the computing resources required would result. Provided with ample computing power, there are several new mathematical complexities. According to Equation (2.7), a coupled system of equations must now be solved, and even if one supposes that the Coulomb gauge  $\nabla \cdot \mathbf{A}$  can be enforced so that

$\nabla \times \nabla \times \mathbf{A}$  becomes  $-\Delta \mathbf{A}$  in the second equation, solutions for its linearized version are not eigenfunctions. Notwithstanding this fact, consider the problem of specifying the space containing pairs  $(u, \mathbf{A})$  that solve the coupled problem. Presuming similar conditions regarding the applied magnetic field  $\mathbf{h}_0$ , it should follow that  $\nabla \times \mathbf{A} = \mu \mathbf{h}_0$  sufficiently far from the sample. It seems promising to choose  $\mathbf{A}_0$  satisfying the most desirable gauge conditions and the above relation, then to regard the unknown vector potential  $\mathbf{A}$  and field  $\mathbf{h}$  as perturbing  $\mathbf{A}_0$  and  $\mathbf{h}_0$  when the order parameter becomes nontrivial. One must determine how the function  $\mathbf{A}$  should in this case be regarded. If taken to be identically zero outside of  $\Omega$ , in which case any induced effects are neglected, then one must enforce the condition  $\nabla \times \mathbf{A} \times \hat{n} = \mathbf{0}$  according to the physical boundary conditions, assuming (as in the current problem) that no charges or sources are present on  $\Gamma$ . This is in addition to the GL boundary condition from Equation (2.7), and thus there are Neumann-type conditions to enforce regarding the tangential components of  $\nabla \times \mathbf{A}$ , as well as additional conditions to enforce upon the normal components of  $\mathbf{A}$  which depend upon those chosen for  $\nabla u \cdot \hat{n}$ . Even if it is possible to make the selections  $\mathbf{A} \cdot \hat{n} = \nabla u \cdot \hat{n} = 0$ , it seems that the specification of closed form functions spanning the desired solution space which satisfy these or similar conditions might not always be possible. If this perturbational approach is not deemed favorable, then otherwise a different corresponding complication must be considered. Regardless of whether it is assumed that  $\mathbf{h} = \mathbf{h}_0$  outside of  $\Omega$ , or instead outside of some well-chosen surface enclosing  $\Omega$  to estimate the field induced outside of the sample, the corresponding magnetic field must be continuous across any such ‘boundary,’ again assuming the simplest properties regarding the materials on either side. Thus, there correspond existence requirements for the partial derivatives of  $\mathbf{A}$  on the same such boundary, and (in the simplest situations) some combination of the partial derivatives of the component functions of  $\mathbf{A}$  must equal a constant at the boundary. Again, this requirement comes in addition to that specified by the GL problem itself, and if a favorable gauge selection is required as well, this approach seems no less complex. Based upon the geometry of interest, it may be possible to numerically compute functions satisfying these or similar collections of boundary requirements, and it seems obvious that there are cases in which this would represent the only possible option. Clearly, the strategy employed when studying such extensions must be to first consider the simplest geometries in three dimensions.

A more immediate extension to consider is perhaps the case of the “thin

annulus.” The eigenfunctions of  $\mathcal{L}$  are available in closed form, and similar to those specified for the operator on  $D$ . Several similar phenomena could undoubtedly be observed or verified in such a study, and the specification of where these similarities are observed to end could offer a means of obtaining a larger understanding of both problems.

The other type of GL modeling extension to consider is that for layered superconducting systems at high-temperature; representing problems that are of current technical interest to the design of systems that exhibit low resistivity in more desirable temperature ranges. This additionally requires a more specific modeling of anisotropy and nonhomogeneity in the superconducting regions. Perhaps the most widely studied model is the so called Lawrence-Doniach Model, wherein an adaptation of the functional  $\mathcal{E}$  to account for the coupling effects between superconducting layers is made (see [2]). Of course, this corresponds to a more complex PDE problem at the very least. A complete evaluation of the potential applicability of GNGA or a similar algorithm to these types of problems is not provided here. However, such an application may be possible after a suitable collection of assumptions, even if designed only to first evaluate the practical aspects of such an endeavour, are made.

There are several improvements and extensions to consider for the simulation software used in this or similar GNGA numerical applications. Specific to this problem, the bifurcation algorithms could be better generalized so that a single function is called to specify a bifurcation point, given estimates on any sort of branch that might be encountered. Not only would this help streamline any higher-level procedures that might need to be invoked, but also the detection of any unexpected types of bifurcations (if they exist) would be clarified. The computational aspects discussed in the fourth chapter concerning the minimization of the execution time used when forming the search direction function at each Newton iteration are fairly complete, although some improvements might be possible after even a more complete understanding is obtained. The most useful addition to the collection of simulation routines would be a high-level control script by which solutions exhibiting certain properties could be effectively searched for in a reasonable time frame.

The numerical method detailed in this research clearly has the advantage of providing deep insight into the mathematical phenomena inherent in a given PDE problem. This is offset to some degree by the significant theoretical complications resulting from the need to specify a basis for the solution

space; however when methods of this type can be practically applied, the results obtained are certain to stimulate a more in-depth understanding of and interest in a given problem.

# Bibliography

- [1] Adams, Robert A. *Sobolev Spaces*. New York: Academic Press, Inc., 1975.
- [2] Bauman, Patricia and Ko, Yangsuk. "Analysis of Solutions to the Lawrence-Doniach System for Layered Superconductors," 2005.
- [3] Berger, Jorge and Rubinstein, Jacob (Eds.). *Connectivity and Superconductivity*. Springer-Verlag Berlin Heidelberg, 2000.
- [4] Berger, Melvyn S. *NonLinearity and Functional Analysis*. New York: Academic Press, Inc., 1977.
- [5] Bethuel, F., Brezis, H. and Hel in, F. *Ginzburg-Landau Vortices*, Boston: Birkh user, 1994.
- [6] Deo, P. Singha, Schweigert, V. A. and Peeter, F. M. "Magnetization of Mesoscopic Superconducting Disks," *Phys. Rev. Lett.*, **79**,23(1997), pp. 4653-4656.
- [7] Du, Qiang. "Computational simulation of type-II superconductivity including pinning phenomena," *Phys. Rev. B*, **51**,22(1995), pp. 16194-16203.
- [8] Du, Qiang, Gunzburger, Max D. and Peterson, Janet S. "Analysis and Approximation of the Ginzburg-Landau Model of Superconductivity," *SIAM Review*, **34**,1(1992), pp. 54-81.
- [9] Gilbarg, G. and Trudinger, N. S. *Elliptic Partial Differential Equations of Second Order*, (2d ed.). Springer-Verlag Berlin Heidelberg, 1977, 1983.

- [10] Giles, J. R. *Introduction to the Analysis of Normed Linear Spaces*, Australian Mathematical Society Lecture Series **13**. Cambridge; Cambridge University Press, 2000.
- [11] Golubitsky, Martin and Stewart, Ian. *The Symmetry Perspective*. Basel; Boston; Berlin: Birkhäuser, 2002.
- [12] Helffer, Bernard. *Semi-Classical Analysis for the Schrödinger Operator and Applications*, Lecture Notes in Mathematics **1336**. Springer-Verlag Berlin Heidelberg, 1988.
- [13] Hislop, P. D. and Sigal, I. M. *Introduction to Spectral Theory With Applications to Schrödinger Operators*, Applied Mathematical Sciences **113**. Springer-Verlag New York, Inc., 1996.
- [14] Jaffe, Arthur and Taubes, Clifford. *Vortices and Monopoles*, Progress in Physics, A. Jaffe and D. Ruelle, Eds. Boston: Birkhäuser, 1980.
- [15] Lévy, L.-P. *Magnetism and Superconductivity*. Springer-Verlag Berlin Heidelberg, 2000.
- [16] Lions, J. L. and Magenes, E. *Non-Homogeneous Boundary Value Problems and Applications (I)*. Springer-Verlag Berlin Heidelberg, 1972.
- [17] Neuberger, John M., Rice Jr., Dennis R. and Swift, James W., “Numerical Solutions of a Vector Ginzburg-Landau Equation with a Triple Well Potential,” *Int. Jour. Bif. Chaos*, **13**,11(2003), pp. 3295-3306.
- [18] Neuberger, John M. and Swift, James W. “Newton’s Method and Morse Index for Semilinear Elliptic PDEs,” *Int. Jour. Bif. Chaos*, **11**,3(2001), pp. 801-820.
- [19] Neuberger, John M., Swift, James W. and Sieben, Nándor, private communication.
- [20] Neuberger, John W. *Sobolev Gradients and Differential Equations*, Lecture Notes in Mathematics **1670**. Springer-Verlag Berlin Heidelberg, 1997.
- [21] Sattinger, D. H. *Group Theoretic Methods in Bifurcation Theory*, Lecture Notes in Mathematics **762**, A. Dold and B. Eckmann, Eds. Springer-Verlag Berlin Heidelberg, 1979.

- [22] Schechter, Martin. "Essential Self-adjointness of the Schrödinger Operator with Magnetic Vector Potential," *Jour. Func. Anal.*, **20**(1975), pp. 93-104.